INTERANNUAL VARIABILITY OF SUMMER PRECIPITATION IN TEXAS AND ITS IMPLICATION TO SUMMER DROUGHT

A Dissertation

by

BOKSOON MYOUNG

Submitted to the Office of Graduate Studies of
Texas A&M University
in partial fulfillment of the requirements for the degree of

DOCTOR OF PHILOSOPHY

August 2007

Major Subject: Atmospheric Sciences

INTERANNUAL VARIABILITY OF SUMMER PRECIPITATION IN TEXAS AND ITS IMPLICATION TO SUMMER DROUGHT

A Dissertation

by

BOKSOON MYOUNG

Submitted to the Office of Graduate Studies of
Texas A&M University
in partial fulfillment of the requirements for the degree of

DOCTOR OF PHILOSOPHY

Approved by:

Chair of Committee,	John W. Nielsen-Gammon
Committee Members,	Larry Carey
	Ping Chang
	Gerald North
	Ramalingam Saravanan
	Courtney Schumacher
Head of Department,	Richard Orville

August 2007

Major Subject: Atmospheric Sciences

ABSTRACT

Interannual Variability of Summer Precipitation in Texas and

Its Implication to Summer Drought. (August 2007)

Boksoon Myoung, B.S., Yonsei University;

M.S., Texas A&M University

Chair of Advisory Committee: Dr. John W. Nielsen-Gammon

Since Texas normally receives most of its precipitation in the warm season, precipitation deficits in summertime may bring serious agricultural and hydrological disasters. While the underlying physical processes of summer precipitation deficit and drought are unclear, they can be understood in terms of convective instability. This research is designed to investigate how convective instability influences monthly mean precipitation in Texas in the summertime and to examine the modulation of convective instability and precipitation by upper-level circulations, soil moisture, vertical motion, and low-tropospheric warm air transport using NCEP/NCAR reanalysis data. Statistical approaches including correlation analysis, multiple linear regression analysis and back trajectory analysis were used to reveal the underlying dynamics of their linkage and causality.

The results show that warming at 700 mb and surface dryness result in excessive convective inhibition (CIN), leading to precipitation deficits on a monthly time-scale.

Temperature at 700 mb (Tlt) and surface dewpoint have little correlation suggesting different processes contribute to warming at 700 mb and surface dryness, respectively.

Correlation analysis among the surface variables emphasizes the role of soil moisture on the dewpoint and thermodynamics at the surface. Back trajectory analysis indicates that a significant contributor to warming at 700 mb is the inversion caused by warm air transport from the Rocky Mountains and the Mexican Plateau where the surface potential temperature is greater than 307.5K rather than by subsidence. It was found that downward motion and warm air transport are enhanced in Texas when upper-level anticyclonic circulation develops in the southern US.

Upper-level anticyclonic circulations in the southern US strongly affect Texas summertime precipitation by modulating the principal processes as follows. They increase CIN not only by enhancing warm air transport from the high terrain but also by suppressing occurrence of disturbances. The resulting reduced precipitation and dry soil significantly modulate surface conditions, which elevates CIN and decreases precipitation. The aforementioned chain-reaction of upper-level anticyclone influences can be understood in the context of CIN.

DEDICATION

To my father whom I look forward to meeting in heaven

ACKNOWLEDGEMENTS

I would like to express my gratitude to my advisor, Dr. John W. Nielsen-Gammon for his consistent guidance and support throughout this project. I also appreciate my other committee members, Dr. Gerald North, Dr. Larry Carey, Dr. R. Saravanan, Dr. Courtney Schumacher, and Dr. Ping Chang for helping me take a broad view on the subject.

Certainly, I would like to thank my parents and family in Korea. Their deepest love and their consistent support provided me the motivation to finish this work.

Lastly, and most importantly, I thank my Lord, Jesus Christ, who gave me the strength to persevere throughout the challenges of completing this research.

TABLE OF CONTENTS

LIST OF TABLES

LIST OF FIGURES

FIGURE Page

FIGURE Page

CHAPTER I

INTRODUCTION

In the cool season, when the polar jet migrates southward and the subtropical jet intensifies, upper-level synoptic-scale disturbances interact with surface waves, so, precipitation in Texas is dominated by cold, warm, and stationary fronts associated with baroclinic systems. In summer, as the contrast of the temperature between ocean and land becomes insignificant, the subtropical jet weakens, and the polar jet migrates to the north, rainfall associated with upper-level disturbances reduces and convective precipitation prevails over Texas (Clark 1960; Mintz 1984).

Since Texas receives most of its precipitation between April and September, climatologically, and potential evapotranspiration is high during that time, a summertime precipitation deficit in Texas may bring serious agricultural failure in the growing season. According to Koster et al. (2004), strong interaction between land and precipitation through soil moisture is present in the south-central US. Therefore, reduced precipitation over a certain time may induce further precipitation deficit by land-atmosphere interactions. Since drought results from the accumulated effect of deficient precipitation over time, serious droughts can be caused by an initial precipitation deficit.

In the past, Texas has suffered tremendous hydrological and agricultural damages

---

This dissertation follows the style and format of the *Journal of the Atmospheric Sciences.*

from summer droughts. For example, the state-wide warm season droughts of 1996 and 1998 produced widespread crop failure and $5 and $6 billion were lost through agricultural damage in each event (NCDC 2006). More wide-ranging drought in 1980 in the south-central and eastern US was associated with $20 billion damage in agriculture and related industries. Hao and Bosart (1987) estimated 1300 deaths due to the heat waves that accompanied and were enhanced by the latter warm season drought.

Prediction skills of monthly and seasonal precipitation need to be substantially improved. The National Oceanic and Atmospheric Administration's (NOAA) Climate Prediction Center (CPC) issues seasonal forecasts for United States temperature and precipitation for leads out to 12.5 months. Only marginal skill has been found for CPC's seasonal precipitation forecasts (van den Dool et al. 1998). The forecast skill for summers is smaller than that for winters and this is partially due to the unclear linkage between tropical SST anomalies and subtropical and extratropical climate variability in summers. One of the difficulties in establishing the relationships between SST anomalies and summer precipitation variations in the south-central US is the significant influence of local processes and feedbacks associated with soil moisture (Atlas et al. 1993; Helfand and Schubert 1995).

Due to the severity and frequent occurrence of droughts, many efforts have been made to determine the origins and development process of droughts in the Great Plains (Trenberth et al. 1988; Trenberth and Branstator 1992; Trenberth and Cuillemot 1996; Lyon and Dole 1995; Sud et al. 2003). Most studies have focused on the 1988 drought in the Great Plains and found significant remote influence from anomalous sea surface

temperature (SST) in the tropical and extratropical Pacific and local influence from reduced soil moisture; the 1988 drought was initiated by the former through induction of upper-level anticyclonic circulations and maintained by the latter. This result was consistent with the inferred causes of droughts in south-central US in 1980 and 1998 (Namias 1982; Hong and Kalnay 2002).

However, those studies have not made clear the physical and dynamical contributions of the remote and local forcings to the precipitation deficit. The response of precipitation to the forcings is not linear because of the complicated precipitation processes including planetary boundary layer (PBL) processes, moisture transports, temperature inversions above the PBL and so on. Texas droughts may differ from those experienced in the Great Plains due to the different latitudes and proximity to moisture sources, implying different relative importance of tropical and mid-latitude dynamics. At present, there is no comprehensive theory that explains the physical and dynamical processes of precipitation deficit in summer months of Texas.

Thus, we propose examining interannual variability of summertime precipitation in Texas and investigating the significant factors contributing to the variability. This would 1) reveal the underlying dynamics of precipitation deficit, 2) shed light on the physical and dynamical mechanisms of the initiation and maintenance of summertime droughts in Texas and improve their prediction, and 3) help to comprehend how land-atmosphere feedback and large scale circulations that were inferred to play crucial roles in the previous US drought studies directly and indirectly affect the convective precipitation.

In this study, we argue that the most direct physical influences on summertime drought in Texas can be represented by conventional indices used in convective forecasting. We will investigate how convective instability influences monthly mean precipitation in Texas in summertime and how convective instability and precipitation are modulated by large-scale processes such as upper-level circulations and by local processes such as soil moisture, vertical motion, and warm air transport. This will be accomplished by statistical methods such as linear correlation and regression analyses among the parameters representing physical and dynamical properties or processes.

Chapter II provides a brief background of the current knowledge of a summary convective precipitation diagnosis and of the formation and maintenance mechanism of warm season droughts in the central US including the Great Plains. The chapter then presents the specific issues to be addressed by this research. Chapter III outlines the data and methods used in this study. Chapter IV investigates characteristics of summertime Texas precipitation and modulation of precipitation by convective instability. The chapter then examines the most significant parameters affecting convective instability. Controlling mechanisms on the aforementioned parameters will be explored in chapter V. Chapter VI elucidates the large-scale influence on convective instability and precipitation and integrates the principal processes controlling interannual variability of summer precipitation in Texas. It includes the cascade of influences and pathways between large scale circulations and local precipitation. The major results and conclusions of this study are summarized in chapter VII.

CHAPTER II

BACKGROUND

A. Summer precipitation in Texas

In summertime, as the subtropical jet weakens and the polar jet migrates to the north near the Canadian boarder, convective precipitation becomes the primary characteristic of summertime rainfall in Texas (Clark 1960; Mintz 1984). We will review studies that address significant factors controlling convective precipitation on various time-scales less than a season. Many such studies of frequency and intensity of convective precipitation have considered tropical convection.

Three necessary ingredients for deep convection were suggested by Doswell (1987): ample moisture in the lower troposphere, a substantial "positive area" with a steep enough lapse rate, and sufficient lifting.

The first ingredient is usually represented by high precipitable water (PW). PW, defined as the vertically integrated total mass of water vapor per unit area for a column of the atmosphere, is the amount of water that would fall to the surface if all moisture in the atmosphere were condensed and precipitated out. Although PW does not exactly correspond to the expected rain total due to the complicated precipitation processes and moisture convergence that may increase the amount of moisture into a region, it has generally a positive relationship with precipitation (Sato and Kimura 2003; Brenner 2004). This positive relationship is not only because higher PW indicates larger amounts

of moisture to condense and precipitate out but also because it increases the second ingredient, convective instability. Water vapor is a source of positive buoyancy in the atmosphere since the density of moist air is lower than the density of dry air at the same pressure and temperature, and due to the latent heat that would be released when the water vapor condenses in a updraft. Therefore, a moist air parcel is more unstable than a dry air parcel.

While PW can be increased by enhanced surface evaporation and/or low-level moisture convergence, the latter tends to more significantly modify PW over the deep convective regions in the tropics (Maloney and Hartmann 1998; Brenner 2004). It has been very well known that moisture convergence associated with the low-level jet (LLJ) is also linked with nocturnal thunderstorm activity in the Great Plains (Hering and Borden 1962; Augustine and Caracena 1994; Higgins et al. 1997a)

The second ingredient corresponds to convective instability, which is commonly assessed by examining convective available potential energy (CAPE). CAPE is the vertical integral of parcel buoyancy between the LFC and the equilibrium level (EL):

$$CAPE = R\int_{P_{LFC}}^{P_{EL}} (T - T')d \ln p$$

where T′ is the temperature of a parcel, T is that of the environment, P_{LFC} is the pressure of LFC, P_{EL} is the pressure of EL, and R is a gas constant. This equation is a simplified version of CAPE. T′, T, and R can be replaced by virtual temperature of a parcel Tv′ and that of the environment Tv and gas constant for dry air Rd, respectively.

CAPE depends on the temperature and moisture of a parcel and the vertical profile of the environmental temperature. Over tropical oceans, variations of CAPE in

space and time are mostly influenced by surface wet-bulb temperature (Tw), especially on short timescales (Williams and Renno 1993; Ye et al. 1998; DeMott and Randall 2004). Variations of lapse rate play a secondary role since temperature variations in the mid- and upper-troposphere are negligible due to the balance of adiabatic cooling and subsidence warming associated with updraft and downdraft areas. The dependence of CAPE on Tw is also found on a monthly timescale (DeMott and Randall 2004).

Several physical processes can modify CAPE by altering the vertical thermodynamic structure: convection, large-scale dynamics, radiation, and surface fluxes. Using a GCM, testing the effect of the individual physical processes on the linear relationship between CAPE and Tw, Ye et al. (1998) found that surface evaporation and convection are the most significant contributing processes while the large-scale vertical motion does not influence the relationship. Surface evaporation directly changes boundary layer moisture content, and convection tends to warm the free atmosphere by subsidence in the cloud-free region as well as to dry the boundary layer. However, vertical motion that is most prominent in the mid-troposphere hardly modifies boundary layer thermodynamics.

Physically, CAPE refers to the maximum kinetic energy per unit air mass that can be attained by the moist convection, and therefore puts an upper limit on the cumulus updraft vertical velocity (Emanuel 1994). The maximum upward velocity achieved by a parcel is given by

$$w = \sqrt{2CAPE}$$

Although observational studies have shown that the vertical velocity estimated from the amount of CAPE is substantially greater than the actual vertical velocity (Williams et al. 1992; Kingsmill and Wakimoto 1991), the relationship between CAPE and convection is qualitatively indicated by the positive correlation between observed parcel buoyancies and updraft velocities in oceanic convection (Ye et al. 1998).

On the other hand, for an ascending parcel to realize positive potential energy above LFC, it needs to overcome negative energy through the stable layer to reach the LFC. This negative energy is named convective inhibition (CIN) and is defined as follows:

$$CIN = -R\int_{P_{sfc}}^{P_{LFC}} (T - T')d\ln p$$

By definition, CIN is controlled by the original temperature and moisture of the lifted parcel and by the environmental temperature profile below the LFC. Often, CIN exists due to the presence of a capping inversion (Carlson 1983; Lanicci and Warner 1997; Stensrud 1993). In general, the capping inversion has been attributed to subsidence and topography. Such an inversion is frequently observed in the southern, central and eastern part of US in spring. Elevated mixed layers (EML) are responsible for this. EMLs originate over the high terrain of the Rocky Mountains and Mexican Plateau where the boundary layer often has a tendency for being particularly heated on account of the enhanced surface sensible heat flux associated with dry soil. Some parts of tropical oceans are also influenced by capping inversions (Kloesel and Albrecht 1989; Williams and Renno 1993).

Due to a restraining inversion and CIN, deep convection may be prevented from

occurring over a wide area despite substantial CAPE. In such a case, the atmosphere needs sufficient kinetic energy to carry parcels to the LFC for deep convection or sufficient large-scale ascent to produce absolute instability from potential instability. This nature of atmospheric convection requires the third ingredient, a disturbance as a lifting mechanism.

Lifting mechanisms have been discussed extensively in the literature. They include gravity waves, see-breeze type circulations, outflow from mature storms, frontal circulations, jet streak circulations, and drylines (Colby 1984; Weckwerth 2000). Despite large CIN, the existence of strong low-level convergence forced by a cold front or outflow can allow the boundary layer air to reach LFC so that thunderstorms can develop and become organized into large-scale convective systems (Rasmussen and Blanchard 1998).

It is generally accepted by forecasters that convection typically is initiated by mesoscale or smaller scale events listed above rather than by large scale vertical motion (Doswell 1987). The initiation of convection is dependent on whether dynamic lift is large enough to overcome CIN (Mapes 2000; Ziegler et al. 1997). Colby (1984) employed a one-dimensional model to investigate thermodynamic conditions prior to the onset of deep convection in Kansas in springtime 1979. The modeling study demonstrated that while large CAPE and low CIN prior to the onset of deep convection prevailed, convection started where CIN was a minimum but not where CAPE was a maximum. Weak convergence associated with differential surface heating occurred, but minimization of CIN through surface heating with moderate soil moisture allowed

turbulence in the boundary layer to lift boundary layer air to its LFC. Consistent with other observational studies (Colby 1980 and Foote and Wade 1982), this study emphasizes the connection of minimization of CIN to onset of convection.

Meanwhile, on the seasonal or subseasonal time-scale, large-scale thermodynamic conditions tend to determine convective instability and control the frequency and intensity of convection in tropics (Fu et al. 1999). This point of view is supported by assuming that the crucial role of mesoscale processes is to provide the lifting which is required to initiate deep moist convection. Then, on the time-scale larger than a week or so, mesoscale processes, i.e. disturbances to lift air in the boundary layer, may become less significant, and thermodynamic structure is more important for governing convection. Doswell (1987) proposed that, with this assumption, the interaction between mesoscale and large scale controls the intensity and evolution of the consequential convection.

With respect to the thermodynamic structure that is directly related to convection, most of the focus by researchers has been on convective instability. In an effort to evaluate convection in a changed climate, variations of tropical CAPE have been studied extensively. Over the past several decades, positive trends in both precipitable water and large-scale temperature in tropics have been reported, which appear to result in increased CAPE, but no specific link was found between CAPE and convective frequency or intensity (Gaffen et al. 1991; Williams and Renno 1993; Brown and Bretherton 1997; Gettleman et al. 2002; DeMott and Randall 2004). This feature is not limited to the

tropical region. Globally, a positive tendency in global mean precipitation is not obvious despite increased atmospheric instability (Tsonis 1996).

As discussed above, the weak connection between CAPE and precipitation in the tropics is partially due to the existence of CIN, the negative energy below the LFC. Mean values of CIN in the tropics are generally a factor of ten smaller than in mid-latitudes, but a small amount of CIN is frequently able to present a substantial obstacle to the release of potential instability and limits outbreaks of convection in the tropics although there is widespread availability of energy for instability (Williams and Renno 1993).

The significant role of CIN in regulating initiation of deep convection is also described in Fu et al. (1999). In light of how thermodynamic structures control initiation of convection in the tropical Amazon, two key players were found: a convectively unstable profile and CIN. Especially in the south Amazon, a high correlation was found between CIN and frequency of convective cumulus. Land surface warming from winter to spring possibly destabilizes the atmosphere. In addition, large-scale circulations have a tendency for inducing cooling and moistening in the troposphere above 850 mb. Also, the circulations not only supply moisture to the PBL through entrainment but also remove temperature inversions. These processes decrease CIN and increase lapse rates, promoting increased frequency of convection.

The study of Fu et al. (1999) suggests that changes of large scale thermodynamic conditions are likely to modulate the frequency and strength of the convection on a monthly and seasonal time-scale. The control by large scale thermodynamic conditions

of convection may be due to the interaction between dynamic processes and thermodynamic processes on a time-scale greater than a month or so. According to their example, large scale dynamics may be expected to control moisture and the stability of the lower troposphere, altering the extent to which the environment favors convection.

B. Warm season droughts in the central US

Precipitation deficit in summer can cause warm season drought. Warm season drought tends to result in catastrophic damage to agriculture since it has a devastating effect on crop yields in the growing season, and the heat waves that often accompany drought jeopardize human health. For example, the Great Plains' drought in 1988 was associated with record high temperatures and widespread forest fires that burned nearly 4.1 million acres of forest, a Mississippi river discharge 40% of normal (a record low), and roughly 40 billion dollars in economic losses (Sud et al. 2003). The 1980 drought was responsible for nearly 1300 deaths due to the intense heat (Hao and Bosart 1987).

The central United States experienced a number of severe droughts during the last century. Major droughts in the 1930s and the 1950s were the most severe and long lasting and affected the south-central US and the Great Plains. Catastrophic decadal drought in the 1930s was accompanied with dust storms so that it produced the "Dust Bowl". Rather less severe multiyear drought occurred in the early 1910s, 1920s, and in the mid-1960s. The frequent occurrence of multiyear droughts in the Great Plains

implies that multiyear droughts are a regular characteristic of the Great Plains climate (Woodhouse and Overpeck 1998) and are expected to recur as normal climate fluctuations in the future as well.

Nevertheless, most GCMs were unable to simulate the major US summer droughts of the past few decades-those of 1980, 1988, and 1998 (Namias 1982, Lyon and Dole 1995). The one in 1988 covered much of the contiguous US and most severely affected the Great Plains, and the others in 1980 and 1998 affected the south-central and the south-eastern US, respectively. They developed quickly and lasted only for several months during spring and summer. Even today, some present GCMs in present have not succeeded in simulating the 1988 drought (Sud et al. 2003).

The devastating outcomes for large areas of the country and the uncommon severity of the 1980, 1988, and 1998 droughts were accompanied by abrupt changes of upper-level circulations, which made them attractive cases for diagnostic study. While the 1980 and 1998 droughts in the south-central US should project characteristics and mechanisms of Texas drought much more than the 1988 drought in the Great Plains, a larger number of studies have been contributed to the latter. The three have similarities in terms of initiation and maintenance mechanisms. This section reviews published studies of the causes and maintenance of the multi-month warm season US droughts in 1980, 1988, and 1998.

1. Remote forcing

One of the distinctive features of central US droughts is a positive height anomaly over regions affected by drought, clearly seen in upper-tropospheric height fields. This is often observed prior to and during the peak of the drought (Namias 1982; Trenberth et al. 1988; Chang and Wallace 1987; Trenberth and Branstator 1992; Lyon and Dole 1995; Chen and Newman 1998). Fig. 2.1 shows the height anomalies in Jun-Aug of 1980 and Apr-Jun of 1988 associated with droughts in the Great Plains and the south-central US, respectively. According to Namias (1982), these anticyclonic circulations serve as blocks to cyclonic activity from the Pacific by displacing storm tracks north of the US/Canadian border, which results in the precipitation deficit. Lyon and Dole (1995) speculate that the anticyclone may reduce moisture transport from the Gulf of Mexico to the central US by changing flow patterns.

As seen in the case of the 1988 Great Plains drought (Fig. 2.1.(a)), this positive height anomaly is often accompanied by other positive anomalies over the Pacific and/or over the Atlantic that are significantly different from climatology (Mo et al. 1991). Fig. 2.1.(a) also depicts the negative anomalies positioned between the positive anomalies. This characteristic has been inferred to originate from propagation of stationary planetary waves. Anomalously warm SSTs are prone to induce abnormal low-level convergence and convective activity. Associated upper-tropospheric divergence provides a forcing for Rossby waves by the advection of vorticity (Trenberth et al. 1998).

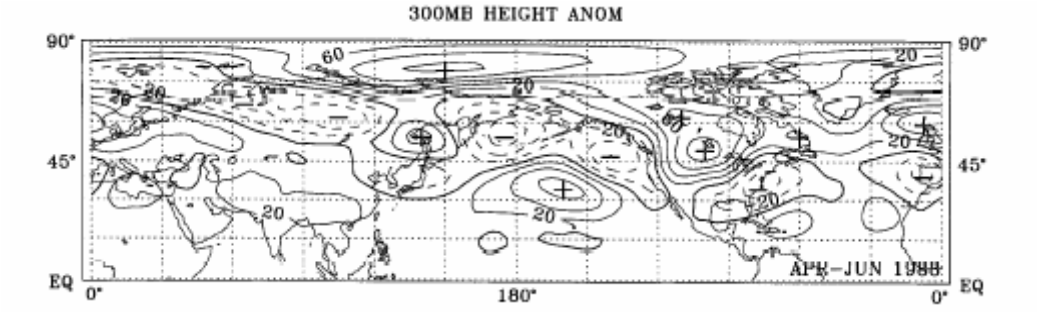

(a)

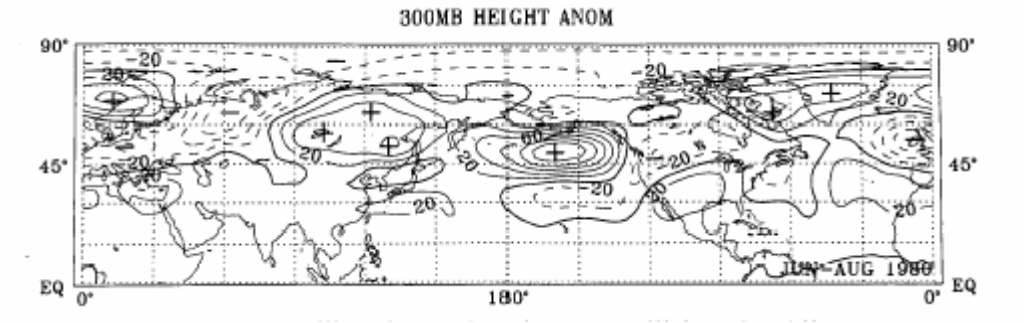

(b)

Fig. 2.1. Time average 300-mb height anomalies a) for April-Jun 1988 and b) for Jun-Aug 1980. (Lyon and Dole (1995))

Various models have been employed to study SST influence on droughts, such as simple primitive equation models, atmospheric general circulation models, and coupled general circulation models (Trenberth et al. 1988, 1992; Lyon and Dole 1995; Atlas et al. 1993; Sud et al. 2003). The goal of previous modeling studies that focused on the 1988 drought was to reproduce the observed upper-level height anomalies in the spring and summer of 1988 by SST forcing. Since a strong La Niña event occurred in the tropical Pacific in 1987/1988, cold SST anomalies in the eastern tropical Pacific were pronounced at the early stage of the 1988 drought. Depending on their intensity and

location, these SST anomalies may disrupt atmospheric heating patterns in the tropics. Thus, such heating anomalies could have initiated the circulation anomalies across North America, resulting in the drought.

Trenberth et al. (1988) noted that highly anomalous tropical convection revealed in outgoing longwave radiation (OLR) field was associated with the major SST anomalies. They hypothesized that the anomalous flow pattern observed in the spring of 1988 was forced primarily by a northward shift of diabatic heating over the eastern tropical Pacific. To test the hypothesis, a five-layer primitive equation stationary wave model linearized about climatological June conditions was forced by the poleward shifted anomalous heating. The model showed a significant response that was similar to the upper-level anomalous circulations observed in North America during the 1988 drought (Trenberth and Branstator 1992).

However, simulations of height patterns associated with drought are highly model-dependent. The barotropic linear model of Lyon and Dole (1995) failed to capture the same locations of the anticyclonic circulations over the tropical Pacific and US and the pattern of wave activity flux observed. Their model is similar to the one of Trenberth et al. (1988) but linearized about spring and summertime mean flow rather than about climatological June conditions. In addition, in an attempt to identify potential source regions for the anomalous stationary wave, a local conservation relation for quasi-geostrophic stationary waves introduced by Plumb (1985) was applied. Although the Plumb flux diagnostic does not necessarily identify the original physical forcing region, it suggests that the central North Pacific is a potential source region for the anomalous

wave pattern observed in the spring of 1988.

While most studies of the 1988 drought focused on monthly and seasonal characteristics, Chen and Newman (1998) by analyzing the temporal evolution of streamfunction on time-scales shorter than a month, found that the April-May-June seasonal height anomaly was dominated by several rapidly intensifying and decaying wave trains, the strongest ones in early and mid-late June. The evolution of 10-day low-pass anomalies of streamfunction and OLR suggested that a propagating Rossby wave forced in the western Pacific was responsible for the abrupt development of the anticyclones, a conclusion that is also supported by a linear time-dependent barotropic model. It is likely that the GCMs' failure in predicting the 1988 drought is partially attributable to the incapability of the models to simulate this abrupt development of upper-tropospheric anomalous circulation. This study suggests that the 1988 drought should be considered not as a steady seasonal event, but rather as a succession of anomalous events that resulted in a serious hydrological deficit. Furthermore, they discussed that precipitation deficit and abnormally high surface temperature that prevailed over the study region in Apr and May although the circulation anomaly aloft was not strongly anticyclonic during either month. This feature implies a significant role of local surface forcing and atmospheric forcing e.g. atmospheric initial condition on drought. The former has been studied broadly in terms of feedback of soil moisture on precipitation, which will be discussed in the next section. Although the latter has been investigated less extensively, Hong and Kalnay (2002) shed light on the significant role of atmospheric initial condition on drought.

In an attempt to elucidate causes of the 1998 drought, Hong and Kalnay (2002) tested three hypotheses: if each of SST forcing, soil moisture forcing, and atmospheric initial condition favors prolonged deficit of precipitation. The third one was referred to as internal forcing in their terminology. Anomalous SST was distinct because positive ENSO was present in the antecedent winter in 1997/1998 although its intensity had weakened by the month of simulation, May 1998. To test the hypotheses, a global spectral model (GSM) and a regional spectral model (RSM) were employed. The initial atmospheric condition and soil moisture came from NCEP-NCAR reanalysis data and observed SST data were used. While the ocean (and land) surface forcing played significant roles at the early stage of the drought, the internal forcing also had a nontrivial impact on the initiation of the drought. Given SST and soil moisture anomalies from 1998, atmospheric initial conditions corresponding to May 1993 rather than May 1998 resulted in a positive precipitation anomaly similar to the pattern observed in May 1993. This experiment showed that the internal forcing had a significant impact on the initiation and early stage of the 1998 drought.

Meanwhile, SST over the Atlantic may influence US droughts. It was found that the position of the anticyclone over the Great Plains is linked with the strength and position of the surface subtropical high over the Atlantic (Helfand and Schubert 1995). In its normal position, the air from the Gulf of Mexico provides ample moisture into the Great Plains. But if it is located farther east and north, the Great Plains becomes dry since moist air is directed to the eastern coast (Forman et al. 1995). The position of this

subtropical high tends to be connected to SSTs in the Gulf of Mexico and over the Atlantic (Oglesby 1991).

2. Local forcing

The drought studies listed above have observed protracted dry conditions after the remote forcing disappeared so that they investigated mechanisms responsible for the maintenance of drought. The important role of soil moisture in determining the mean climate and its variability has been studied extensively (Rowntree and Bolton 1983; Garratt 1993; Betts et al. 1996). It has been suggested that the US droughts in 1980, 1988, and 1998 were initiated by remote forcing, i.e. SST anomalies, and maintained by local forcing, i.e. feedback of soil moisture (Namias 1982; Lyon and Dole 1995; Trenberth et al. 1996; Hong and Kalnay 2002; Sud et al. 2003).

Over the ocean, the SST plays an important role in forcing the atmosphere and its circulation, and over the land, so does soil moisture. The former is observed daily, and ocean surface is considered saturated so that understanding its role is rather simple. However, soil moisture is neither observed routinely in most locations nor uniform, and it is greatly influenced by precipitation on a short time-scale. Although in the last few decades a great amount of effort studying the land-atmosphere system has brought huge improvements in the understanding of the feedback between soil and atmosphere, the influence of soil moisture on precipitation is a subject of continuing investigation.

Traditional moisture budget analysis has been often used to estimate surface evaporation. With respect to moisture content, this method seeks factors relevant to reduced precipitation during a drought period by evaluating inter-relationships between each factor (e.g. evaporation and moisture flux divergence) and precipitation (Hao and Bosart 1987; Lyon and Dole 1995). Moisture budget equation describing the excess of surface evaporation (E) over precipitation (P) can be written as

$$E - P = \frac{\partial q}{\partial t} + \nabla \bullet Q$$

where q is the precipitable water (PW) and Q is the moisture flux. On monthly or seasonal time-scales, the change of the precipitable water is negligible so that a balance exists among evaporation, precipitation, and moisture flux divergence.

Using this method, Lyon and Dole (1995) found that reduced precipitation month by month in 1988 corresponded to a decreased monthly mean evaporation rate possibly representing decreased soil moisture. The decreasing trends in both precipitation and evaporation occurred despite the fact that an anomalous positive moisture flux convergence occurred over the drought region in the later months of 1988 drought. One might imagine that moisture flux divergence (convergence) would prevail during the period of drought (flood), which may result in decreased (increased) moisture content in troposphere and then, decreased (increased) precipitation. However, Trenberth et al. (1996) showed that moisture flux divergence in 1988 was not larger than during the 1993 flood in the same area, emphasizing little connection of moisture flux divergence to precipitation variability. Although these studies did not prove a direct response of precipitation to soil moisture explicitly, they suggest that decreased evaporation that

seems to be associated with reduced soil moisture likely maintains drought in its later stages.

Research on the effect of soil moisture on precipitation mostly relies on modeling studies because of the convenience of isolating control factors. Many GCM and regional climate model (RCM) studies showed a significant role of soil moisture in maintaining drought conditions in the Great Plains (Oglesby and Erickson 1989; Oglesby 1991; Sud et al. 2003; Hong and Kalnay 2002). In simulations of the 1988 (Atlas et al. 1993) and 1998 (Hong and Kalnay 2002) US droughts, reduced soil moisture resulted in decreased rainfall as well as increased surface air temperature. In the work of Oglesby and Erickson (1989), this feature was consistent in the experiments of both prescribed and initialized negative anomalies in soil moisture.

However, although the observational and modeling studies described above found an influence of soil moisture on precipitation, the physical processes of their coupling are still unclear. It is often assumed that precipitation would primarily derive from local evaporation and, then, enhanced evaporation due to wetter soil would increase the moisture content of the troposphere and draw air closer to saturation and precipitation. However, soil moisture only regulates the ratio of sensible heat flux to latent heat flux that is named the Bowen ratio. Although the smaller Bowen ratio associated with wetter soil increases latent heat flux and decreases sensible heat flux, the resulting amount of precipitation is not directly affected by a decreased Bowen ratio (Betts et al. 1996). This may be partially due to an indirect effect of the Bowen ratio. Increased latent heat flux and decreased sensible heat flux induced by decreased Bowen

ratio reduce entrainment of drier free-atmosphere causing a shallower PBL and an increase in wet-bulb temperature affecting precipitation. Schar et al. (1999) argued that wet soil tends to increase precipitation efficiency rather than to provide moisture to fall out by rainfall in Europe. In their RCM study to examine sensitivity of summertime precipitation to soil moisture, wet soil induced a shallow boundary layer, high moist entropy, low level of free convection (LFC), and large net radiative energy flux that together increased the potential for convection. Moisture to fall out by precipitation was provided from the ambient atmospheric flow. Thus, the direct and indirect physical mechanisms of feedback between soil and precipitation still need to be clarified.

With respect to changes in the land-surface boundary condition, soil moisture influences not only the Bowen ratio but also surface albedo. It was proposed by Charney (1975) that dry soil increases the albedo of the surface, causing downward motion to be enhanced to compensate for radiative cooling in order to reach thermodynamical equilibrium (hereafter, the albedo hypothesis). Consistent attention has been paid to the albedo hypothesis in US drought studies because subsiding motion is known to prevail over the drought regions (Chang and Smith 2001; Hao and Bosart 1987).

Originally the albedo hypothesis was proposed to explain the drought in Sahel where evaporation changes are small. The effect of surface albedo change seems to be significant over the Sahel region (Charney 1977; Sud and Fennessey 1982; Cunnington and Rowntree 1986), but it is controversial that this theory can be applied to more heavily vegetated regions in the subtropics. Over the Great Plains, with a GCM, Charney et al. (1977) found that influence of surface albedo changes on summer precipitation was

much less than over desert regions. Furthermore, Sud and Fennessey (1984) reported that elevated surface albedo can reduce aridity over the semi-arid region including the US Great Plains.

The previous discussions of changes of Bowen ratio and albedo linked with soil moisture change imply that the sensitivity of precipitation to soil wetness varies by location. One of the reasons that change of precipitation does not correspond to that of soil moisture is the supply of moisture by transport from outside of the region. Using a GCM, Sud and Fennnessy (1984) and Sud and Smith (1985) found that over semi-arid regions in their model, notably India, an increased convergence of moisture produced by enhanced sensible heating in the planetary boundary layer was sufficient to compensate for the moisture deficit caused by reduced evaporation caused by dry soil.

In the case of the Great Plains of US, while modeling studies of Fennessy and Shukla (1999) and Oglesby and Erickson (1989) also support the importance of dry soil on US drought, they emphasize that moisture flux may reduce the feedback of dry soil on precipitation by providing moisture for precipitation in the 1988 drought. The COLA GCM employed in Fennessy and Shukla (1999) showed that while precipitation and evaporation was found to be significantly less when the model was initialized by June 1998 soil moisture than by climatological soil moisture, the difference in precipitation was half the difference in evaporation because of the moisture flux convergence over the Great Plains.

Demonstrating that moisture availability is sensitive to moisture flux divergence as well as surface evaporation, these studies imply that a careful treatment is needed for

moisture availability for precipitation by investigating not only the soil condition but also the atmospheric circulation determining moisture transport into the region. This is related to the precipitation recycling problem, which is defined as the contribution of the locally evaporated water to the precipitating water in the same region (Brubaker et al. 1993; Trenberth 1999). While the relative importance of regional evaporation to advected moisture on local precipitation substantially depends on location and season, it significantly varies with the size of the area. Contribution of local evaporation tends to be small for small spatial scales and increase for larger scales. For a given region, the effect of surface evaporation (moisture transport) would be significant on local precipitation where the feedback of recirculation of precipitation is strong (weak).

C. Motivation and hypotheses

Comparison of the aforementioned studies of the 1980 and 1998 droughts with those of the 1988 drought indicates that there exist similarities of warm season droughts between Texas and the Great Plains in terms of the predominance of 1) development of positive height anomaly in upper-troposphere at the early stage of the droughts and 2) dry soil at the later stage: the former initiated the US droughts in 1980, 1988 and 1998, and the latter maintained them.

However, there are also some differences in drought characteristics in between Texas and the Great Plains. The most obvious one is the spatial pattern of the positive

height anomalies in the upper-troposphere as seen in Fig. 2.1. While one of the positive height anomalies in the North Pacific is paired with the other in North America, the locations of the anomalies in the 1988 drought (Fig. 2.1.(a)) are quite different from those in the 1980 drought (Fig. 2.1.(b)) in their latitudes, even allowing for the differences in the location of drought. This feature suggests that forcings driving the upper-level height anomalies and the response of the atmosphere may be different in Texas and the Great Plains, respectively.

The role of moisture transport on precipitation is not the same in Texas and the Great Plains. While an increased moisture flux associated with LLJ provides ample moisture in Texas, it not only transports large amount of moisture to the Great Plains but also facilitates convection by enhancing low-level convergence as a lifting mechanism in the Great Plains (Higgins et al. 1997a). Higgins et al. (1997a) found that when moisture transport and moisture flux convergence by LLJ enhances nocturnal precipitation over the Great Plains, a commensurate amount of precipitation along the Gulf decreases.

In addition, there would be mechanistic differences of warm season droughts in Texas and the Great Plains with respect to the precipitation processes. Convective precipitation is the primary characteristic of summertime rainfall in Texas. While convective precipitation occurs in the Great Plains as well, rainfall in the Great Plains is often associated with baroclinicity and storm track dynamics. Thus, rainfall anomalies over the Great Plains are greatly affected by changes of large-scale circulations in the upper-troposphere. For example, the aforementioned development of quasi-stationary upper-level positive height anomalies blocks cyclone activity and then reduces

precipitation. However, amounts of rainfall in Texas should be directly influenced by modulation of factors controlling convective precipitation (e.g. convective instability) and anomalous upper-level circulations likely affect precipitation by changing those factors.

We claim that previous drought studies do not generally provide a mechanistic understanding of precipitation processes, which should be sensitive to location and season. Those studies have not made clear the physical and dynamical contributions to the precipitation deficit. Concerning summer drought in Texas, we need better understanding of the processes that modulate convective precipitation. Accordingly, in this section, we discuss the important factors that would be expected to control convective precipitation in Texas on various time-scales less than a season. For example, from the fact that precipitation is reduced as subsidence is enhanced, we cannot immediately determine whether convection is suppressed by the subsidence inversion or by decreased instability induced by the subsidence. For better understanding and modeling of summer drought, it is necessary to comprehend how land-atmosphere feedback and large scale circulations directly affect the convective instability and associated precipitation.

As discussed previously, on monthly and seasonal time-scale, thermodynamic characteristics seem to be crucial to control long-term variability of tropical deep convection (Fu et al. 1999; Firestone and Albrecht 1986; Kloesel and Albrecht 1989). This may be because the changes in convective instability, especially CIN, are prone to control initiation of deep convection (Fu et al. 1999). Since the precipitation

characteristics of Texas in summertime are similar to those in the tropics in that convective precipitation prevails, these findings suggest that thermodynamic characteristics and changes in convective instability would be significant to the variation of summer precipitation in Texas. Thus, it will be investigated how variability of summer precipitation in Texas will be modified by convective instability on a monthly time-scale.

Although we will examine variability of monthly mean precipitation, our major interest is in the thermodynamic structure associated with Texas summer droughts. As noted previously, since the life cycle and mechanistic characteristics of the summer droughts in Texas are similar to those over the Great Plains, it is expected that upper-level anticyclonic circulation, subsidence, and reduced soil moisture may play significant roles causing precipitation deficit as well on the assumption that drought is regulated by monthly time-mean thermodynamic conditions. We attempt to determine influences of the typical feature of droughts in the central US on precipitation deficit in Texas by examining changes in thermodynamic structure and convective instability.

Fig. 2.2 illustrates possible causes and pathways of precipitation deficit in summertime in Texas. It includes the upper-level anticyclone and reduced soil moisture that have been emphasized in the previous US drought studies. We do not claim that Fig. 2.2 shows a complete set of processes causing precipitation deficit that are associated with the upper-level anticyclone and reduced soil moisture. However, these pathways are

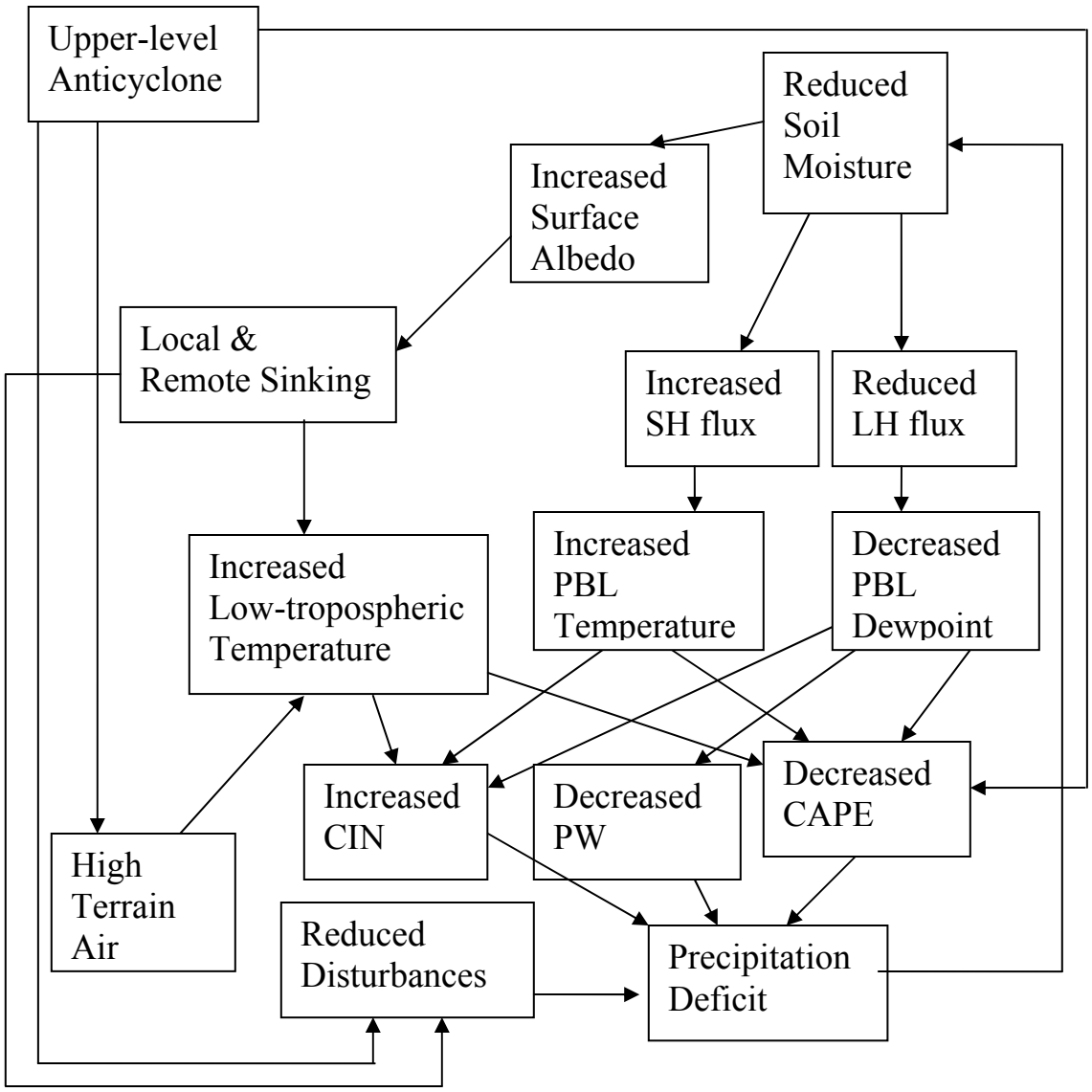

Fig. 2.2. Schematic showing possible causes of precipitation deficit in summertime Texas.

inferred to play major roles on inducing decrease in precipitation based on current knowledge of land-atmosphere interactions and precipitation dynamics. Here, the processes will be briefly described since each pathway will be extensively discussed in detail in later chapters.

An upper-level anticyclone and sinking motion tend to result in precipitation deficit by suppressing occurrence of disturbances and then convection. The relatively warm mid-troposphere temperatures associated with the anticyclone would also affect CAPE. Also, sinking motion may increase low-tropospheric temperature by causing subsidence inversion and thereby increase CIN and reduce CAPE. An inversion can be also caused by warm air advection from the high terrain over the Mexican Plateau and Rocky Mountains. This advection may be associated with changes in upper-level circulations.

With respect to soil moisture, dry soil increases not only the Bowen ratio driving an increase of sensible heat flux and a decline of latent heat flux, but also surface albedo enhancing local subsidence (the albedo hypothesis). The former increases entrainment of drier free-atmosphere air into the PBL, which is likely to result in large CIN and small PW and CAPE. The resulting precipitation deficit makes soil drier, which gives a positive feedback on precipitation. While no direct relationship exists between an upper-level anticyclone and reduced soil moisture, the former tends to affect the latter through induction of decrease in precipitation.

In the context of convective instability, we will examine and discuss the components of Fig. 2.2 in sequence, starting with precipitation deficit. Variables are

chosen to represent each component suitably and statistical results of correlation and regression analyses among the variables will reveal the processes that most strongly control summer precipitation deficit in Texas.

First, we hypothesize that summer precipitation in Texas is strongly controlled by local parameters governing convective precipitation frequency and intensity on monthly-averaged time scales. Here, the local parameters are CAPE, CIN, and PW. Relatively little consideration will be given to the occurrence of mesoscale lifting due to the fundamental difficulties in estimating frequency and intensity of disturbances. Among the three, the most significant parameter(s) will be determined.

Next, it will be hypothesized that the important local parameters are controlled by local surface-based processes. Here, the local surface-based processes refer to pathways that are mainly controlled by soil moisture. This hypothesis will address (1) what changes in the vertical thermodynamic structure influence the most significant parameter(s) and (2) how those changes are affected by surface conditions and large-scale circulations such as soil moisture, vertical motion, transport of high terrain air, upper-level anticyclones, and so on. By making attempts to determine what the most important local parameters on precipitation deficit are and which local and/or remote processes modulate the parameters, we will explore how thermodynamic structure, convective instability, large scale circulation, and surface conditions prohibit occurrence and intensity of convection and, hence, lead to precipitation deficit and Texas summer drought.

CHAPTER III

DATA AND METHOD

A. Data

The monthly precipitation data used in this study is US climate division data obtained from National Climatic Data Center (NCDC) of NOAA. Texas is composed of 10 climate divisions (Fig. 3.1) and the eastern divisions climatologically receive larger precipitation than the south-western divisions in summertime (not shown). To test whether interannual variability of summer precipitation varies significantly by location, we categorized the 10 climate divisions into three regions: mountain region (division 1, 5, 6, and 9), northern region (division 2, 3, and 4), and coastal region (division 7, 8, and 10). While 68% of state-wide precipitation comes from the northern plain region, interannual variability of precipitation for one of the regions was highly correlated with those for the other regions, implying that mechanistic characteristics of precipitation of the three regions are uniform. Thus, an area-weighted, state-wide averaged precipitation was calculated for each month and used as a primary monthly mean precipitation data.

Because the precipitation values are bounded by zero, they tend to have a lognormal distribution. Thus, the state-wide averaged precipitation amounts were transformed using the natural logarithm. Hereafter, PRCP refers to the transformed values if there is no additional note.

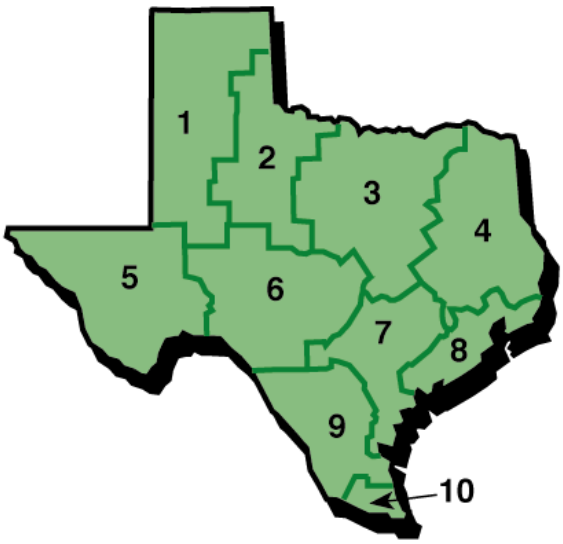

Fig. 3.1. Map showing climate divisions of Texas.

The data for analysis of the probability distribution function (PDF) of Texas precipitation are from US_Mexico daily precipitation analysis gridded at 0.25˚x0.25˚. This dataset is derived from NCDC daily co-op stations, other daily station data received by CPC, and daily accumulations from hourly precipitation dataset. Its monthly averaged

precipitation in Texas is highly correlated with the aforementioned precipitation.

The third data set is NCEP/NCAR reanalysis data (Kalnay et al. 1996) gridded at 2.5˚x2.5˚. The NCEP Medium Range Forecast spectral model and the operational NCEP Spectral Statistical Interpolation were used for the NCEP–NCAR assimilation. The assimilation is performed at a horizontal resolution of T62 and 28 sigma levels in the vertical. Data sets include diagnostic variables like evaporation, soil moisture, sensible and latent heat fluxes that are generated by the GCM's physical parameterizations as well as instantaneous variables like temperature, specific humidity, height, and winds. The former is less reliable than the latter because they are more influenced by the model parameterization. While the variables are available monthly and four times daily, every six hours (0000, 0600, 1200, 1800 UTC) on 17 pressure level, we utilize monthly mean values averaged at the 11 grid points within Texas.

The time domain for this study covers summer months from 1948 to 2003, especially July and August when convective precipitation prevails. The long time span of the reanalysis data allows a comprehensive analysis covering 56 years.

B. Method

In the present study, linear correlation analysis is performed among precipitation, convective instability parameters, surface variables, and tropospheric variables (whose

definition and computation will be described below) to reveal the relationships among the variables. In addition, we use the linear regression analysis to determine the parameters or variables most relevant to precipitation. The resulting Pearson correlation coefficients indicate the strength of a linear relationship between the two fields. Assuming independent, normally distributed data, 0.34 is roughly the 99% confidence limit for a non-zero correlation. Such statistically significant relationships will be indicated by a star in the tables and graphics that follow.

We will compare magnitudes of correlation coefficients to determine, for example, which variables are more or less correlated, or which pathways are more important on controlling a variable. To do so, we need to examine whether two correlation coefficients differ significantly each other. Z_1 and Z_2 corresponding to correlation coefficients, r_1 and r_2, drawn from samples of sizes N_1 and N_2, are computed, respectively. Then, we use the fact that the test statistic

$$z = \frac{Z_1 - Z_2}{\sigma_{Z1-Z2}}$$

where

$$Z = \frac{1}{2}\ln\left(\frac{1+r}{1-r}\right)$$

and

$$\sigma_{Z1-Z2} = \sqrt{{\sigma_{Z1}}^2 + {\sigma_{Z2}}^2} = \sqrt{\frac{1}{N_1 - 3} + \frac{1}{N_2 - 3}}$$

is normally distributed. It is assumed that the population of r has a normal symmetric distribution. A large number of the correlation analyses are focused on the month of July in this study. In this case, N_1 is equal to N_2 at a sample size of 56.

Table 3.1 shows a significance level at which a selected value of r_1 is significantly different from r_2.

Table 3.1. Significance level of r_1 and r_2.

r_1 and r_2	Significance level
0.8 and 0.7	76.6%
0.7 and 0.6	62.2%
0.6 and 0.5	52.0%

For a difference of 0.1 in correlation coefficient, significance level decreases as r decreases. The small sample size in this study makes significance level relatively lower than would be found for the same r_1 and r_2 with a larger number of sample sizes. According to the significance test above, r_1=0.80 is referred to being significantly different from r_2=0.69 at the 90% level. We do not attempt to perform the significance test of a difference between correlation coefficients systematically, but Table 3.1 will simply provide a guide line of statistical inferences for a difference in two correlation coefficients.

Although correlation analysis doesn't identify causality between two variables, understanding the physical mechanisms between the two often allows us to determine their causality. For example, a significant positive correlation was found between temperature and vertical motion at a given pressure level and location: warming linked with descending motion. Because relatively warm air tends to ascend due to buoyancy, downward motion cannot be caused by the buoyancy of the warm air. Instead, because downward motion causes adiabatic warming, subsidence must be driving the positive correlation. Physical reasoning combined with correlation analysis makes it possible to infer causality between many of the correlated variables. This technique is used in this study to find pathways causing deficit of convective precipitation. Great caution is needed to conclude causation inferences because some group of "third variables" can be causing variance in both variables as well.

1. Precipitation and convective instability parameters

In order to explore relationships between the convective instability parameters and precipitation, CIN and CAPE are computed using monthly mean vertical profiles of temperature and dewpoint averaged across Texas. The general meteorology package (GEMPAK) is used to compute CIN, CAPE, LCL and LFC. For PW, monthly mean precipitable water from the reanalysis is averaged over Texas.

2. Precipitation and atmospheric variables

Among the various fields obtained from the NCEP/NCAR reanalysis data, atmospheric variables that may play a significant role in modulating convective instability and associated precipitation were selected to examine the synchronous relationships to precipitation. The variables are divided into two classes according to the effective levels: surface and tropospheric variables. Table 3.2 is the list of the acronyms and symbols for the surface and tropospheric variables. Surface variables include soil moisture (SM), sensible heat flux (SH), latent heat flux (LH), surface dewpoint (Td), and surface temperature (Ts). From these quantities, surface dewpoint depression, DP=Ts-Td, is calculated at each grid point and then averaged across Texas. The same procedure is applied to equivalent potential temperature (θe) defined as

$$\theta_e = T_e \left(\frac{p_0}{p}\right)^{\frac{R}{c_p}} \approx \left(T + \frac{l_v}{c_p} r\right) \left(\frac{p_0}{p}\right)^{\frac{R}{c_p}}$$

where T_e is equivalent temperature; T is temperature of air at pressure p; p_0 is standard reference pressure (1000 mb); R is specific gas constant for air; c_p is specific heat of dry air at constant pressure; l_v is latent heat of evaporation; and r is mixing ratio of water vapor in air. Surface dewpoint, Td, and surface dewpoint depression, DP, are measures of specific and relative humidities, respectively. Surface equivalent potential temperature, θ_e, measures moist static energy.

Tropospheric variables include moisture flux divergence (MFD), 500-850 mb average vertical motion (OMG), and temperature at 700 mb (Tlt). Moisture flux was computed directly from winds and specific humidity on the respective model pressure levels and its divergence was integrated vertically. MFD ($\nabla \bullet (q\vec{V})$) consists of the advection term, ADV ($\vec{V} \bullet \nabla q$), and the divergence term, DIV ($q\nabla \bullet \vec{V}$), where q is the specific humidity and $\vec{V}$ is the horizontal wind. Since precipitation is best correlated with vertical motion at 700mb (not shown), mean vertical motion between 850 and 500 mb was selected. OMG is the change of pressure following an air parcel, and is negative for upward motion. Extreme variation of temperature at 700mb (Tlt) may have a significant impact on the amount of CIN and substantial effect on the amount of CAPE. In summer, the top of the PBL in most parts of Texas is below 700 mb (Nielsen-Gammon, personal communication). Thus, Tlt is expected to represent free-atmospheric processes that cannot be necessarily described using the surface variables.

In the next chapter, we will examine the linkages among these variables, convective instability parameters, and precipitation.

Table 3.2. Frequently used acronyms and symbols.

Category	Acronym or symbols	Meaning
Surface	SM	soil moisture
Surface	SH	sensible heat flux
Surface	LH	latent heat flux
Surface	Td	surface dewpoint
Surface	Ts	surface temperature
Surface	DP	dewpoint depression
Surface	Thetae	surface equivalent potential temperature
Tropospheric	ADV	advection term of moisture flux divergence
Tropospheric	DIV	divergence term of moisture flux divergence
Tropospheric	MFD	moisture flux divergence
Tropospheric	OMG	500-850 mb mean vertical motion
Tropospheric	Tlt	temperature on 700 mb

CHAPTER IV

PRECIPITATION PROCESSES AND CONVECTIVE INSTABILITY IN TEXAS IN JULY

A. Precipitation and convective instability parameters

First, we investigate whether monthly precipitation is strongly controlled by local convective instability parameters that are known to govern convective precipitation frequency and intensity on shorter time scales. Monthly anomalies of PRCP and convective instability parameters in July and August are plotted in Fig. 4.1. Note that 2 samples in August were omitted in Fig. 4.1 because their CINs were unavailable in those months. CIN and CAPE obtained from the monthly mean temperature profile and surface dewpoint are different than the instantaneous values of CIN and CAPE which are used in the reanalysis model's convective scheme. Among CIN, CAPE, and PW, PRCP is most strongly coupled with CIN.

The negative relationship between CIN and precipitation can be caused by the influence of CIN on precipitation or vice versa. Since CIN is a measure of the amount of energy needed to initiate convection, precipitation is suppressed when CIN is relatively high. On the other hand, convective activity and rainfall do not decrease CIN necessarily:

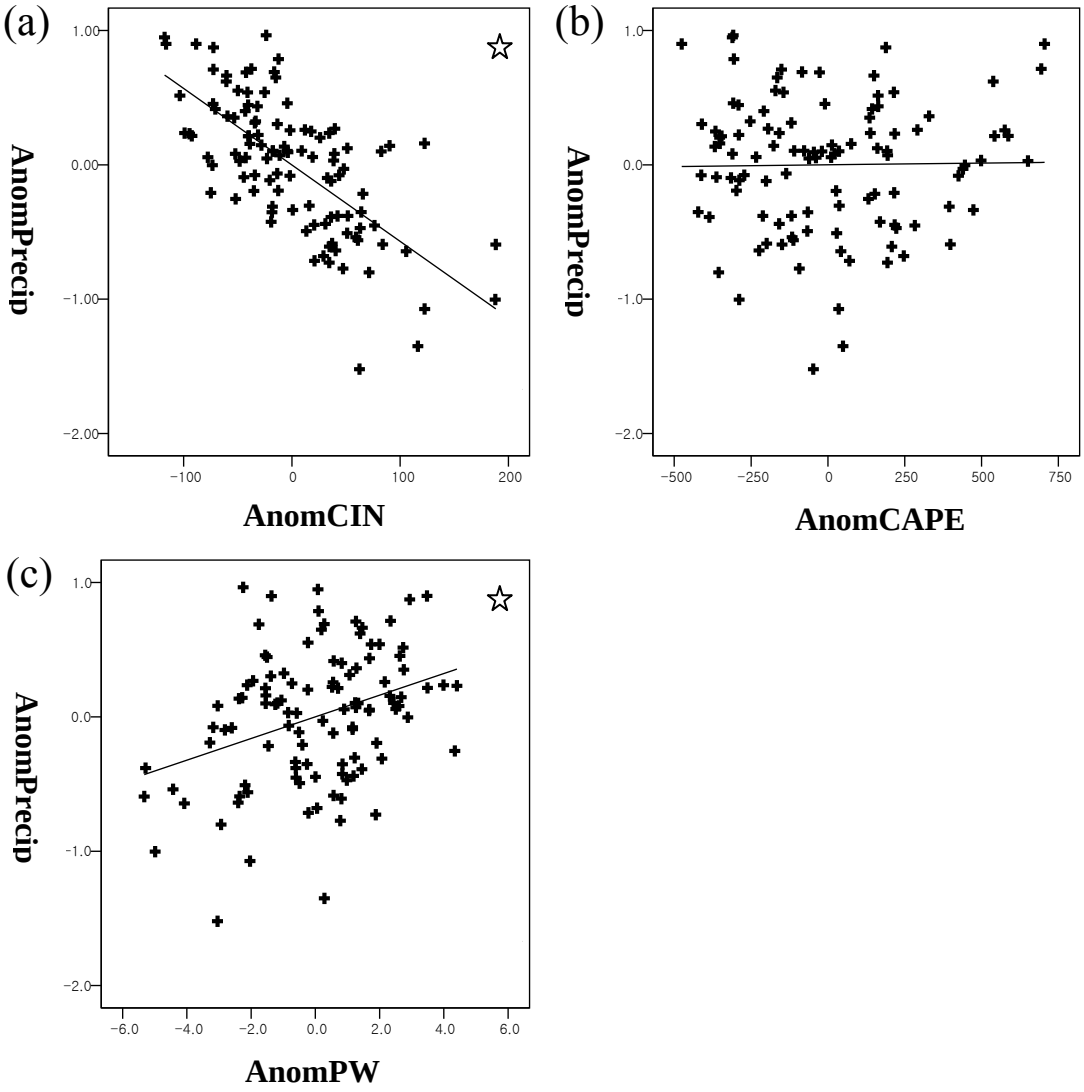

Fig. 4.1. Scatter plot between PRCP (inches) and a) CIN (J/Kg), b) CAPE (J/Kg), and c) PW (kg/m^2). They are monthly anomalies in July and August.

the downdrafts compensating convective updrafts tend to generate capping inversions in the low-troposphere and the recovery of the boundary layer is less than a day or so (Zipser 1977) although small CIN is induced by humid and cool surface air instantaneously. Therefore, the negative correlation between CIN and PRCP indicates that on a monthly time-scale, the amount of precipitation tends to be controlled so strongly by CIN.

CAPE is directly related to the maximum potential vertical speed of updrafts so that higher values tend to indicate greater potential for severe weather on short time-scale (Emanuel 1994). However, Fig. 1.(b) shows a poor correlation between CAPE and PRCP. Convection does not inevitably occur until CIN is first removed, even if substantial CAPE exists. This is consistent with PRCP being correlated with CIN significantly (-0.68) at the 99 % confidence level and essentially uncorrelated with CAPE (0.02). In addition, because convective activity can destroy large CAPE (Demott 2004), the monthly averaging process may reduce the relationship between CAPE and subsequent precipitation.

An analogous discussion can be applied to the relationship between PW and PRCP. On one hand, substantial moisture is a prerequisite for rainfall. On the other hand, precipitation reduces liquid-phased moisture that is transformed from water vapor in troposphere, which directly results in a decrease of PW. However, the latter effect becomes less significant than the former effect once positive feedback of the subsequent wet soil enhances PW through increased surface evaporation. Consequently,

precipitation on a monthly time scale tends to be positively coupled with PW at correlation coefficient equal to 0.34 (Fig. 4.1.(c)), which is significant at the 99% level.

The results of Fig. 4.1 suggest that thermodynamic characteristics and changes in convective instability are significant to the interannual variability of summer precipitation not only in tropics but also in Texas. Monthly mean precipitation in summertime in Texas is modulated primarily by the amount of CIN rather than by that of CAPE or PW, which is consistent with Fu et al. (1999). Meanwhile, coupling between PRCP and CIN in July (-0.75) is stronger than in August (-0.61). The smaller correlation coefficient in August may be due to the more frequent occurrence of tropical disturbances. As mentioned previously, convective instability was not present in the two months out of the 56 months in August. Thus, for better quality of result, further analyses will focus on the month of July from now on.

Fig. 4.2 illustrates the relationships between precipitation and convective parameters in July. It is consistent with Fig. 4.1 in that PRCP is most coupled with CIN (-0.75), moderately with PW (0.43), and least with CAPE (0.33) with tighter relationships compared to those in Fig. 4.1. Here again, CIN and PW are significantly linked with precipitation at the 99% level, but CAPE is not. This is odd because a moderate coupling is found between CIN and CAPE (-0.62, not shown). The coupling between CIN and CAPE may be because both are greatly influenced by origin conditions of a parcel. Nevertheless, precipitation is tightly coupled with CIN and poorly with CAPE in Fig. 4.2. This implies that there is another factor(s) besides surface conditions

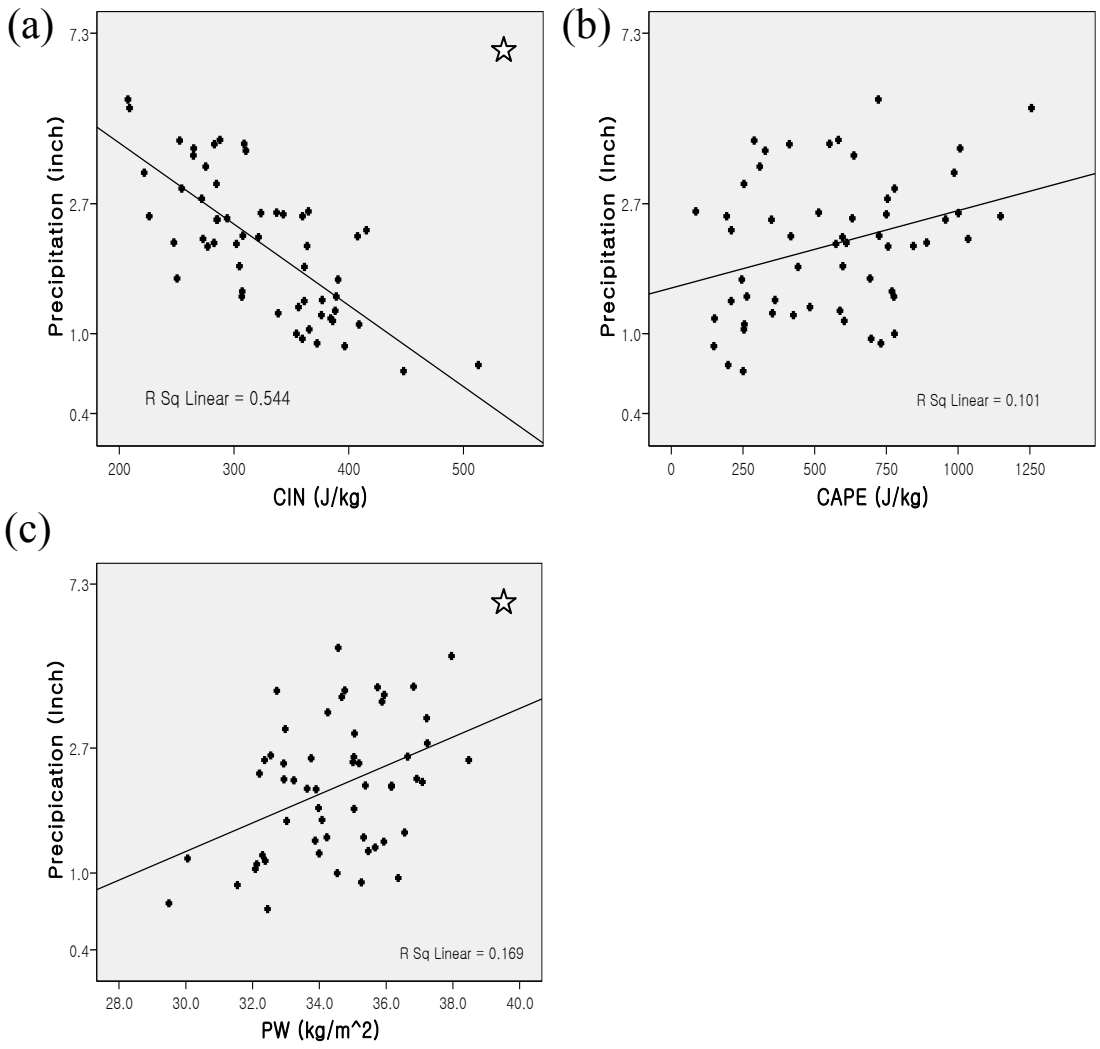

Fig. 4.2. Scatter plot between PRCP and a) CIN, b) CAPE, and c) PW only in July.

controlling CIN but not CAPE, and thereby exerting a strong influence on monthly precipitation. This will be discussed in the following section.

Variations in monthly mean precipitation can be caused by modification in the frequency of rainfall events, or in the intensity of rainfall per event, or a combination of both on a daily time-scale. CIN is likely to be associated with initiation convection (Mapes 2000). Reduced precipitation is expected to be due to a scarcity of convective rainfall events due to excessive CIN, due to reduced precipitation intensity per event, or due to both.

The fact that CIN is the most relevant convective instability parameter to July precipitation suggests that dry summer months in Texas are due primarily to the reduced number of rain days, or reduced frequency of deep convection, caused by increased CIN. To test this hypothesis, the probability distribution function (PDF) of daily July precipitation in Texas was investigated with respect to number of rain days and their average precipitation intensity. Rainy day is defined as a day which daily precipitation is greater than or equal to 1 mm. For each July, we calculated number of rain days and precipitation intensity, e.g. averaged rain amount per rain days, at each grid point. The two were then averaged over all the grid points in Texas to obtain July mean series for number of rain days (RD) and precipitation intensity (PI).

(a)

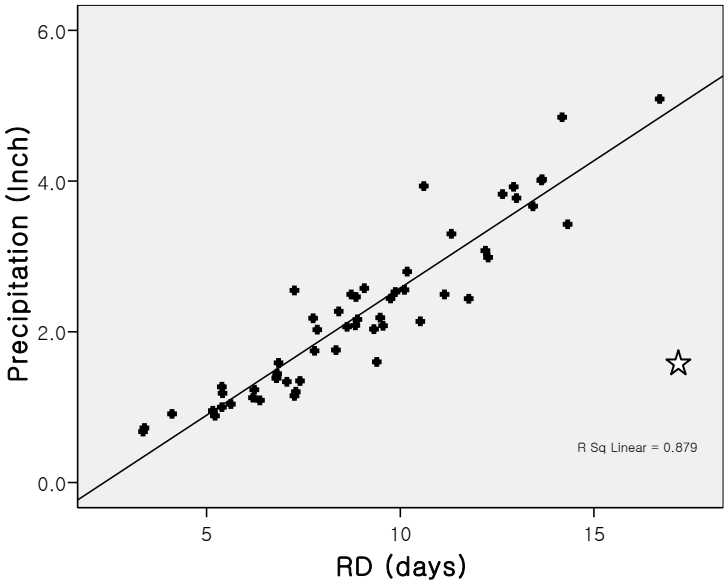

(b)

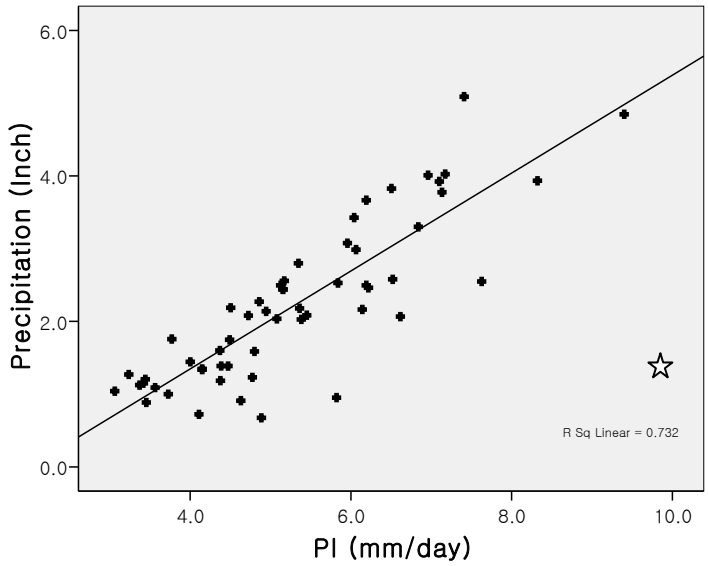

Fig. 4.3. Scatter plots between precipitation without the natural log transform and a) the number of rain days (RD) in natural log scale and b) precipitation intensity (PI).

Fig. 4.3 is a scatter plot of PRCP with RD and PI. Both RD and PI are significantly correlated with total precipitation (PRCP) at the 99% confidence level (0.94 and 0.81, respectively), and RD and PI are also positively coupled (0.65, not shown). This feature implies that dry (wet) months are caused by both fewer (more) rain days and lower (higher) intensity. Groisman et al. (1999) reported that an increase of both rain days and intensity was interconnected with an increase of summertime total precipitation in Norway (for the period 1900-1995), the USA and Australia (for the period 1910-1999). However, in Northeastern Italy, a negative trend observed in rain days was linked with an increase in rainfall intensity, which resulted in a weak reduction in total precipitation in winter and summer (Brunetti et al. 2001). In fall, decreasing trends were found in rain days, precipitation intensity, and total precipitation. However, long-term increasing or decreasing trends in the three variables do not necessarily correspond to the positive or negative relationships of their interannual variations. Our study shows that while less precipitation is correlated with fewer rain days and reduced intensity, the total precipitation is more influenced by the former in Texas in summertime.

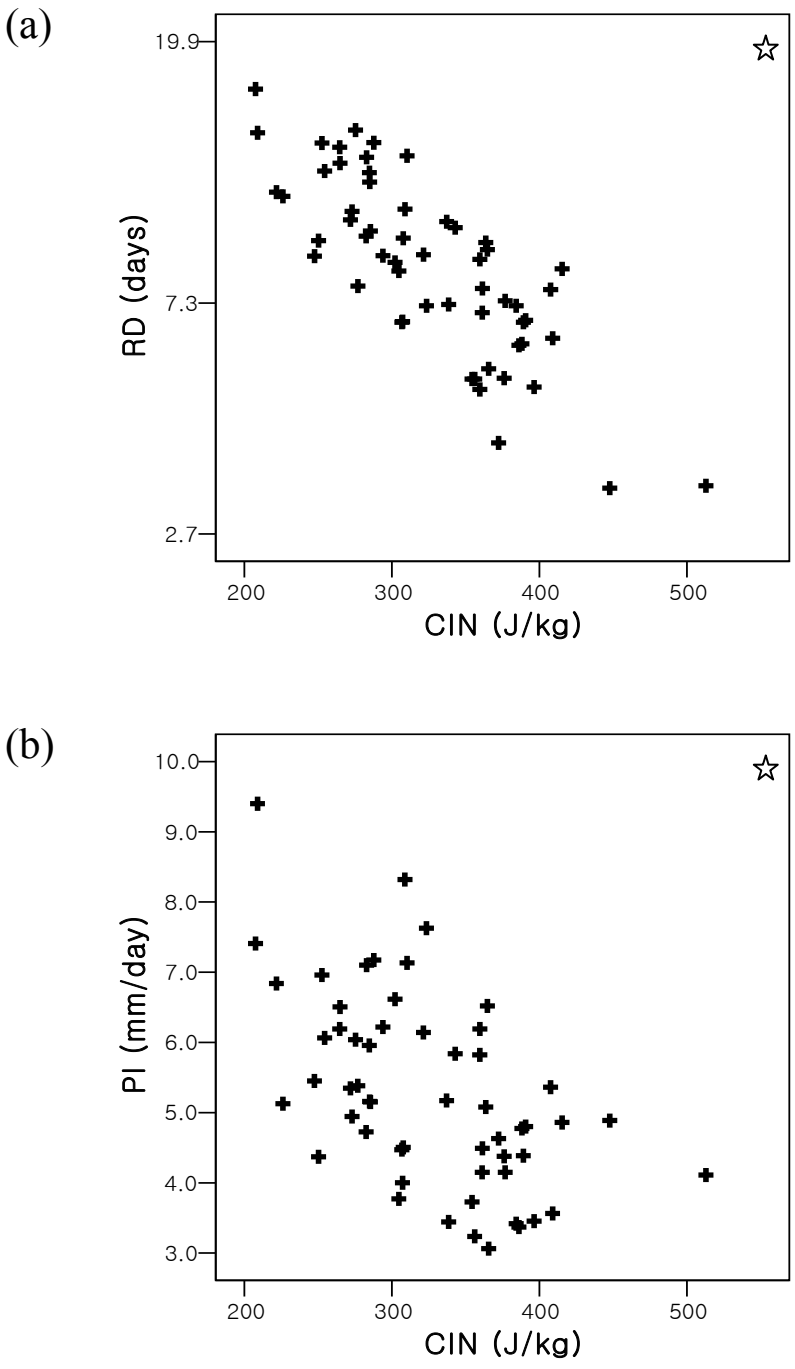

Fig. 4.4. Scatter plots between CIN and a) RD in natural log scale and b) PI.

Linkage of CIN with RD and PI is depicted in Fig. 4.4. While an increase of CIN is associated with a decrease both in rain days and intensity, stronger coupling of CIN with RD (-0.80) than with PI (-0.55) suggests that larger CIN tends to reduce number of rain days. Combining the results of Fig. 4.3 and Fig. 4.4, Fig. 4.5.(a) illustrates the correlation coefficients of CIN with RD, PI, and PRCP. Similar illustrations are shown for CAPE and PW as well. It seems that the tight coupling of CIN with PRCP (-0.75) is due to its strong correlation with RD rather than with PI. This is supported by comparison of Fig. 4.2.(a) to Fig. 4.4. CIN shows a more significant and stronger one to one relationship with RD (-0.80) than with PRCP (-0.75). For CAPE, although it is more tightly connected to PI than to RD, the magnitudes of the correlations are substantially smaller than to those of CIN (Fig. 4.5.(b)). PW does not seem to affect RD, PI, and PRCP as much as CIN does, either (Fig. 4.5.(c)). When one recalls that CIN is the energy needed to initiate convection, it seems plausible to conclude that CIN controls the number of rain days and the number of rain days affects the monthly precipitation.

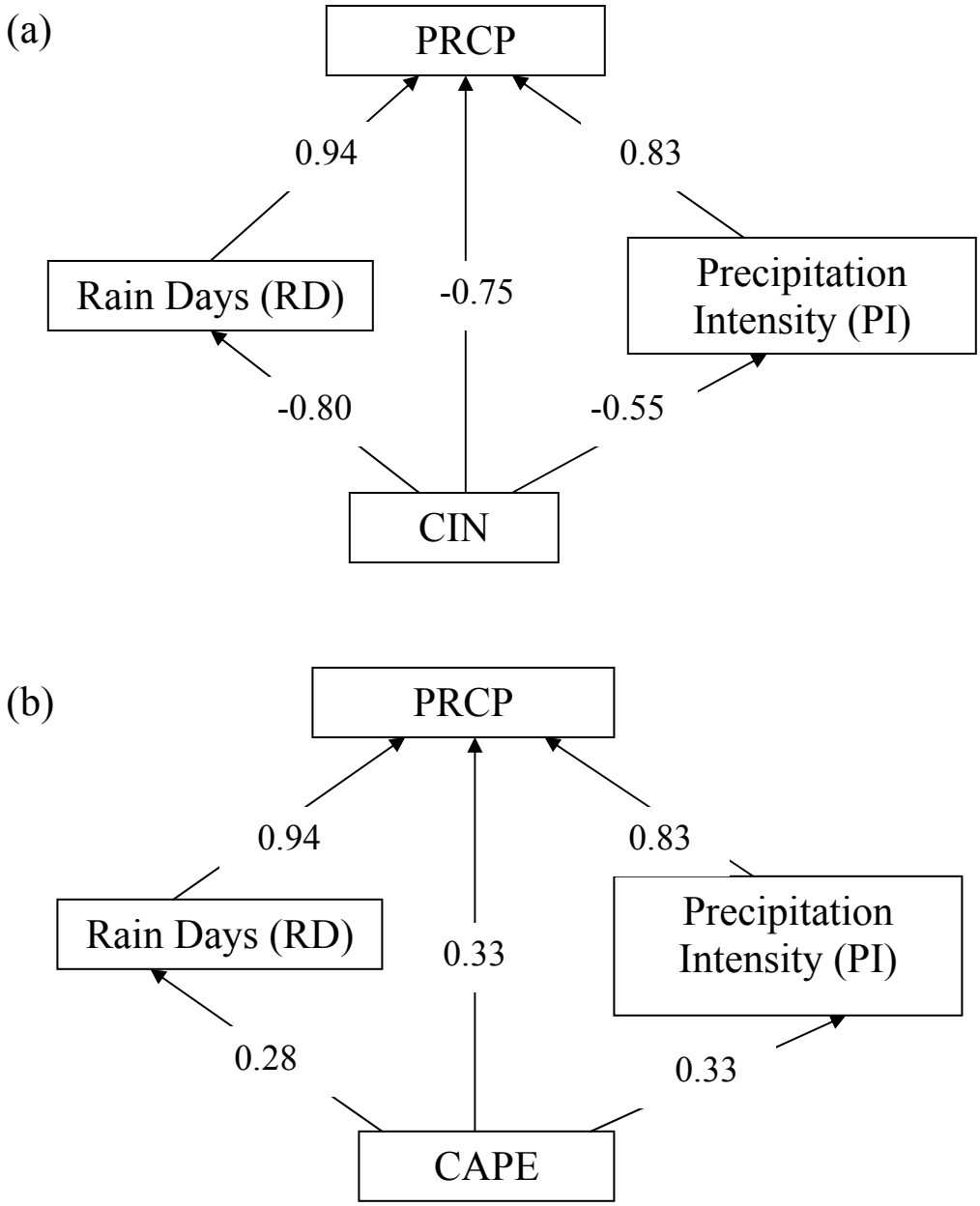

Fig. 4.5. Schematic illustrating correlation coefficients of a) CIN, b) CAPE, c) PW with RD, PI, and PRCP.

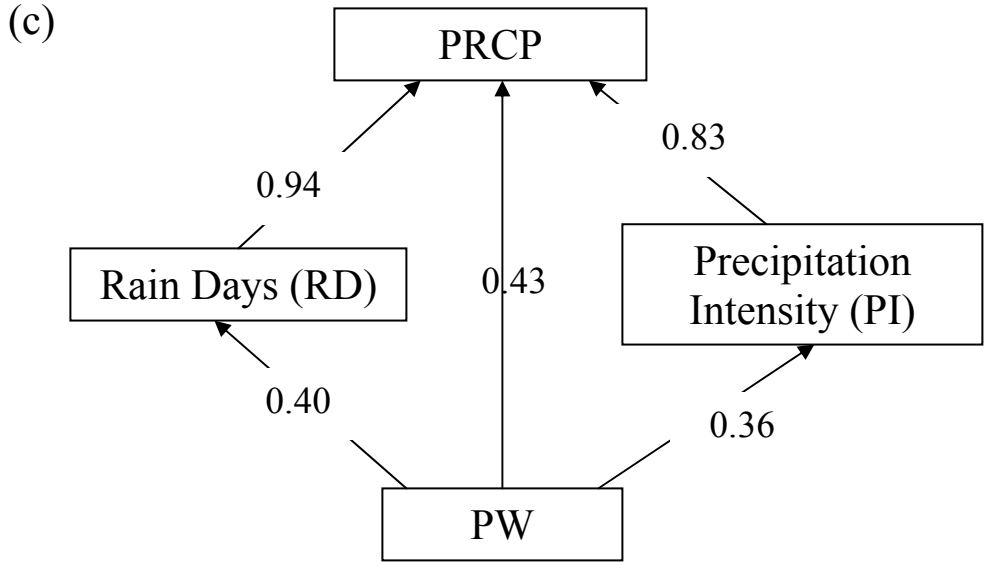

Fig. 4.5. (*Continued*)

B. Parameterization of CIN

Fundamentally, CIN is determined by surface temperature and dewpoint and the vertical temperature distribution, ignoring virtual temperature effects. Since the vertical temperature distribution is continuous, the estimation of CIN by one or two variables reduces the degree of freedom of the system. An effective simplification would be strongly correlated with the actual CIN and would identify the variables that have the most significant effect on CIN. The successful parameterization of CIN will lead us to investigate modulation of local land-surface processes and large scale circulations on those variables, CIN, and precipitation, which will be described in chapter V.

The parameterization of CIN also allows us to test the hypothesis that CIN is controlled by local surface-based variables that represents surface-based processes. If CIN is most efficiently parameterized by surface conditions, the hypothesis will be accepted. We assume that Tlt is an accurate proxy for the free-tropospheric temperature just below the LFC. Then, linear regression analysis on CIN with various combinations of independent variables using Ts, Td, and Tlt is employed, and the result is shown in Table 4.1. Among the univariate and bivariate predictors, (Tlt-Td) produces the closest fit to CIN while (Ts-Td) and the

Table 4.1. Results of linear regression analysis on CIN. Adjusted coefficient of determination (R_a^2), coefficients of each independent variable ($\beta_0, \beta_1,$ and β_2), multicollinearity (VIF), and significance (S) and insignificance (I) of the independent variable(s) at a 95% of confidence level.

Independent	R_a^2	β_0	β_1	β_2	VIF	Sig (95%)
Ts	.630	-982.4	46.7	N/A	N/A	S
Td	.580	1156.7	-44.2	N/A	N/A	S
Tlt	.238	-58.7	37.7	N/A	N/A	S
Ts-Td	.847	33.6	31.5	N/A	N/A	S
Ts+Td	-0.180	281.3	0.9	N/A	N/A	I
Tlt-Td	.951	774.2	48.5	N/A	N/A	S
Ts,Td	.845	-50.2	33.4	-29.8	1.23	S/S
Td, Tlt	.951	771.2	-49.2	47.1	1.02	S/S
(Ts-Td),Td	.845	-50.2	33.4	3.5	3.61	S/I
(Ts-Td),Tlt	.884	-108.2	29.3	16.1	1.21	S/S
(Tlt-Td), Ts	.951	840.3	50.5	-2.8	3.24	S/I

bivariate regressions including (Ts-Td) provide reasonably good approximations of CIN. The moist static energy approximated by (Ts+Td) estimates CIN poorly.

Before discussing how Tlt controls CIN, we want to validate our assumption: Tlt represents free-atmospheric processes. To test whether Tlt truly represents free-troposphere processes or is just a proxy for surface conditions in the context of CIN, we

used two linear regression models to see whether the departure of Tlt from that predicted by Ts is significant.

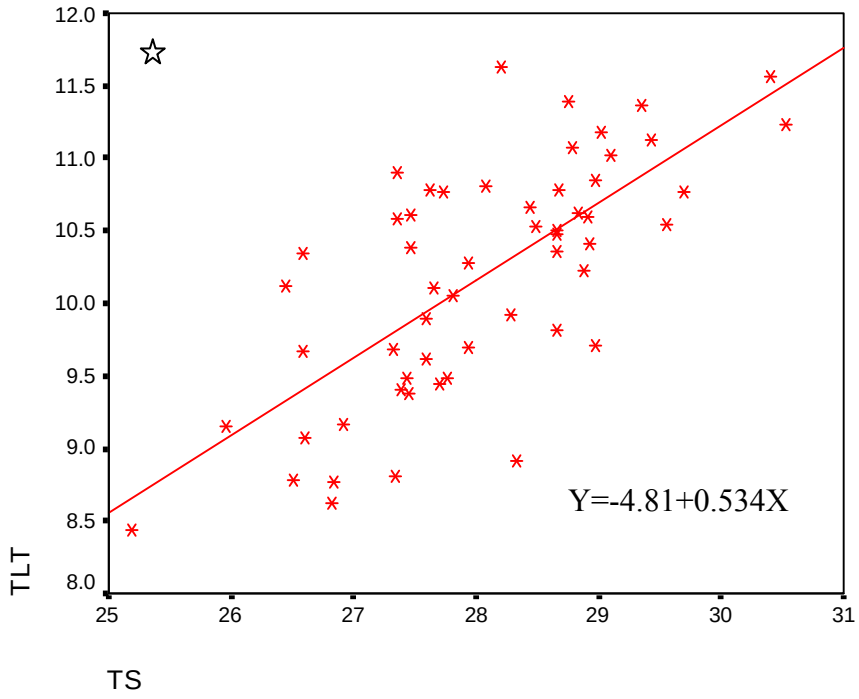

Fig. 4.6. Scatter plot between Ts and Tlt with regression line.

In the first model, Tlt^a is determined by first-order linear regression of Tlt on Ts (Fig. 4.6), i.e.,

$$T_{lt}^{a} = a + b * T_s, \quad \text{(a=-4.81 and b=0.534)}$$

where a and b are the intercept and the slope of regression equation, respectively. The corresponding lapse rate,

$$\Gamma_1 = \frac{-(a+(b-1)*Ts)}{\Delta P}$$ (K/mb) between surface and 700mb

is proportional to Ts. Then, LFC is also controlled by surface condition, Ts and Td, and the system determining CIN is closed by them.

In the second model, Tlt has two parts; one is T_{lt}^{a} that increases linearly with Ts and the other is a departure of Tlt from T_{lt}^{a}. The latter is the residual from the previous regression model (RES) defined as following:

$$T_{lt2} = T_{lt}^{\ a} + RES$$

$$= (a + b * T_s) + RES$$

$$RES = T_{lt2} - (a + b * T_s)$$

where the lapse rate,

$$\Gamma_2 = \frac{-(a+(b-1)*Ts+RES)}{\Delta P}$$ (K/mb) between surface and 700mb.

RES in this model allows influence of free-atmospheric processes on CIN, which is independent of heating within PBL. T_{lt2} is the observed temperature on 700 mb, Tlt, while T_{lt}^{a} is the predicted temperature from the surface temperature, Ts.

In the regression analysis for CIN, Ts and Td were used in the first model as independent variables while Ts, Td, and RES were used in the second model. Table 4.2 represents result of the linear regression analysis of the two models of CIN. The result of the first model has been already shown in Table 4.1, but, for convenience purposes, is repeated here.

Table 4.2. Adjusted coefficient of determination and mean square error of the two models.

Independent variable	Ra^2	MSE
Ts , Td	0.845	610
Ts, Td, RES	0.917	329

The second model improved predictability of CIN compared to the first model. In addition, the *f-test* suggests RES should be added in the model at a 95% confidence level (not shown). This result confirms that anomalous 700 mb temperature affects CIN independent of surface variables.

Fig. 4.7 illustrates the relationships between CIN, Td, Ts, Tlt, and SH. Tlt is coupled with CIN less tightly than are Ts and Td. Nevertheless, superior performance of the model employing (Tlt –Td) over (Ts-Td) as an independent variable emphasizes the independent significance of Tlt for determination of CIN. The result that low-tropospheric temperature as well as surface conditions have a significant impact on monthly convective instability and precipitation is unique, because previous studies have focused on the role of surface conditions on droughts (Namias 1982; Lyon and Dole 1995; Trenberth et al. 1996; Hong and Kalnay 2002; Sud et al. 2003).

Why does Ts play a secondary important role to control CIN compared to Tlt although it is tightly coupled with CIN? The answer is found in the physical relationship

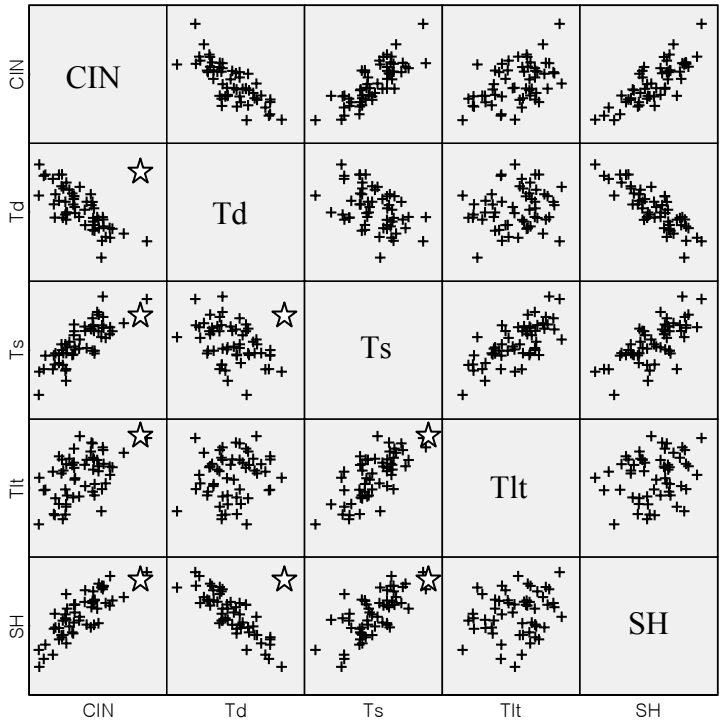

Td: surface dewpoint
Ts: surface temperature
SH: sensible heat flux
Tlt: temperature on 700 mb

Fig. 4.7. Monthly average scatter diagrams between CIN, Td, Ts, Tlt, and SH.

between Ts and Tlt. In Fig. 4.7, a tight relationship is found between Ts and Tlt (0.71), which indicates hotter 700mb as surface warms. Simultaneous warming at the surface and at 700 mb can be caused by anomalous heating of surface air so that the top of the PBL reaches up to 700 mb or by entrainment of anomalous warm low-tropospheric air into the ordinary PBL.

There is a distinct difference between these two processes although both result in a positive relationship between Tlt and Ts. Once the PBL develops and reaches 700mb, mixing tends to equalize potential temperature within the PBL, which will result in a tight positive relationship between Tlt and Ts. In this case, SH that determines PBL depth would be linked with Tlt as well as with Ts, which contradicts to the previous assumption that Tlt represents free-atmospheric processes. On the contrary, when the top of the PBL is lower than 700mb, air above the top of the PBL will still be entrained into the PBL. When warm air transport occurs aloft, entrainment of warm air into the boundary layer can cause an increase of PBL temperature and Ts. In the later scenario, surface temperature would be directly influenced by SH and indirectly by temperature above the top of PBL, but SH would not affect temperature above the top of PBL.

Therefore, the key is whether SH is linked with temperature above the top of PBL, represented by Tlt in this study. Reanalysis data set reveals that Tlt is weakly associated with SH (0.20) while correlations between Tlt and Ts and between Ts and SH are relatively strong (0.71 and 0.69), respectively (Fig. 4.7). This supports the hypothesis that coupling of Tlt with Ts is primarily due to the entrainment of 700 mb air, or air with similar thermodynamic characteristics to that at 700 mb into the ordinary PBL.

Employing linear regression analysis, we now test whether both Tlt and SH significantly contribute to the variation of Ts. Table 4.3 illustrates that Tlt and SH being mutually independent produce a much closer fit to Ts than either of Tlt and SH alone does, so that both significantly contribute to Ts.

Table 4.3. Adjusted coefficient of determination (R_a) of regression models on Ts employing Tlt and SH as independent variable(s).

Independent variable	R_a^2
Tlt	.489
SH	.463
Tlt, SH	.801

Although lack of samples may cause the poor correlation between Tlt and SH, this result is consistent with Stensrud (1993) who investigated the influence of elevated residual layers (ERLs) on surface boundary layer development. Using a simple slab mixed-layer model, he found that ERLs with a strong and shallow inversion at their base do not appreciably mix with the PBL, but ERLs with deeper inversion layer are likely to be rapidly entrained downward. One may ask why Tlt is not coupled also with Td when the entrainment of ERL air that is usually warmer and drier than the air within boundary layer is enhanced. However, temperature is nearly independent of dewpoint at 700 mb (not shown). Although 700 mb air is extremely warm and dry in certain months, the PBL

becomes dry only when the boundary layer develops quickly enough that the drying by entrainment is greater than the moistening by the surface moisture flux (Stensrud 1993).

Going back to the original question, why Tlt rather than Ts plays a critical role to determine CIN, we found that surface temperature, Ts, is affected by both temperature at 700 mb (Tlt) through entrainment and surface sensible heat flux (SH). In Fig. 4.7, SH is tightly linked with surface latent heat flux (LH) and Td through soil moisture (refer to chapter V). Since Tlt is independent of SH and Td, the variability of CIN is explained mostly by Td and the rest is explained by Tlt rather than by Ts.

Now, the rest of this section will be devoted to describing how low-tropospheric warming directly controls CIN. Fig. 4.8 shows a schematic illustrating how Tlt modifies CIN. The pressure depth between LCL and LFC, $P_{LCL-LFC}$, is defined as

$$P_{LCL-LFC} = P_{LCL} - P_{LFC,}$$

where P_{LCL} and P_{LFC} are the pressures at LCL and LFC, respectively. Wet-bulb depression, $T_{dpr,}$ increases (decreases) as dewpoint depression and LCL increase

(decrease). CIN is proportional to the area shaded in Fig. 4.8 that is determined by $P_{LCL-LFC,}$ $T_{dpr,}$ and vertical temperature profile from the surface to LFC.

Meanwhile, T_{dpr}* $P_{LCL-LFC}$ seems to be a good approximation of CIN. R_a^2 of the regression model of CIN using T_{dpr}* $P_{LCL-LFC}$ as a predictor is equal to 0.9. This suggests that CIN is nearly independent of details of the temperature profile between surface and LFC on a monthly time-scale. Therefore, changes in CIN may be estimated by changes in T_{dpr}* $P_{LCL-LFC.}$

As the moisture in the soil drops, atmospheric conditions also change, as indicated with dashed lines in Fig. 4.8. Decreased SM and increased Bowen ratio are generally associated with an increase of Ts (Ts′), a decrease of Td (Td′), and an increase of T_{dpr} (T_{dpr} ′) (Betts et al. 1996). While Tw is not affected by a change of the Bowen ratio, intensified development of the PBL and entrainment of drier air above the top of the PBL tend to cause a decrease of Tw (Tw′). As a result of the enhanced wet-bulb depression, the LCL increases (LCL′). The LFC also tends to increase (LFC′) due to the decrease of Tw and/or the warming in the lower-troposphere. If Tlt doesn't

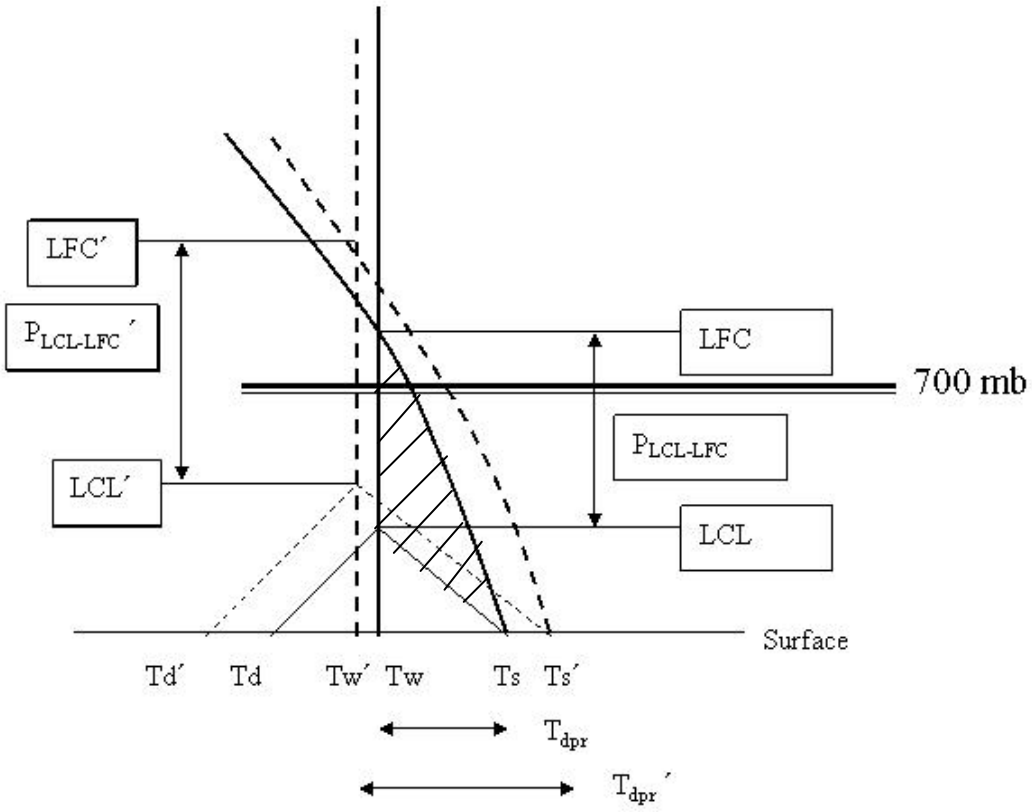

Fig. 4.8. Schematic illustrating increase of CIN associated with the increase of Ts and Tlt, and the decrease of Td and Tw in dry month. Thick lines show dry and moist adiabats.

correspond to the increase of Ts, e.g., is fixed, the LFC increase tends to be less but is still present due to the decrease of Tw. In this case, $P_{LCL-LFC}$ may decrease due to a greater increase of the LCL than the LFC. Thus, without low-tropospheric warming, the increase of CIN will not be as substantial.

Fig. 4.9 is consistent with the schematic. Elevation of CIN is accompanied by increases of both the LCL and the LFC. LCL is tightly linked with the surface variables, Ts, Td, and DP, but is not significantly correlated with Tlt. However, LFC has significant correlations with Tlt as well as with Ts, Td, and DP, indicating that the LFC tends to be influenced both by surface conditions and by the 700 mb temperature. Fig. 4.10 shows that $P_{LCL-LFC}$ is significantly sensitive to CIN and Tlt, but insensitive to Ts. This supports the idea that $P_{LCL-LFC}$ tends to be modified by Tlt rather than Ts although both LFC and LCL are influenced by Ts.

It is concluded that low-tropospheric warming as well as low surface humidity combine to result in extreme CIN. This can initiate and maintain summertime Texas drought. The regression model for PRCP indicates that about 54% of the interannual variation in precipitation is explained by (Tlt-Td). In the following chapter, we will investigate which local variables are tightly linked with Tlt and Td and what processes control them to modulate convective instability, mainly through CIN. Since Tlt is only weakly correlated with Td, factors and pathways controlling Tlt and Td will be examined separately.

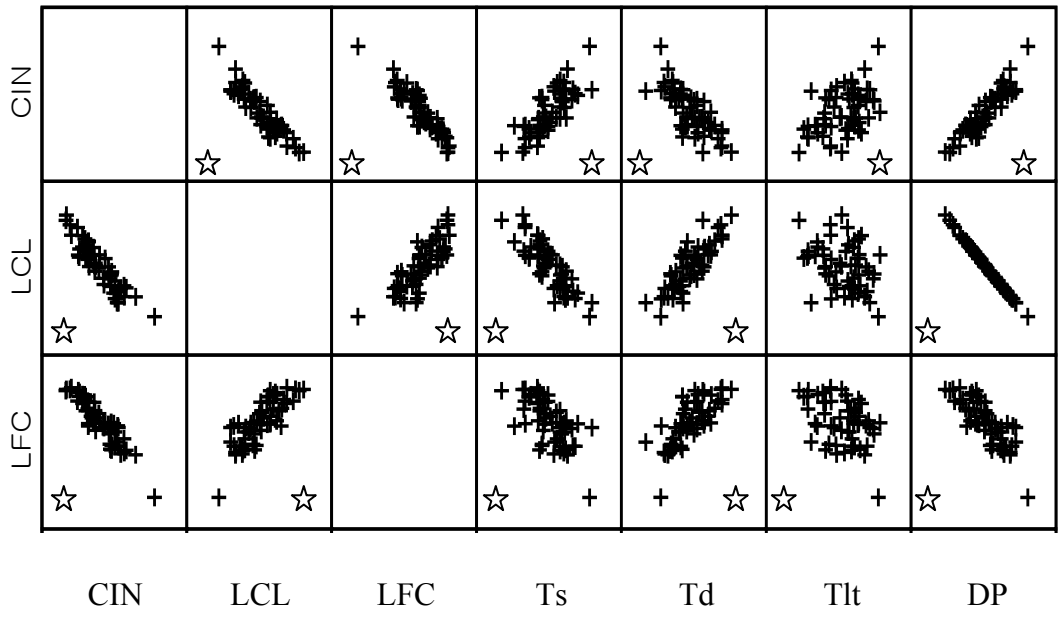

Fig. 4.9. Same as in Fig. 4.7 but among CIN, LCL, LFC, Ts, Td, Tlt and dewpoint depression.

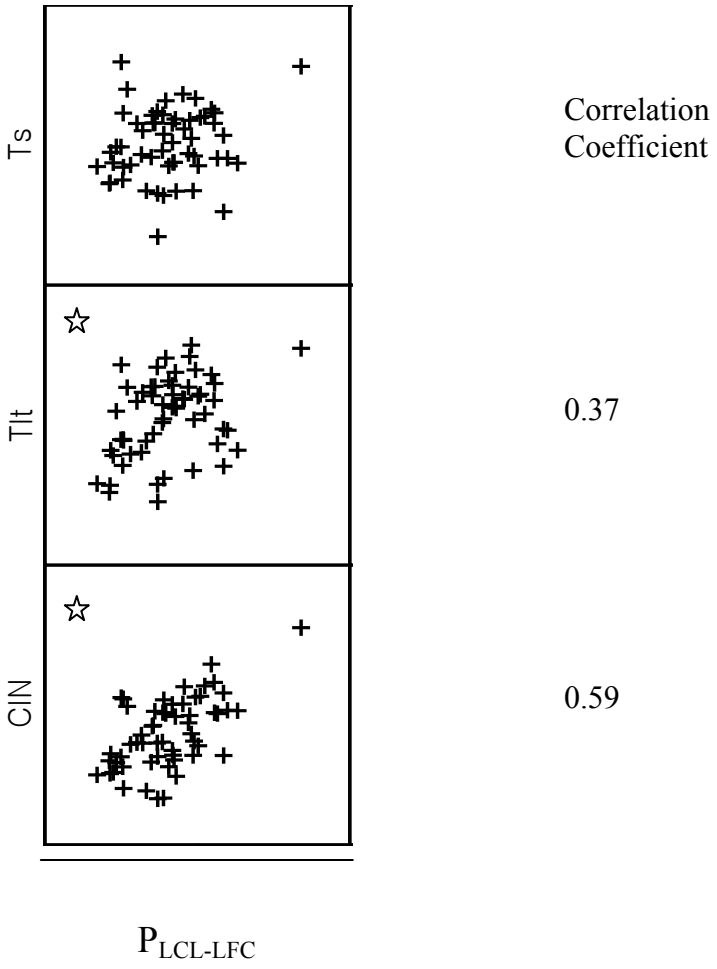

Fig. 4.10. Scatter plots between $P_{LCL-LFC}$ and a) dewpoint depression, b) Ts, and c) CIN with correlation coefficient.

CHAPTER V

IMPACT OF REDUCED SOIL MOISTURE AND WARM AIR TRANSPORT ON PRECIPITATION DEFICIT

A. Local atmospheric variables controlling the key parameters of CIN

To find processes modulating Td and Tlt, relationships of Td and Tlt with several surface variables (SM, SH, LH, and Ts) and tropospheric variables (ADV, DIV, MFD, and OMG) are shown in Fig. 5.1. The definitions of the variables are found in section III.B.2. Td is strongly coupled with those surface variables. These couplings are caused primarily by modulation of SM (Betts et al. 1996). There are two processes by which SM can affect Td through changing the surface heat fluxes. With an ample supply of soil moisture and associated increase in the Bowen ratio, surface evaporation LH is enhanced, which accompanies an increase of Td (direct effect). On the other hand, as SH decreases, reduced mixing of surface air with dry low-tropospheric air in PBL keeps Td from dropping substantially (indirect effect). Thus, both effects result in the increase of Td when rainfall enhances SM, which is consistent with the high correlation coefficients between Td and SH (-0.85) and between Td and LH (0.85) in this study.

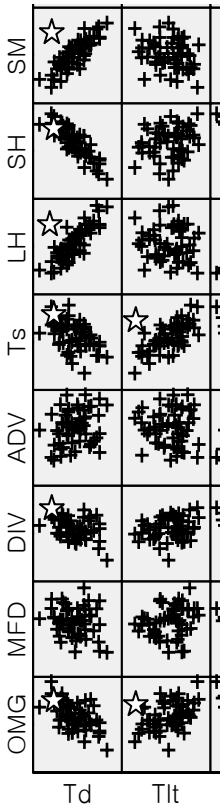

ADV: advection term of moisture flux divergence
DIV: divergence term of moisture flux divergence
MFD: moisture flux divergence
OMG: vertical motion
Tlt: temperature on 700 mb
SM: soil moisture
SH: sensible heat flux
LH: latent heat flux
Td: surface dewpoint
Ts: surface temperature

Fig. 5.1. Same as in Fig. 4.7 but between Td and Tlt and the surface and tropospheric variables.

Td is moderately linked with OMG (-0.55) but it is linked with DIV (-0.35) with a marginal significance at the 99% level. Since OMG does not influence Td directly, Fig. 5.1 suggests that surface processes associated with soil moisture are the primary modulators of Td dominantly, which will be discussed in detail in the following section.

In contrast, Tlt is rarely linked with the surface variables except with Ts (0.71). The linkage with Ts was found to be due to the entrainment of free-atmospheric air into the PBL. Tlt is significantly coupled with OMG with a positive relationship: downward (upward) motion is associated with high (low) Tlt. Since warm air tends to ascend due to the buoyancy, the positive relationship between Tlt and OMG implies that OMG is the cause and Tlt is the effect. In other words, subsidence can cause low-tropospheric warming, which increases CIN resulting in precipitation deficit. However, the correlation coefficient between Tlt and OMG is 0.45, which is only marginally significant at the 99% confidence level. This implies that there might be other processes besides subsidence that lead to warming at 700 mb.

In this section, it was found that Td is tightly coupled with SH, LH, and SM. This implies the existence of strong couplings among the surface variables through soil moisture. Soil moisture regulates the Bowen ratio that significantly controls Ts, Td, and DP. Therefore, it is expected that soil moisture content plays a critical role to modify CIN through Td and thereby affect precipitation. Section V.B will be devoted to describing surface processes controlled by soil moisture and their influences on precipitation.

On the other hand, Tlt is linked with OMG. OMG seems to influence Tlt but their correlation coefficient (0.45) is not large suggesting there would be other mechanisms controlling Tlt. Those mechanisms will be investigated in section V.C.

B. Soil moisture, CIN, and precipitation

Fig. 5.2 shows relationships of the surface variables and PRCP. Each surface variable except θe exhibits a significant link with PRCP as well as with SM at the 99% confidence level. (Hereafter, the surface variables refer to SH, LH, Td, Ts, and DP excluding θe). The relation of the surface variables with PRCP resembles that with SM, but with opposite signs and smaller correlation coefficients, except that the correlation coefficient of Ts with PRCP is as much as that with SM. These features indicate significant influence of rainfall on the surface variables through controlling SM on monthly time-scale.

Now, we will discuss how soil moisture content affects each surface variable from theoretical aspects in literatures and to applying them to our results. Once rainfall occurs, SM increases immediately. It is known that the partitioning of the excess of net radiation onto the surface into SH and LH (described by the Bowen ratio) is controlled by the availability of water for evaporation (Betts et al. 1996). On the other hand, SM influences surface albedo as well. Consequently, wet soil tends to enhance LH and to

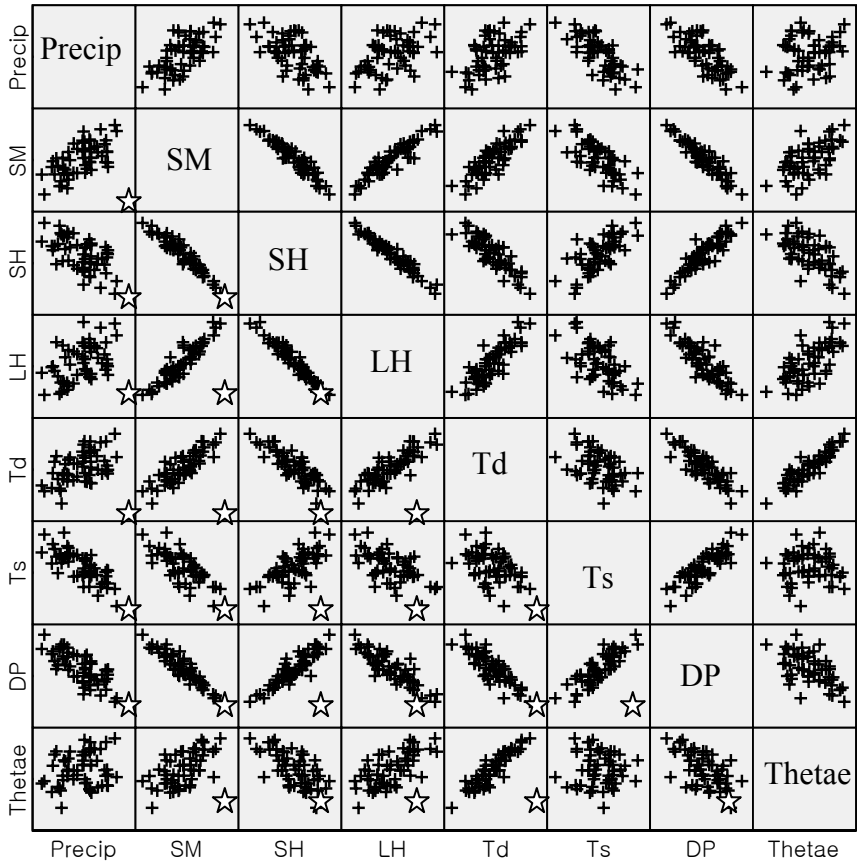

SM: soil moisture
SH: sensible heat flux
LH: latent heat flux
Td: surface drewpoint
Ts: surface temperature
DP: dewpoint depression
Thetae: surface equivalent potential temperature

Fig. 5.2. Same as in Fig. 4.7 except between CIN, precipitation, and the surface variables in Texas.

reduce SH and surface albedo. For Td, the direct effect (increase in LH) and indirect effect (decreases in SH) of SM result in their strong relationship, as described previously.

For Ts, the influence of SM on that is rather complicated. Changes in soil moisture influence not only the Bowen ratio but also the surface albedo (Betts et al. 1996; Findell and Eltahir 1999). Wet soil results in a decrease of surface albedo, which leads to increasing solar radiation into the surface. In addition, increase of longwave back radiation from the low-troposphere to the surface due to the increased evapotranspiration and greenhouse gas effect of water vapor results in an increase of net terrestrial radiation (Eltahir 1998; Schar et al. 1999). With respect to surface energy balance, this should be compensated by an increase in outgoing longwave radiation and/or in total surface fluxes (the sum of SH and LH) on the surface. While Charney (1975) asserted vertical motion in the troposphere acts to oppose the change in net terrestrial radiation, with subsidence for net cooling by increased albedo associated with dry soil, the atmospheric responses to surface radiative warming in the subtropics remain under debate (Charney 1977; Reiply 1976). If the increase of net terrestrial radiation results in enhanced surface fluxes with constant Bowen ratio, it will result in elevation of Ts. However, the negative correlation between SM and Ts (Fig. 5.2) means that the decrease of Ts accompanied by a decrease of Bowen ratio prevails over the increase of Ts accompanied by a decrease of albedo when SM increases.

Couplings of Ts are not as tight as those of Td with SM, SH, and LH, which implies the existence of significant factors controlling monthly mean surface temperature other than soil moisture. One of them is the entrainment of free-atmospheric

air into the PBL, as discussed in the previous section. We showed that 80% of the variation in Ts is explained by Tlt and SH. Cloud effect and feedback may be important (Bony et al. 2006). Although Lyon and Dole (1995) pointed out that no change in net terrestrial radiation is likely to occur because of enhanced cloudiness and reduced incoming solar radiation into the surface as soil moisture increases, the modulation of surface radiation budget and surface temperature by clouds is very complicated. The influence of the change in the radiation budget on surface temperature depends on cloud amount and optical properties for both short and longwave radiation so it remains quite uncertain (Stephens and Webster 1981; Woodhouse and Overpeck 1998).

The last two variables, DP and θe, are associated with the difference and sum of Ts and Td, respectively. An increasing tendency of Td and decreasing tendency of Ts in association with increasing SM implies a decrease in dewpoint depression. This explains the negative relationship between SM and DP in Fig. 5.2. According to the definition of θe in chapter III, at constant pressure, θe is proportional to $(T + \frac{l_v}{c_p} r)$. The latter in turn is determined by Ts and Td since a larger mixing ratio, *r*, implies a greater Td. Due to the opposite response of Ts and Td to SM change, the response of θe to SM is not as simple as that of DP to SM.

Increased LH and decreased SH causing increase of Td and decrease of Ts affect θe not directly but indirectly: they reduce entrainment of drier free-troposphere, which results in elevation of Td as well as θe. Increase in Ts by itself would lead to increase in θe, so the natural positive correlation between Ts and θe exists. However, indirect effects of wet soil increase θe despite decrease in Ts. This mechanism is consistent with the

positive relationships of θe with Td (0.91) and with SM (0.61) and a weak relationship between θe and Ts (-0.03) in Fig. 5.2.

Due to the opposed influences of Ts and Td associated with SM on θe, θe is not tightly correlated with soil moisture as much as other surface variables are, and it is poorly coupled with PRCP, while DP is tightly related with SM and precipitation. Similar results were found in Findell and Eltahir (1999) who examined physical pathways linking soil moisture to subsequent rainfall in summer Illinois. Our result using reanalysis data in Texas are consistent with theirs using observational data in Illinois.

Until now, we have focused on the responses of the surface variables to enhanced SM from rainfall. In contrast, when precipitation deficit is prolonged, dry soil condition influences the surface variables in the opposite direction. Decreased moisture content in soil leads to an increase in the Bowen ratio as well as enhanced surface albedo. Changes of the surface heat fluxes directly and indirectly affect Td. Reduced surface evaporation by decreased LH and enhanced PBL mixing by increased SH both induce decreases in Td. While increased albedo results in a decrease of net terrestrial radiation, increasing SH induces elevation of Ts. Correspondingly, the dewpoint depression is enhanced and θe is reduced. The processes in dry months are consistent with the relationships of SM with the surface variables observed in wet months.

Tight relationships among the surface variables likely originate from the strong interactions between the surface and the atmosphere of the planetary boundary layer (PBL) through feedbacks between soil moisture and precipitation (Betts et al. 1996; Koster et al. 2004). Koster et al. (2004) emphasized the strong coupling between soil

moisture and precipitation over the south-central US as well as the Sahel, equatorial Africa, and India from the ensemble simulations of 16 AGCM models although only half of the models show a statistically significant coupling strength.

So far, we have discussed how rainfall influences the surface variables through changing soil moisture content on a monthly time scale. It is for this reason that magnitudes of the correlation coefficients of the surface variables with SM are greater than those with precipitation. Are these couplings between precipitation and the surface variables entirely due to the response of soil moisture to rainfall? While Koster et al. (2004) pointed out that the impact of SM on precipitation is much weaker than the other direction of causality, several studies shed light on the existence of a positive feedback of soil moisture on subsequent rainfall (Eltahir 1998 and Findell and Eltahir 1997, 1999). If rainfall influences soil moisture without a feedback, the positive correlation coefficient between soil moisture and subsequent rainfall can not be greater than the serial correlation coefficient of rainfall. Findell and Eltahir (1997) showed that the former is greater than the latter using 21-day mean soil moisture and rainfall in summertime Illinois.

Correlation coefficients between PRCP, SM, and CIN are represented in Fig. 5.3. While the coupling between PRCP and SM (0.66) suggests nothing about the causality between the two, it was inferred that precipitation influences the surface variables through changing soil moisture due to the higher correlation coefficients of the surface variables with SM than with PRCP. However, the existence of an impact of soil moisture on precipitation is suggested implicitly in the correlation coefficients in Fig. 5.3. First, it

is assumed that SM affects CIN causing the correlation coefficient of -0.85, which is supported by the fact that Td is the most critical parameter for CIN. Then, analogous with Findell and Eltahir (1997), if PRCP influences CIN through SM and the surface variables without a feedback, the magnitude of the correlation coefficient of PRCP with CIN (0.75) should be less than that with SM (0.63), but it is not. Therefore, there seems to be a direct connection between PRCP and CIN. As discussed in the first section of this chapter, the negative correlation between PRCP and CIN is because CIN controls precipitation in that convection and precipitation does not inevitably occur until CIN is first removed. Therefore, CIN is greatly influenced by the surface thermodynamic characteristics that are controlled by soil moisture, which controls precipitation. The correlation coefficients in Fig. 5.3 implicitly imply the existence of the response of precipitation to soil moisture (i.e., feedbacks of soil moisture on precipitation) in the context of CIN.

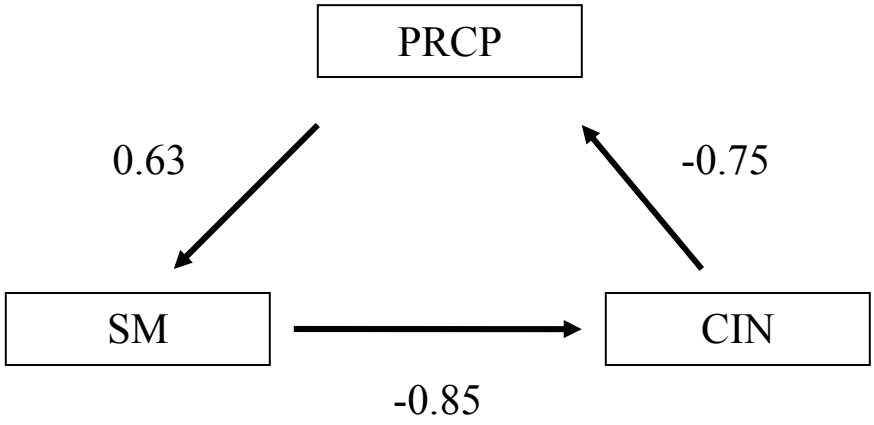

Fig. 5.3. Schematic diagram representing correlation coefficients between PRCP, SM, and CIN.

As a summary, tight couplings among SM, SH, LH, Td, Ts, and DP in Fig. 5.2 emphasize the strong land-atmosphere interaction in Texas in summertime. As previously shown, precipitation affects soil moisture and the latter plays an important role in controlling the surface variables and CIN by acting like a reservoir of water. Through modulating the surface variables (especially Td) and CIN, it is likely that soil moisture gives feedback on precipitation. The two processes would result in strong links of precipitation with CIN as well as with soil moisture.

C. Causes of low-tropospheric warming

In the previous chapter, it was concluded that low-tropospheric temperature as well as surface moisture content act as significant modulators of CIN. Since correlation analysis of Tlt with atmospheric variables showed that Tlt is not affected by surface-based processes, it is still an open question what causes warming in the low-troposphere. In this section, we will investigate dynamic and thermodynamic processes associated with warming at 700 mb.

1. Modulation of temperature at 700 mb

Previously, it was shown that Tlt is not influenced by PBL processes; Ts does not influence Tlt but is affected by it through entrainment of air into PBL. This implies that local drought feedback to the atmosphere by reduced soil moisture and increased sensible heat flux (SH) would not affect the thermodynamic state at 700mb. Without advection, local downward motion and radiative cooling must be in equilibrium, which is often observed in the clear sky regions of the tropics (Gray 1973; Gray and Jacobson 1977). When adiabatic heating in the low-troposphere by subsidence is followed by radiative cooling, it also results in drying in the low-troposphere when convection is inhibited. Since water vapor leads to longwave radiative cooling in troposphere (Manabe and Strickler 1964), a drier troposphere would induce less longwave radiative cooling

and consequent warming. Therefore, if strong descent and the modified radiative properties of a drier atmosphere bring on an increase of Tlt, downward motion and/or low specific humidity at 700 mb should be associated with high Tlt. However, as mentioned previously, OMG accounts for only around 20% of the interannual variability of Tlt and specific humidity at 700 mb is nearly independent of Tlt in this study. Therefore, vertical motion is not primarily responsible for the temperature variation at 700 mb.

Meanwhile, advection of warm air into a region can cause warming at 700 mb as well. Warm (cold) temperature advection refers to the tendency for a temperature increase (decrease) at a specific location caused by movement of air blowing from a warmer (colder) area. However, a noteworthy poor correlation is found between temperature advection and Tlt (not shown). This occurs when temperature advection is computed using either monthly mean or 6-hourly temperatures and winds. Their poor correlation may be due to a time lag between the temperature advection process and actual tendency of temperature change at a specific area. In addition, since temperature advection occurs only when there is a temperature difference between two regions, it is unable to account for a temperature maintained by air flow from a pseudo-permanent heat source or sink. Thus, examination of the correlation between Tlt and temperature advection may fail to identify a heating source on the periphery of Texas that controls the variability of Tlt.

(a)

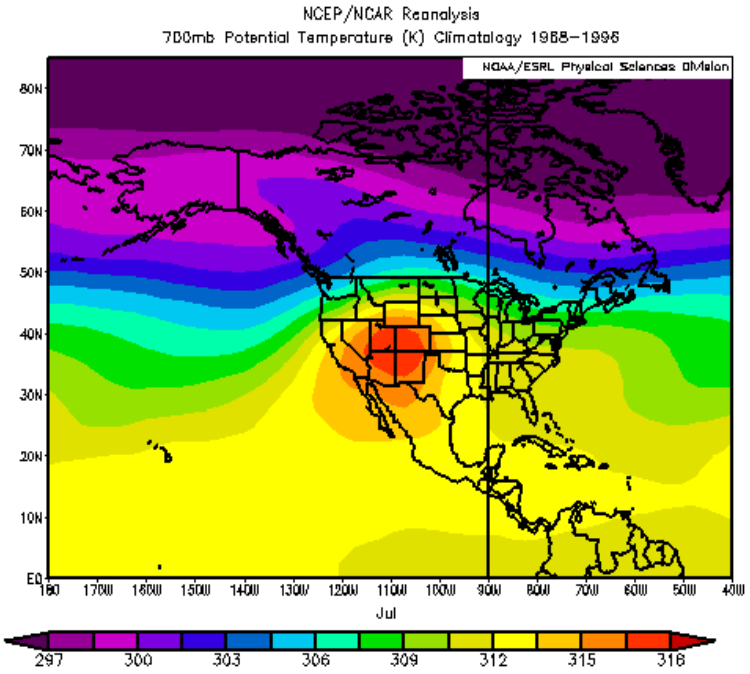

(b)

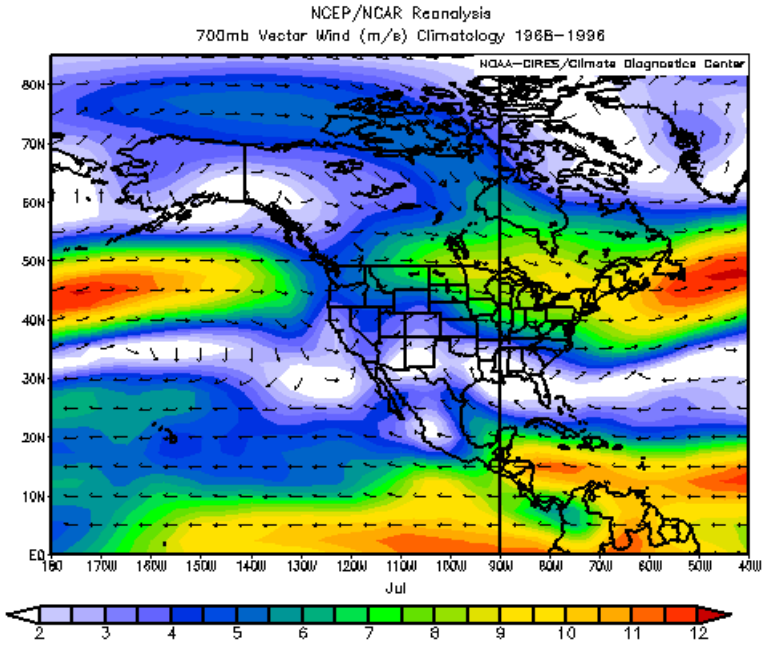

Fig. 5.4. Climatological 700 mb a) potential temperature (K) and b) wind vectors and speed (m/s) for 1968-1998.

The long-term means of potential temperature and vector winds at 700 mb for July 1968-1998 are illustrated in Fig. 5.4.(a) and 5.4.(b), respectively. Fig. 5.4.(a) features a latitudinal temperature gradient to the north and a relatively warm (cold) atmosphere over land masses (oceanic regions). It also shows a warm region over the high terrain to the west of Texas that is affected by surface diabatic heating. Meanwhile, south-easterlies from the Gulf of Mexico or Caribbean are dominant in Texas (Fig. 5.4.(b)) while south-westerlies prevail in Arizona and New Mexico. The former is cooler and more humid than the latter.

Although cool and moist south-easterlies are dominant at 700mb in Texas as seen from the climatological flow pattern in Fig. 5.4b, anomalous changes in wind direction may have a major impact on Tlt. For example, a switch from south-easterlies to westerlies in Texas during the warm seasons might be expected to cause significant increase in Tlt. This speculation motivates us to examine the influence of upstream thermodynamic characteristics on Tlt. In the rest of the chapter, we investigate whether the origins or directions of air entering Texas vary interannually and, if so, whether they affect Tlt.

2. Impact of warm air transport on temperature at 700 mb

To investigate the influences of upstream air on Tlt, we used back trajectory analysis using the Green's functions of the mass continuity equation for a conserved

tracer substance. The trajectory model was kindly provided by Dr. Kenneth Bowman of Texas A&M University. Detailed information and discussions are found in Bowman and Carrie (2002) and Bowman and Erukhimova (2004). Winds are from the NCEP/NCAR reanalysis. They are interpolated to the particle locations linearly in both space and time. Trajectories for a rectangular region containing the state of Texas (104~95W and 28~35N) are computed. Particles are initialized on a regular latitude-longitude grid with 0.25° X 0.25° spacing at 700 mb, which gives 1073 particles total. Trajectories are initialized each day at 18Z at the grid locations and run 4, 8, and 12 days backward for every day in July from 1948-2003. A set of 1736 (31days X 56 years) trajectories is provided for each grid point.

Fig. 5.5 shows origins of 8-day back trajectory analysis. Most parcel origins are from oceanic regions to the east including the Caribbean Sea and the subtropical Atlantic (eastern origins), but other parcels originate over the north-eastern Pacific, the south-western US, and the Gulf of California to the west (western origins).

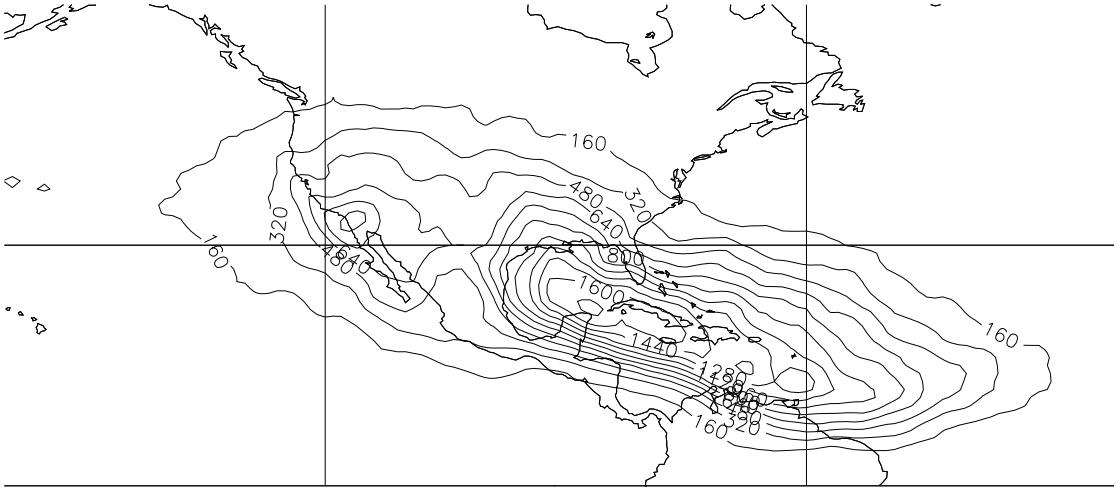

Fig. 5.5. Origins of 8-day back trajectory. The contour interval is 160 per unit area (1°X1° grid box) for 1073 particles during 1736 (31days *56 years) days.

Recalling the high potential temperature region to the west of Texas, first we test whether there are specific origins favoring extremely high destination temperature (DT, which refers to 700mb temperature of a particle in Texas) and thus, whether the number of particles originating over this region controls Tlt. From the PDF of DT for July for 1948-2003, particles with the highest and lowest 20% DT (warm particles and cold particles, hereafter) were selected. Then, their origins were computed and are illustrated in Fig. 5.6. The warm particles (Fig. 5.6.(a)) are associated with mostly western origins although some of them come from the eastern origin areas. In contrast, most of the cold particles come from the eastern origins (Fig. 5.6.(b)). Note that origins of the warm and

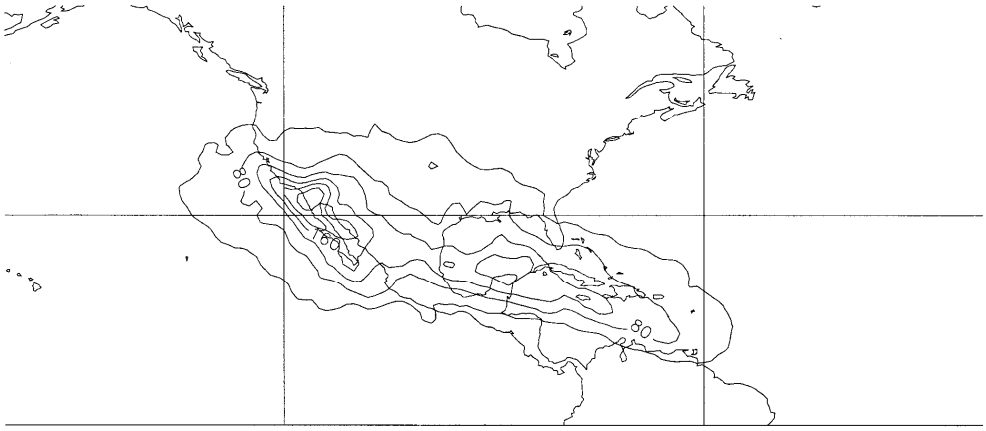

(a)

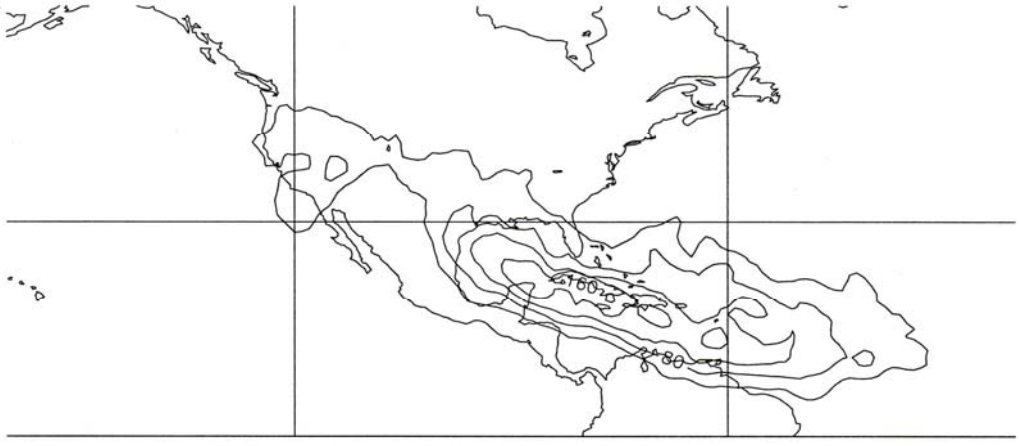

(b)

Fig. 5.6. Origins of a) the warm particles and b) the cold particles.

cold particles vary in location and intensity interannually and Fig. 5.6 represents the cumulative pattern over 56 years.

To examine whether the western origins preferentially produce warm particles, first, at each 1°X1° grid box, the number of cases that warm particles originate in the grid point was counted, and the same for the cold particles. Second, the ratio of warm cases to the total (warm and cold) cases (hereafter, "warm ratio") was computed at the each grid box and illustrated in Fig. 5.7. The warm ratio varies from 0 to 1 and values above 0.5 mean that warm particles are more likely than cold particles. As expected, the western (eastern) origins are associated with a higher (lower) warm ratio. Values of warm ratio greater than 0.6 are found in the south-western US, western Mexico, and the eastern subtropical and tropical Pacific, while those less than 0.4 extend to the North Pacific, southern Canada, and the tropical and subtropical Atlantic.

The definition of the warm ratio was based on the relative prevalence of warm particles to cold particles, referring to the highest and lowest 20 % DT. Now, we want to examine whether the concept of the warm ratio is relevant to all particles as well as the particles with the highest and lowest DT. For all the particles (1073 particles * 31 days * 56 years), we compute the fraction of particles emerging from areas of warm ratio exceeding a certain threshold (ranging from 0.1 to 0.9) for each year and then calculate its correlation coefficient with Tlt.

Fig 5.8 represents these correlations. The strongest correlation, 0.58, occurred with the threshold at 0.5. Regions with the warm ratio greater than 0.5 include the high

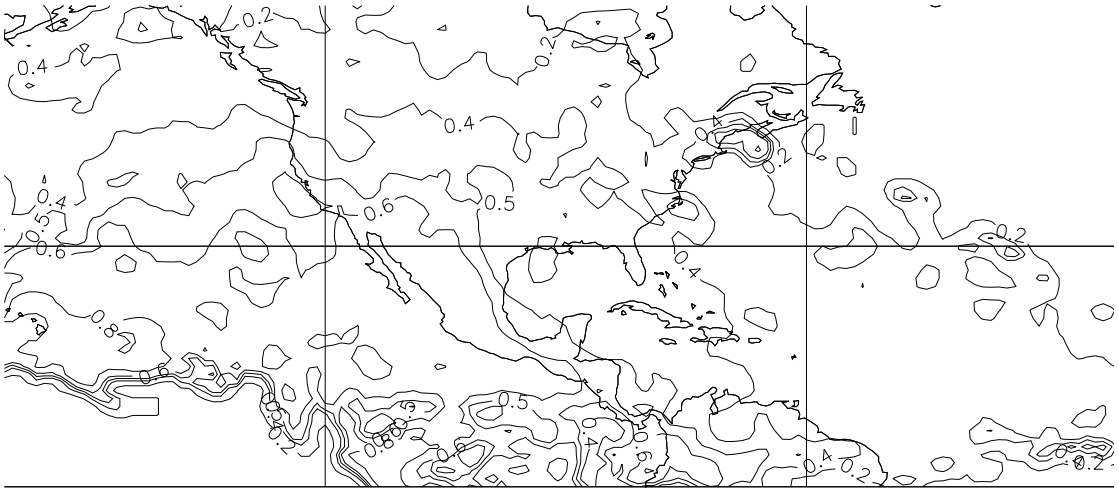

Fig. 5.7. Map showing the warm ratio.

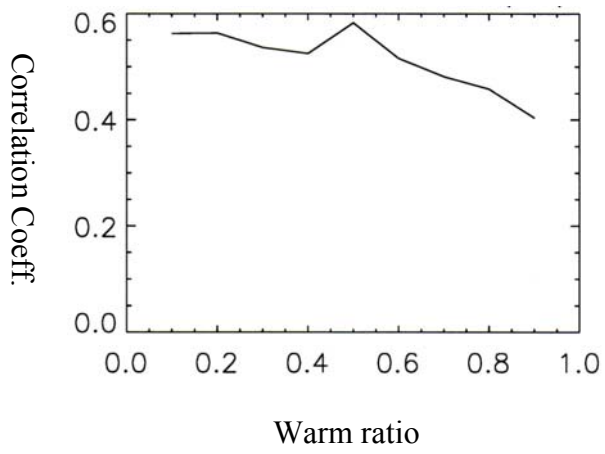

Fig. 5.8. Correlation coefficient of Tlt with the warm ratio.

terrain over the Rocky Mountains and Mexican Plateau, while they exclude the Caribbean and Atlantic where the cold particles emerge. This result indicates that the origins where the warm ratio is greater than 0.5 seems to generate warm particles preferentially and affect Tlt. However, commensurately high correlations (0.56) also correspond to thresholds of 0.1 and 0.2. Those regions cover most of the origin region, indicating that separation of warm origin favoring warm particles from cold origin favoring cold particles is not ideal to find origin regions that strongly control Tlt.

This failure is, first, due to the fact that the origins of the highest 20% DT are not separated geographically from those of the lowest 20% DT (Fig. 5.6). This failure, second, is likely to happen because the warm ratio significantly varies interannually in terms of locations. Recall that Fig. 5.6 represents the cumulative feature of the origins of the highest and lowest 20% DT for 56 years. We performed the same analysis for the highest and lowest 10% and 50% DT, respectively, but none of them satisfied our expectation.

Nevertheless, the fact that high correlation coefficients were found suggests that influences of diabatically heated area to the west of Texas are related with Tlt somehow. If particles are heated over this region, paths rather than origins of particles may be more significant for affecting Tlt. Motivated by this, we conjecture that the ratio of particles that pass over the high terrain to the west of Texas may modulate Tlt due to diabatic heating. According to Lanicci and Warner (1991), the elevated mixed layer (EML) that develops over the high terrain of the Mexican Plateau and Rocky Mountains tends to induce a capping inversion and suppresses of convection over the south-central US in

spring and early summer. EMLs are generated when the warm air in a boundary layer over elevated terrain loses convective contact with the ground as it travels to the east over lower terrain above a moister and cooler air stream from the Gulf of Mexico, causing a capping inversion. Deep and strong capping inversions tend to suppress convection instantaneously. In addition, on the longer timescale, they may cause elevation of CIN not only by elevating low-tropospheric temperature but also by influencing the thermodynamics of the boundary layer.

Since an EML occurs most frequently from Apr to Jun in Texas, it is anticipated to influence the frequency and intensity of convection in July as well. Therefore, we hypothesize that the ratio of particles experiencing diabatic heating over the regions with high surface potential temperature in the Rocky Mountains and the Mexican Plateau regulates Tlt. The geographical distribution of the 12-day back trajectory origins is very similar to that of the 8-day origins (Fig. 5.5) with slightly wider range to the east and west (Fig. 5.9). Although diabatic heating regions over the Rocky Mountains and Mexican Plateau seem to be located between Texas and the western origins found in both 8- and 12-day analyses, we selected 12-day back trajectories hoping that they would include pathways that 8-day trajectories may fail to capture.

To test the hypothesis, the correlation coefficient was investigated between Tlt and the ratio of the particles passing over a diabatically heated area. The diabatically heated area is defined as a region where the monthly mean of surface potential temperature exceeds a certain degree between 305K and 315K. It is also varying

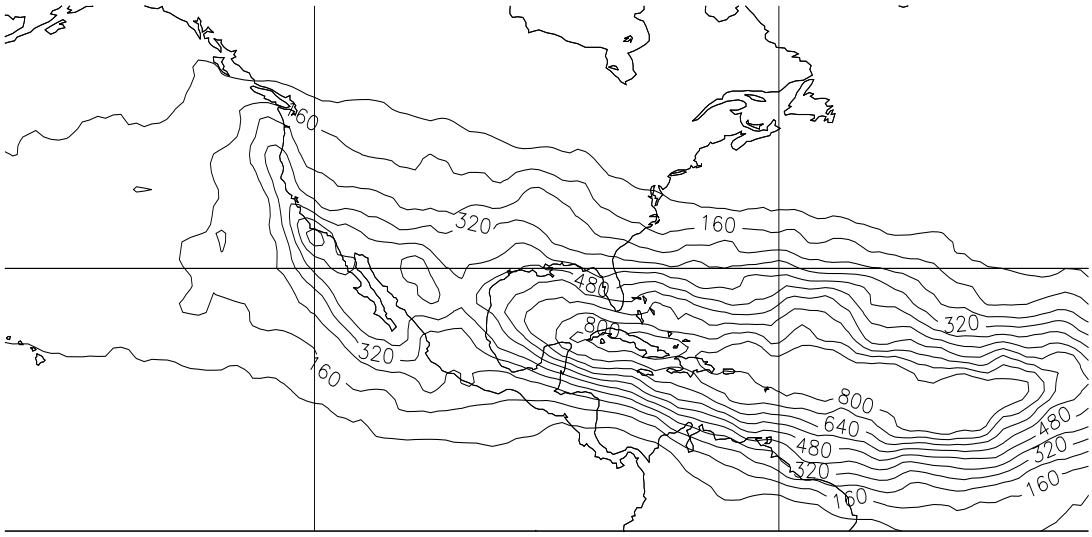

Fig. 5.9. Same as Fig. 5.5 but for 12-day back trajectory. The contour interval is 80.

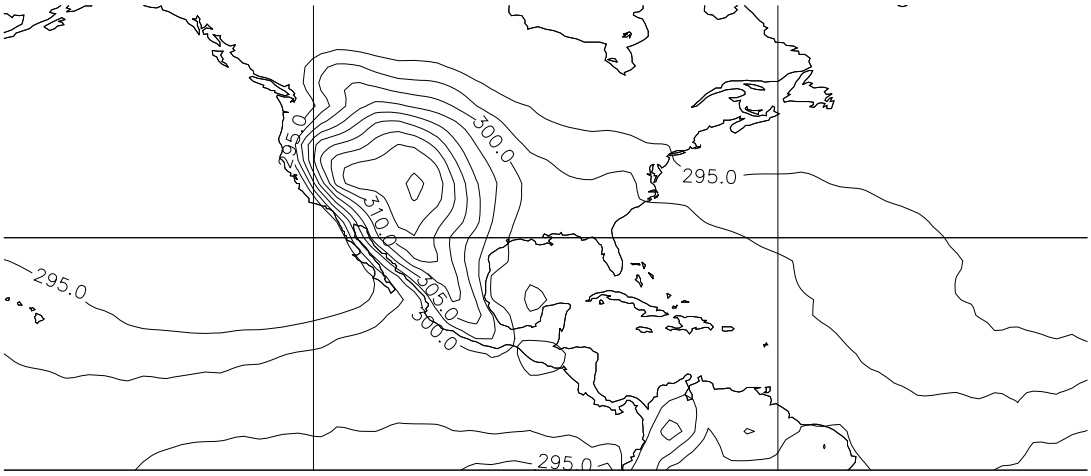

(a)

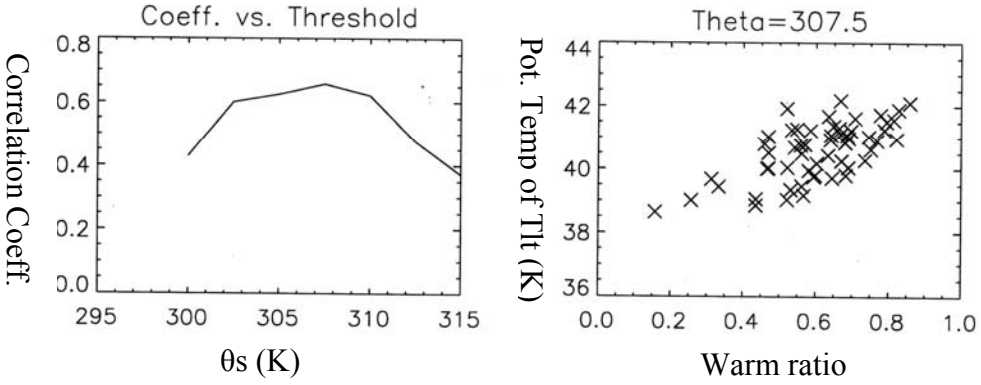

(b) (c)

Fig. 5.10. a) Climatological average of θs (K) for 1948-2003. The contour interval is 2.5(K), b) correlation coefficient of Tlt and RDHP according to θs, and c) scatter plot of RDHP (x-axis) and pontential temperature (°C) of Tlt (y-axis) with 307.5K θs.

interannually, and Fig. 5.10.(a) shows the climatological average of θs. The highest θs is found over the central Rocky Mountain to the west of Colorado, and θs over the Mexican Plateau is relatively high. Fig. 5.10.(b) represents the correlation coefficients between Tlt and the ratio of diabatically heated particles (hereafter, RDHP). The highest correlation, 0.66, occurs at 307.5K θs, whose scatter plot is illustrated in Fig. 5.10.(c). This result clearly indicates that Tlt increases with more air from the diabatically heated area above 307.5K.

One may notice that the region greater than 307.5K θs in Fig. 5.10 slightly overlaps northwestern Texas, which may increase the correlation coefficient unnecessarily. We performed the same analysis excluding the overlapped area in Texas and found that the highest correlation coefficient slightly decreased from 0.66 to 0.62 and the median of RDHP reduced from 0.61 to 0.43. Therefore, this result does not deny the important role of warm air transport from the west on Tlt.

One might assert that the volume of particles from the high altitude area controls Tlt. We investigated the correlation between Tlt and the ratio of the particles passing over the high altitudes rather than the high θs and found that the highest correlation coefficient of Tlt was much less (0.37) than for RDHP. This suggests that high altitude doesn't correspond precisely to greater θs. This may be due to the existence of a difference in solar heating according to the latitudinal variation of solar radiation. In addition, it is likely to occur because of the interannual spatial variation of θs according

to surface thermodynamic conditions. When the diabatically heated area is fixed as all areas with a long-term mean θs of 307.5K, the coefficient dropped to 0.38.

So far, it has been shown that Tlt is significantly modulated by RDHP. As previously demonstrated, warming at 700mb is linked with descending motion as well. Since both can increase Tlt, we want to test the hypothesis that warm air transport (high RDHP) and downward motion (large OMG) contribute to Tlt independently. This hypothesis will be accepted if the regression model on Tlt employing RDHP and OMG as independent variables performs substantially better than that employing either of them.

The result of regression analysis on Tlt using RDHP and OMG is described in Table 5.1. While RDHP produces a better fit on Tlt than does OMG, the regression model using both variables does not show higher performance than that using RDHP alone. Thus, the null hypothesis that RDHP and OMG control Tlt independently is discarded. The rejection of the hypothesis is partially due to the fact that RDHP is not statistically independent from OMG as shown in Fig. 5.11. The positive relationship between RDHP and OMG is an indication that subsidence occurs when influx of diabatically heated air prevails in Texas.

Table 5.1. Adjusted R^2 of the linear regression models of Tlt on RDHP and OMG.

	R_a^2
RDHP	.422
OMG	.189
RDHP and OMG	.420

These results of our study are very interesting. First, subsidence is enhanced in Texas when the influx of diabatically heated particles is dominant, but the elevation of Tlt is caused by the latter rather than the former. This result has been ignored in the previous studies of the 1980 and 1998 droughts that strongly affected Texas. Warm air transport from the elevated terrain may have a significant impact on initiating and maintaining warm season droughts in Texas by increasing CIN. Second, although it is generally expected that an air parcel undergoing diabatic heating would ascend due to buoyancy, it is found in dry months in Texas that diabatically heated particles tend to descend.

In chapter VI, we seek to elucidate mechanisms causing the positive relationship between RDHP and OMG and how they influence CIN and precipitation, thereby integrating our findings from chapters IV and V.

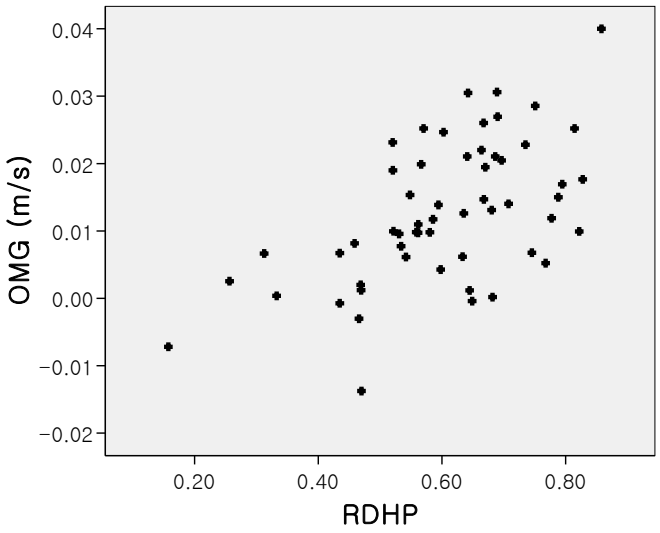

Fig. 5.11. Scatter plot of RDHP and OMG.

CHAPTER VI

ANOMALOUS UPPER-TROPOSPHERIC CIRCULATION AND ITS CHAIN-REACTION INFLUENCES ON PRECIPITATION DEFICIT

A. Causes of the linkage of the ratio of diabatically heated particles with omega

The coupling of strong subsidence with enhanced warm air transport from the west may be the consequence of mechanical descent downstream as the air leaves the mountain area. In that case, downward motion should be stronger or more tightly correlated with RDHP in the lower troposphere rather than in the upper-troposphere. A correlation map of OMG (850-500 mb vertical motion in Texas) with mean 300-400mb vertical motion throughout the region is depicted in Fig. 6.1.(a). Note that correlation coefficients greater than 0.34 are statistically significant at the 99% level. A strong positive relationship is found in the vicinity of Texas indicating that downward motion is not confined only to the lower-troposphere. Fig. 6.1.(b) shows the relationship of vertical motions in between the low-troposphere (500-850 mb) and the upper-troposphere (300-400 mb) in Texas with a reference line, $y = x$. The slope of the scatter plot (1.13) is greater than 1.0, implying that descent is more pronounced in the upper-troposphere than in the lower troposphere. This feature is inconsistent with the conjecture that diabatically heated particles descend due to downslope motion in the lee of the mountains.

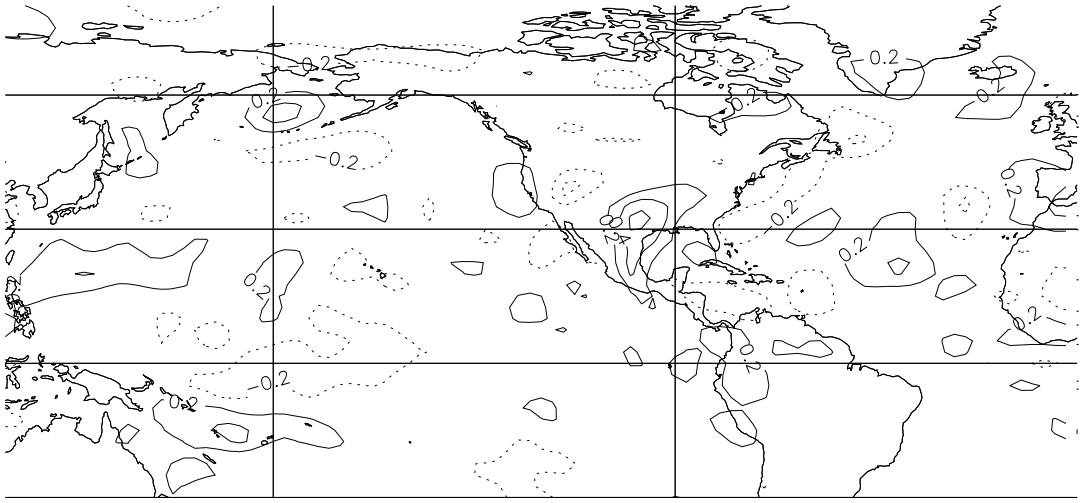

(a)

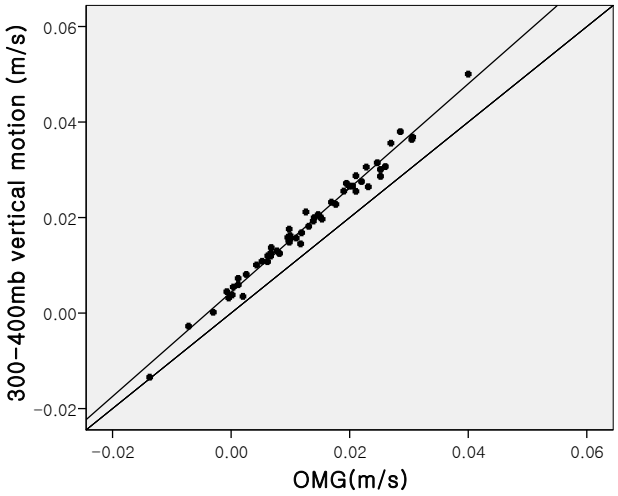

(b)

Fig. 6.1. a) Spatial map of the temporal correlation coefficient between OMG and interannual July mean vertical motion at 200 mb with a regression line. The contour interval is 0.2, b) Scatter plot between OMG and 300-400 mb mean vertical motion in Texas. Reference line is y=x.

The fact that that anomalous vertical motion is distinct not only in the lower-troposphere but also in the upper-troposphere suggests that some large-scale feature that prevails in the troposphere may be involved in the linkage of RDHP with OMG. This speculation leads us to examine the relationships of OMG and RDHP with vorticity and divergence at 200 mb. At 200 mb, divergence (convergence) is directly associated with ascending (descending) motion below due to the constraint of mass conservation, and vorticity patterns indicate large scale circulations and motions (Hoskins et al. 1985).

The 200 mb vorticity and divergence fields were computed interannually from the anomalous winds based on the climatological winds for July, 1948-2003, and their correlation map with OMG is presented in Fig. 6.2. While some areas in the Northern Hemisphere are remotely connected with vertical motion in Texas with weak correlation coefficients, tight relationships occur mainly in North America. More specifically, a strong negative relationship with vorticity is found in the south-western and the south-central US (contours). This indicates that subsidence at 850-500 mb in TX is strongly linked with a possible anticyclonic circulation. For divergence fields (shaded contours), it is confirmed that convergence at the top of troposphere is associated with descent in the low- to mid-troposphere from the negative relationship between divergence and OMG found in Texas and its vicinity.

It should be noted that the aforementioned correlation analyses were performed separately with divergence and vorticity fields, and the results were depicted in one map in Fig. 6.2 for convenience. Thus, Fig. 6.2 does not necessarily imply that the anticyclonic circulation and the convergence that are most significantly coupled with OMG in the surrounding area of Texas occur simultaneously when subsidence is enhanced. To test this, another correlation map was created. First, we computed interannual vorticity averaged over the area in which the magnitude of the correlation coefficient between OMG and vorticity (Fig. 6.2) is greater than 0.2 in the south-western and south-central US. Then, we calculated its correlation coefficient with divergence at each grid point. The spatial pattern of the correlation is expected to indicate which divergence fields are associated with anticyclonic or cyclonic flows in the south-western and south-central US. Shown in Fig. 6.3, the result clearly shows that when anticyclonic (cyclonic) circulation prevails in the south-central US, divergence (convergence) tends to occur to the west and convergence (divergence) occur to the east. This implies that vorticity and divergence fields tightly linked with OMG in Fig. 6.2 are coupled systematically.

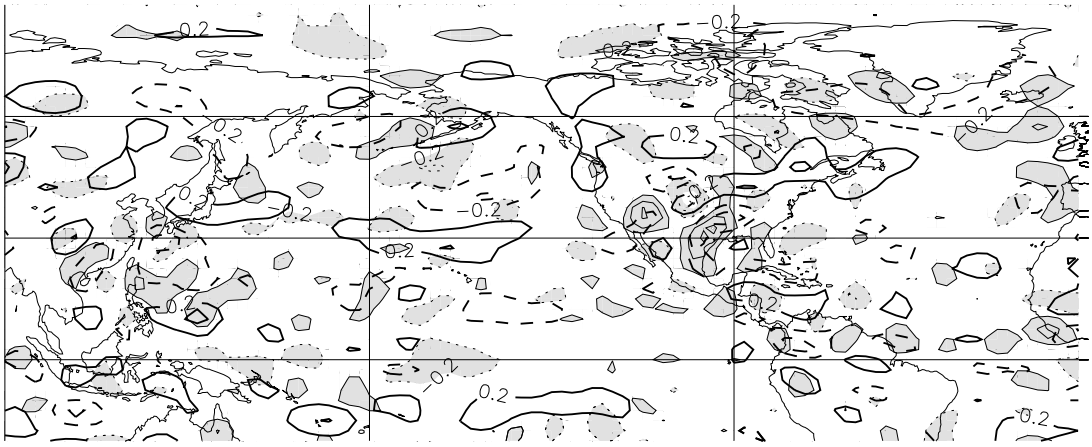

Fig. 6.2. Spatial map of the temporal correlation coefficient of OMG with vorticity (contours) and divergence (shaded contours) on 200 mb. The contour interval is 0.2.

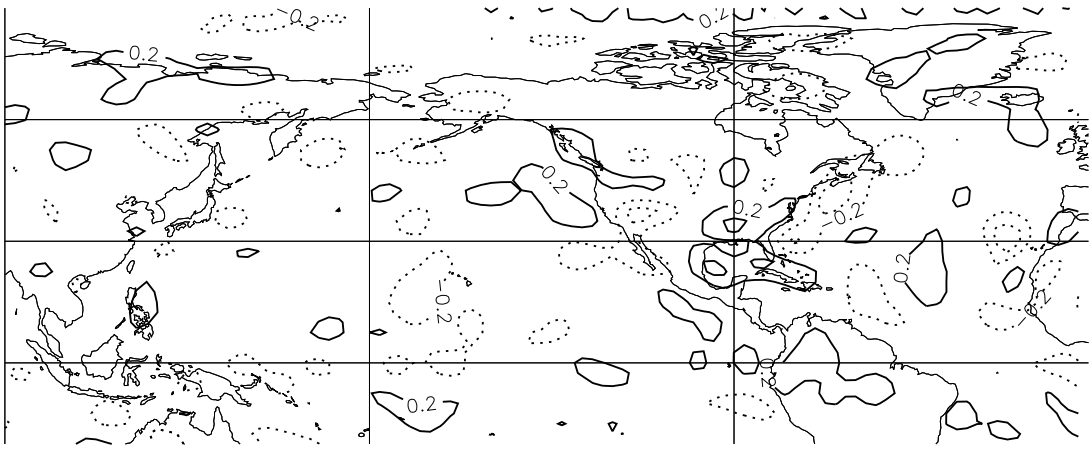

Fig. 6.3. Spatial map of the temporal correlation coefficient between the vorticity over the south-central and south-western US and divergence fields on 200 mb. The contour interval is 0.2.

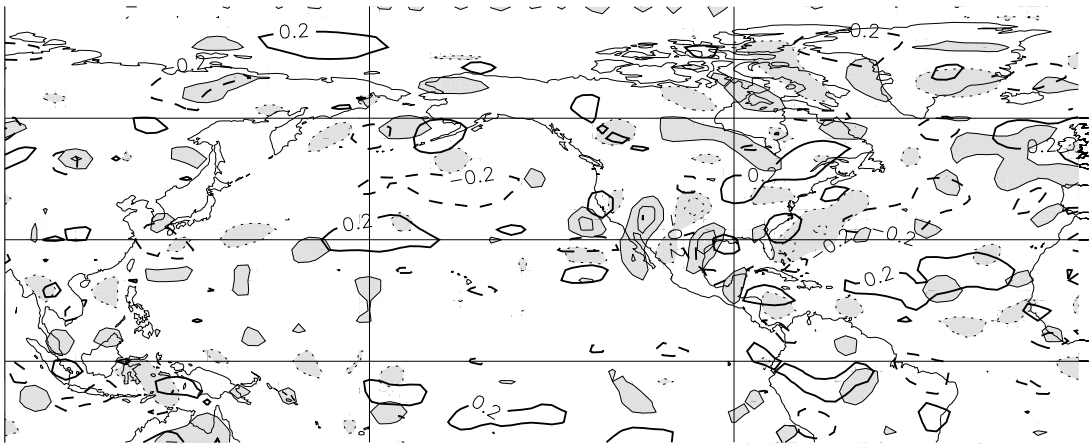

Fig. 6.4. Same as the Fig. 6.2 but with RDHP.

RDHP is also linked with the upper-tropospheric vorticity and divergence on 200 mb. The correlation map between RDHP and divergence and vorticity is illustrated in Fig. 6.4. The results are generally consistent with those of OMG; when RDHP is high, an anticyclone prevails in the south-central and south-western US and convergence is dominant over the eastern Mexico and the Gulf of Mexico, although the location and intensity are slightly different from Fig. 6.2. This feature confirms that upper-tropospheric circulations in the southern US that are linked with the variations of OMG are also coupled with RDHP.

So far, it was shown that an upper-tropospheric anticyclonic circulation over the south-central and south-western US is associated with descent and large RDHP in Texas. The coupling of OMG with vorticity is more distinct at 500 mb than at 200 mb. So is the coupling of RDHP. Fig. 6.5 depicts their relationships to vorticity at 500 mb. While RDHP (Fig. 6.5.(b)) shows a linkage with vorticity in the southern US at 200mb (Fig. 6.4), it is associated with vorticity in the northern Mexico at 500 mb (Fig. 6.5.(b)). The couplings of OMG and RDHP with anticyclonic flow in the southern US are more clearly seen in Fig. 6.6. We defined a 500mb anomalous circulation region as the combined area adjacent to Texas where the correlation coefficient is greater than 0.3 in magnitude in either Fig. 6.5.(a) or Fig. 6.5.(b) and computed the interannual mean vorticity over the region (VOR_{500}). Fig. 6.6 demonstrates the relationships of VOR_{500} with RDHP and OMG. The stronger the anticyclonic circulation, the larger RDHP and OMG in Texas. Both are significantly linked with VOR_{500} and OMG shows a slightly tighter coupling.

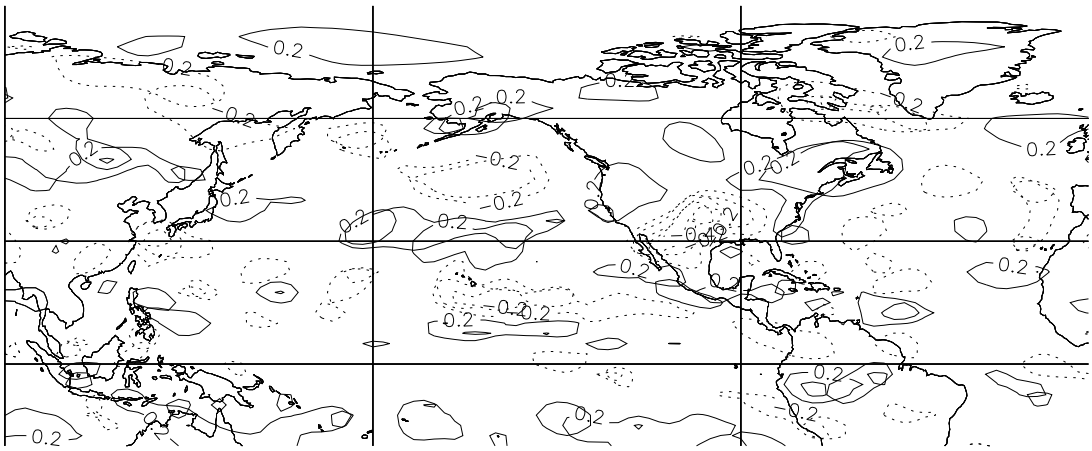

(a)

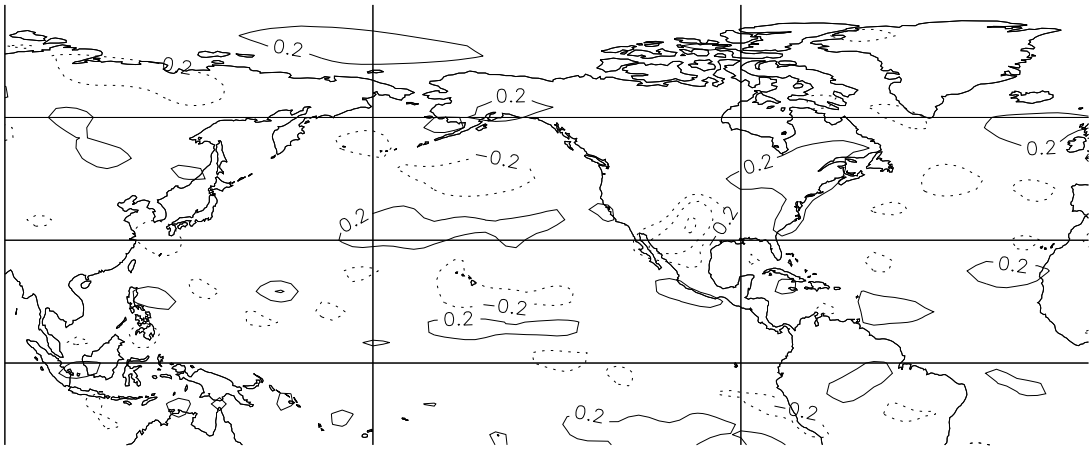

(b)

Fig. 6.5. Spatial map of the temporal correlation coefficient of 500 mb vorticity with a) OMG and b) RDHP. The contour interval is 0.2.

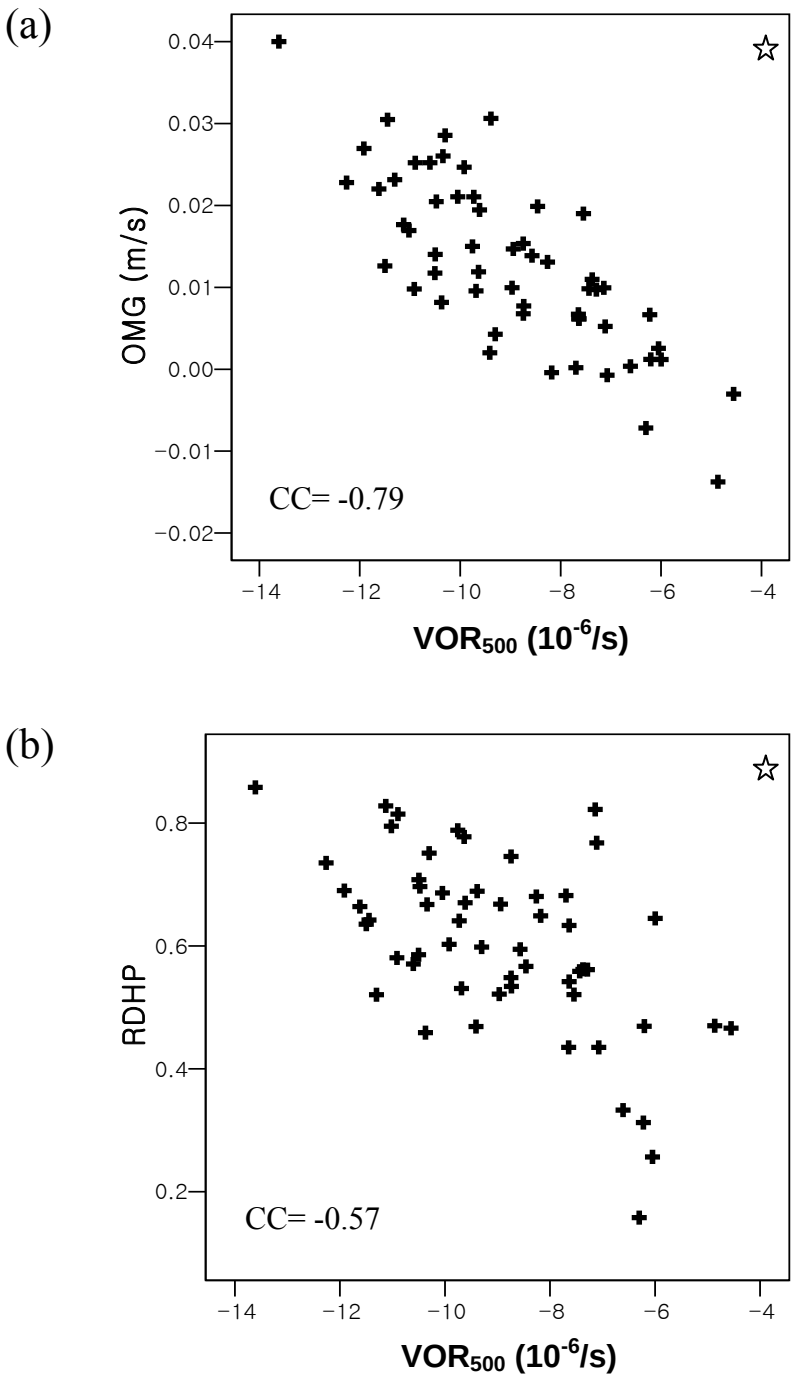

Fig. 6.6. Scatter plots between VOR_{500} and a) OMG and b) RDHP.

Which dynamical and physical mechanisms would explain the linkage of VOR_{500} with OMG and with RDHP? One of the direct influences of the upper-level anticyclonic circulation is to change the flow patterns in troposphere. Due to the existence of a diabatic heating source over the Rocky Mountains and the Mexican Plateau to the west of Texas, Tlt is sensitive to the wind direction. Thus enhancement of warm air transport from the west induced by anticyclonic circulation can increase Tlt significantly.

One example is shown in Fig. 6.7. It presents anomalies in 1000-500 mb thickness and 700 mb vector winds in July 2000 when VOR_{500} and RDHP were extremely high. It features north-westerlies in the western Texas that is expected to be warm due to the diabatic heating over the Rocky Mountains. Northerly and northwesterly winds in the eastern Texas and the Gulf of Mexico indicate the weakening of climatological south-easterlies (Fig. 5.4.(b)) over those regions. These anomalous wind patterns seem to be associated with an upper-level anticyclone illustrated by the positive anomaly in the 1000-500 mb thickness in the central US. When an anticyclone develops over the south-central US, it is likely that climatological south-easterlies cease and, instead, influx of diabatically heated air from the west is enhanced at 700 mb.

However, the physical and dynamical reasons why downward motion is enhanced in Texas when an anticyclonic circulation prevails in the south-central US are not straightforward. In the papers about the 1988 drought in the Great Plains (Trenberth and Branstator 1992; Trenberth and Cuillemot, 1996: Lyon and Dole 1995; Namias 1982), strong subsidence had been inferred to be associated with a quasi-stationary Rossby wave, although it is not examined explicitly. Tropical heating and associated

Rossby wave propagation have remote impacts on regional climate away from the source region through a wave train like feature (Trenberth et al. 1998). Recurrent low-frequency patterns of heating and distant tropospheric response are often called "teleconnections".

Our study also shows an upper-tropospheric circulation feature that seems to be attributed to wave propagation. Going back to the correlation map of OMG with 200mb vorticity and divergence in Fig. 6.2, we see that enhanced low-level upward motion in Texas is also coupled with anticyclonic flow over the North Pacific and cyclonic flow over the north-western US, while it is also associated with circulations over the tropical and subtropical Pacific and over the eastern coast of Canada. This feature of alternating anticyclones and cyclones like a wave train is similar to the height anomaly patterns of the 1980 drought in the south-central US (Fig. 2.1.(b)). In addition, the divergence fields associated with OMG in Fig. 6.3 demonstrate that descending motions occur to the east of the anticyclones over the north-western coast of US and over the south-central US/the

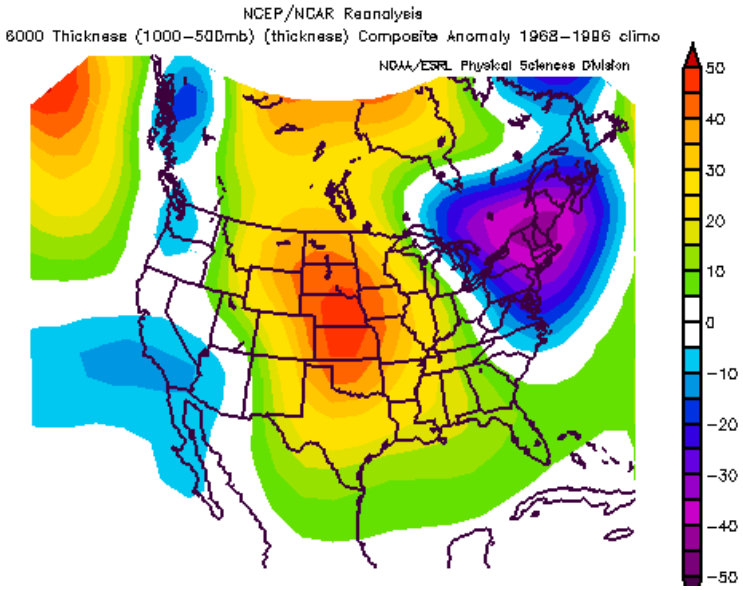

(a)

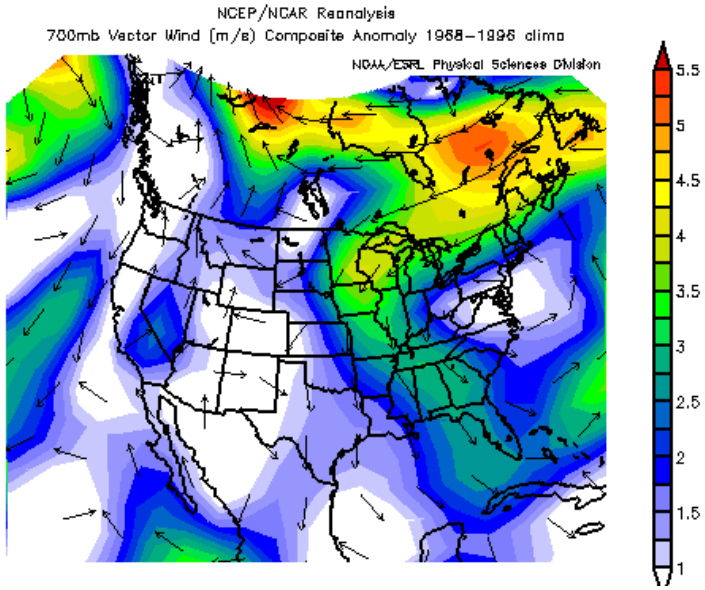

(b)

Fig. 6.7. Anomalies in a) 1000-500 mb thickness and b) vector winds in July 2000.

Gulf of Mexico and that ascending motion takes place to the east of cyclone over the west-central states including Nevada, Utah, and Wyoming. These relationships between vorticity and vertical motion are fairly typical of the dynamics of baroclinic Rossby wave propagation (Hoskins and Karoly 1981; Trenberth et al. 1998; Matthews and Kiladis 2000). Thus, we will examine whether these aspects of the coupling of OMG with upper-tropospheric vorticity and divergence fields are due to the propagation of remotely developed Rossby waves.

According to the quasi-geostrophic omega equation, downward (upward) motion occurs downshear of an upper-tropospheric vorticity minimum (maximum) due to the negative (positive) differential vorticity advection in the upper-troposphere over the surface high (Holton 1992). Therefore, for dynamically-forced subsidence thermal winds have to substantially advect negative vorticity in the south US into the subsidence region in the vicinity of Texas.

Fig. 6.8.(a) illustrates the climatological mean speed and direction of vertical wind shear (i.e., thermal wind) between 200 and 700 mb in July. In the Northern Hemisphere, while strong easterly and westerly shears are found in the Indian Sea and the central Asia, respectively, moderate shear occurs in the central North Pacific and the mid-latitudes in North America. However, relatively weak northerly shear occurs in the regions where upper-level convergence is predominant in the vicinity of Texas in Fig. 6.2. We investigated the possibility that interannual variations of the vertical shear are large in specific years since Texas is located in the margin of the mid-latitude strong shear zone over North America. The interannual variability of 200-300 mb vertical shear

in Texas is shown in Fig. 6.8.(b). In July in Texas, north-easterly and north-westerly vertical shears prevail but their speeds are generally less than 10 m/s. This result suggests that subsidence in Texas in dry months is not caused by differential vorticity advection, rejecting the hypothesis that baroclinic Rossby wave propagation is responsible for the coupling of VOR_{500} and OMG in Texas.

While we do not attempt to find an answer for the strong coupling between OMG and VOR_{500} in this study, one possibility is found in the vertical circulations induced by convective heating in tropics. Such circulations can significantly alter the vertical motion in surrounding areas via locally confined Hadley and Walker type circulations (Gill 1980; Hartmann et al. 1984; Lau and Peng 1987). According to Gill (1980), the steady solution in a shallow water system is characterized by a Kelvin wave to the east of heat source and by a Rossby wave to the west. The former is associated with easterly flows and the latter with westerly flows at the surface, accompanying subsiding motion to the east and west of the heating region. The equatorial radius of deformation in the Gill model is about 1000 km. Those wind patterns are accompanied by large-scale low-level convergence and upper-level divergence that are associated with a strong upper-level anticyclone. The low-level convergent flow over the heating region can lead to additional convection. Thus, the aforementioned vertical motions and large-scale circulations that have horizontal structure of several thousands kilometers in the lower level can modify regional climates of surrounding areas significantly and substantially depending on locations.

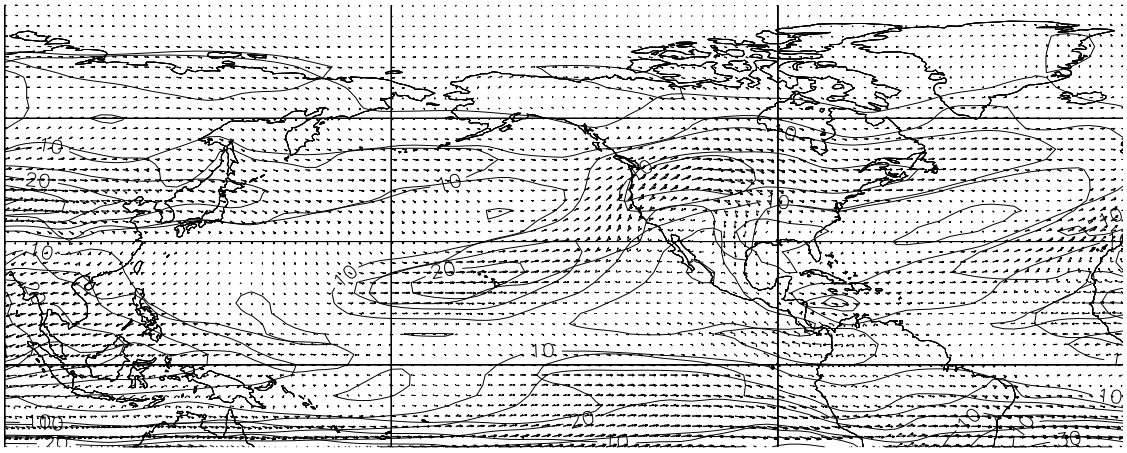

(a)

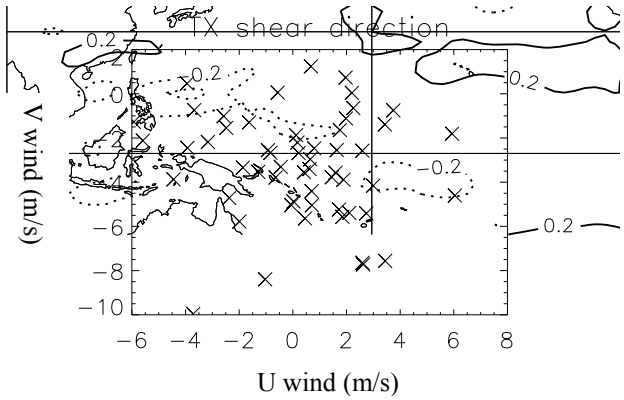

(b)

Fig. 6.8 Climatological mean speed (m/s) and direction of vertical wind shear between 200 and 700 mb in July for 1948-2003.

Climatologically, convective heating is enhanced in the summertime over the south-western US and northern Mexico as well as the eastern tropical Pacific and the Caribbean Sea (Higgins et al. 1997b, Johnson et al. 1987; Schaack and Johnson 1994). Thus, vertical motions and upper-level circulations in Texas can be modified by convective heating in the aforementioned regions. However, the response of atmosphere to tropical heating is sensitive to the vertical distribution of heating, depth of heating, basic flow, and barolinic/barotropic structure of the atmosphere (Schumacher and Houze 2003; Jin and Hoskins 1995), which might make it difficult to find tropical regions that predominantly modulate upper-tropospheric circulation and vertical motion in Texas. Tropical heating that may be responsible for the strong subsidence in dry months remains to be further investigated.

B. Physical connection between upper-level vorticity and precipitation

The aforementioned strong relationships among VOR_{500}, OMG, and RDHP imply that they influence tropospheric variables, CIN, and precipitation as well. In this section, we will discuss how 500 mb vorticity, OMG, and RDHP are linked with precipitation and examine their physical pathways in detail. Fig. 6.9 demonstrates the couplings of OMG, RDHP, and VOR_{500} with tropospheric variables (SM, SH, LH, Td, Ts, Tlt, and DP), CIN, and PRCP. Their correlation coefficients are shown in Table 6.1. First, RDHP is significantly coupled with all tropospheric variables except Td at the 99% level. Since the typical base of the EML in the southern plains (Lanicci and Warner

1991) is at 800 mb and the July mean LFC in Texas is above 700 mb, it is expected that increasing Tlt by EML advection results in a capping inversion. Because the PBL is capped by the lid of the EML, the influence of warm air in the EML on the surface is negligible on a short time-scale so that it would not modify the LCL. However, on a longer time-scale, it affects thermodynamic properties in the boundary layer: it increases surface temperature by entrainment of warm air into the PBL (Stensrud 1993). The combination of frequent development of a capping inversion and surface warming would reduce convection and the likelihood of precipitation by elevating CIN, despite substantial surface moisture. Then, the associated precipitation deficit decreases SM, which in turn controls the surface variables.

The aforementioned processes and pathways are illustrated in Fig. 6.10. RDHP directly affects CIN and then precipitation and soil moisture. The magnitude of correlation coefficients of RDHP supports this hypothesis; RDHP is most tightly correlated with CIN (0.73), next with PRCP (-0.61), and least with SM (-0.56). Tighter relationship of RDHP with SM (-0.56) than those with SH, LH, and Td (0.52, -0.48, and -0.33) suggests that RDHP influences SH, LH, and Td through SM.

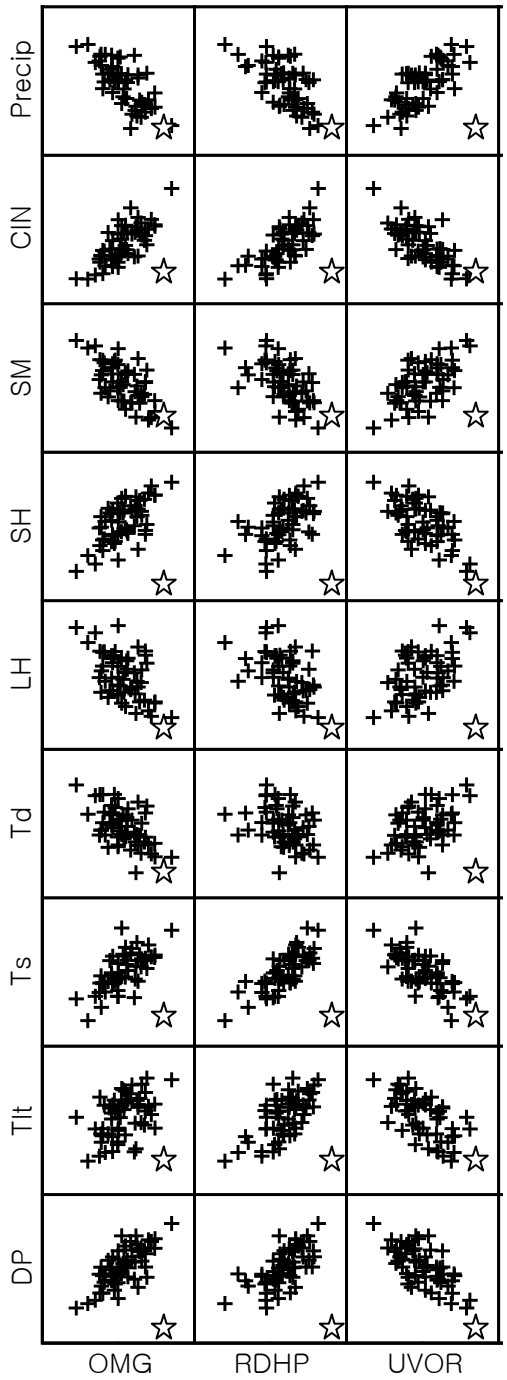

Fig. 6.9. Scatter plots of OMG, RDHP, and VOR_{500} with the surface variables, SM, CIN, and PRCP.

Table. 6.1. Correlation coefficients.

	OMG	RDHP	VOR_{500}
PRCP	-0.73	-0.61	0.73
CIN	0.76	0.73	-0.74
SM	-0.66	-0.56	0.61
SH	0.65	0.52	-0.62
LH	-0.52	-0.48	0.49
Td	-0.55	-0.33	0.44
Ts	0.69	0.78	-0.69
Tlt	0.45	0.66	-0.61
DP	0.73	0.65	-0.67

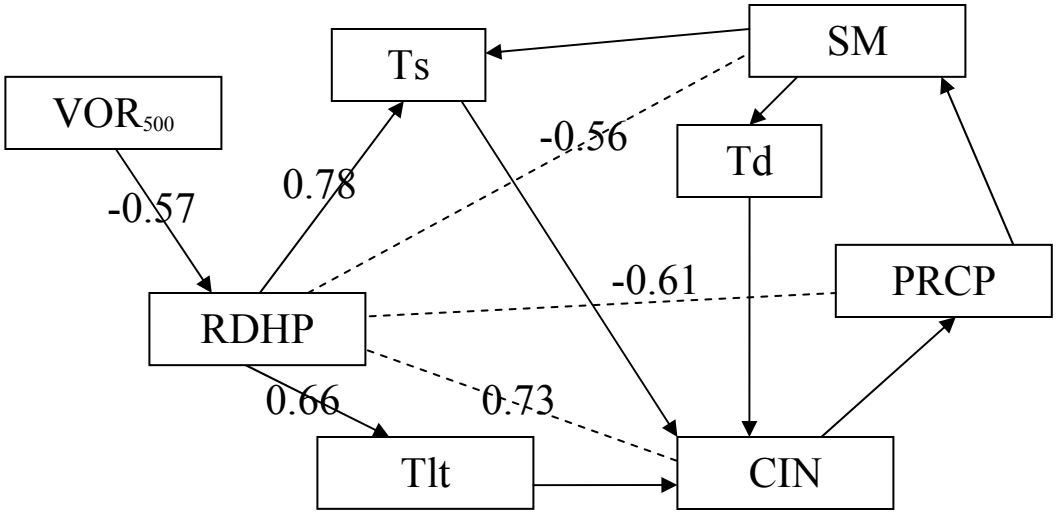

Fig. 6.10. Schematic diagram representing influence of RDHP on CIN, PRCP, and SM.

Second, OMG demonstrates significant correlations with all the tropospheric variables at the 99% confidence level (Fig. 6.9 and Table 6.1). It is more tightly linked with SM, SH, LH, and Td than is RDHP. OMG shares several features of RDHP: tighter relationship with SM (-0.66) than with SH, LH, and Td (0.65, -0.52, and 0.55, respectively). OMG seems to alter Ts rather directly since the magnitude of their correlation coefficient (0.69) is greater than that between OMG and SM (-0.66) although the difference of the two correlation coefficients is statistically not significant. Or else a third process affects both OMG and Ts.

While both large OMG and RDHP can directly contribute to the surface temperature change by adiabatic warming and warm air transport, respectively, RDHP is more tightly linked with Ts (Table 6.1). Then, among OMG, RDHP, and SM, what is the most significant contributing factor(s) on July mean surface temperature? The R_a^2 values of linear regression analyses on Ts using SM, RDHP, and OMG are shown in Table 6.2. While, as a single independent variable, RDHP shows the best fit, adding OMG or SM increases model performance significantly based on the reduced model f-test. However, the reduced model f-test using the last two models indicates that OMG as a independent is not significant at 95% confidence level.

In section IV.C, it was found that Tlt and SH explain 80% of the variance of Ts. When it is recalled that RDHP and SM are the significant regulators of Tlt and SH, respectively, the result in Table 6.2 confirms that monthly mean surface temperature in Texas is primarily modulated by surface energy flux and entrainment of air above the top of the PBL.

Table 6.2 Adjusted R^2 of the linear regression models of Ts on SM, RDHP, and OMG.

Independent variable(s)	R_a^2
SM	.52
RDHP	.60
OMG	.46
SM, OMG	.59
OMG, RDHP	.68
SM, RDHP	.72
SM, RDHP, OMG	.74

On the other hand, despite moderate coupling with SM, OMG is tightly linked with CIN (0.76) as well as PRCP (-0.73). Since CIN, PRCP, and SM are tightly inter-connected each other as shown in section V.B, a direct physical or dynamic linkage of OMG to any of them can cause commensurate correlation coefficients of OMG with the others. When direct connections between OMG and CIN, precipitation, and SM are considered for simplicity, four possible explanations are found as follows (Fig. 6.11).

First, large OMG can affect CIN not only by increasing Tlt and/or Ts but also by suppressing low-level convergence while OMG cannot be influenced by CIN, directly.

Second, OMG may be coupled with PRCP due to the precipitation process: convection associated with strong upward motion results in large amount of precipitation. Although this process has a time-scale less than a day, feedbacks of soil moisture on precipitation may enhance the couplings among OMG, and PRCP on a monthly time-scale. In general, dry soil caused by lack of rainfall increases CIN by which, in turn, inhibits subsequent convection, upward motion, and precipitation. Therefore, a reduced number of convective events would result in a precipitation deficit and then downward motion that is typical in subtropics in summer would be kept undisturbed. Third, SM can influence OMG through the albedo hypothesis. Lastly, other process affects both OMG and the one among CIN, PRCP, and SM.

The first and the third are causality-induced relationships while the second is a physically coupled relationship. Among the first three possibilities, correlation coefficients of OMG with CIN (0.76), PRCP (-0.73), and SM (-0.66) suggest that the first and second are more predominant than the third because if the third is dominant, correlation coefficient between OMG and SM should be highest. However, more precise investigation is needed to find the origin of subsidence and its influence on precipitation deficit in dry months.

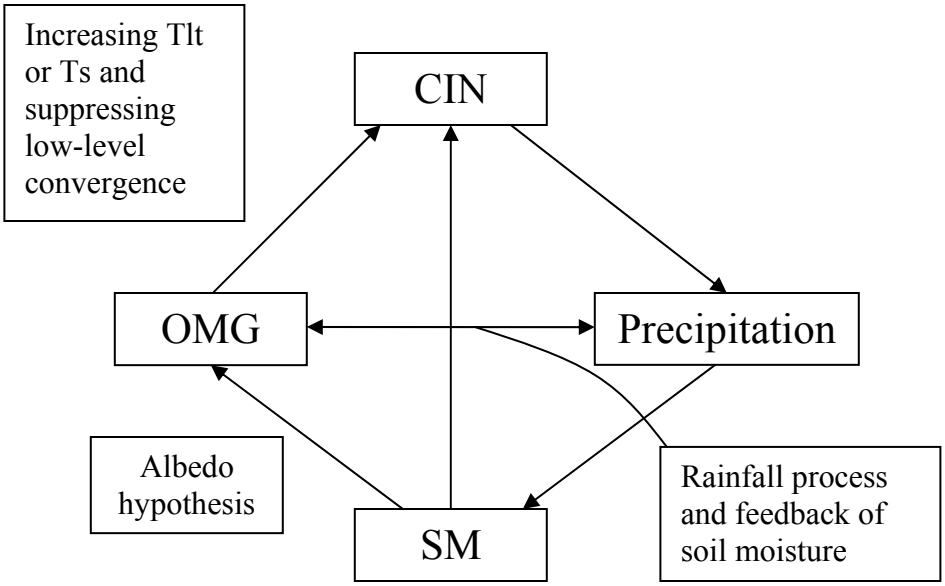

Fig. 6.11. Schematic diagram representing possible pathways and explanations between OMG and CIN, PRCP, and SM.

Lastly, similar to OMG, VOR_{500} is tightly coupled with CIN (-0.74) and PRCP (0.73). This is likely to be due to upper-level anticyclonic circulations not only affecting CIN by increasing RDHP and Tlt but also suppressing occurrence of disturbances. The former is supported by the stronger relationship of Tlt with VOR_{500} (-0.61) than with OMG (0.45).

VOR_{500} seems to have the least impact on Td, one of the most significant contributing factors for CIN. This is perhaps due to the fact that soil moisture, a critical contributing factor on surface moisture content, has a longer time scale than a month, generally a seasonal time scale, although it may be influenced by rainfall instantaneously (Betts et al. 1996; Findell and Eltahir 1999). Soil moisture tends to diminish high-frequency fluctuations and enhance the memory of the land-surface system. Thus, monthly mean precipitation is only moderately coupled with SM.

Fig. 6.12 summarizes the principal processes and pathways examined in this study. Significant processes verified in this study are in solid and unverified but possibly significant processes are in dashed. Once a mid- and upper-tropospheric anticyclone develops over the southern US, it can reduce chances of convection by blocking disturbances despite small CIN. Simultaneously, warm air transport from the high terrain increases Tlt directly and Ts by entrainment of warm air above the top of PBL. Both processes result in a decrease of precipitation by generating a capping inversion or increasing CIN. Notice that no change in SM is involved so far. This speculation is consistent with the tighter relationships of VOR_{500} with precipitation and with CIN than with SM in Fig. 6.9.

Thereafter, reduced rainfall caused by warm air transport by the upper-level anticyclonic circulation starts affecting soil moisture and SH, LH, and Td, subsequently. This is supported by the fact that, as seen in Table 6.1, VOR_{500} is moderately coupled with SM, SH, LH, and Td as well as with Ts and Tlt while RDHP preferentially affects the temperature variables, Ts and Tlt. Furthermore, reduced SM influences precipitation

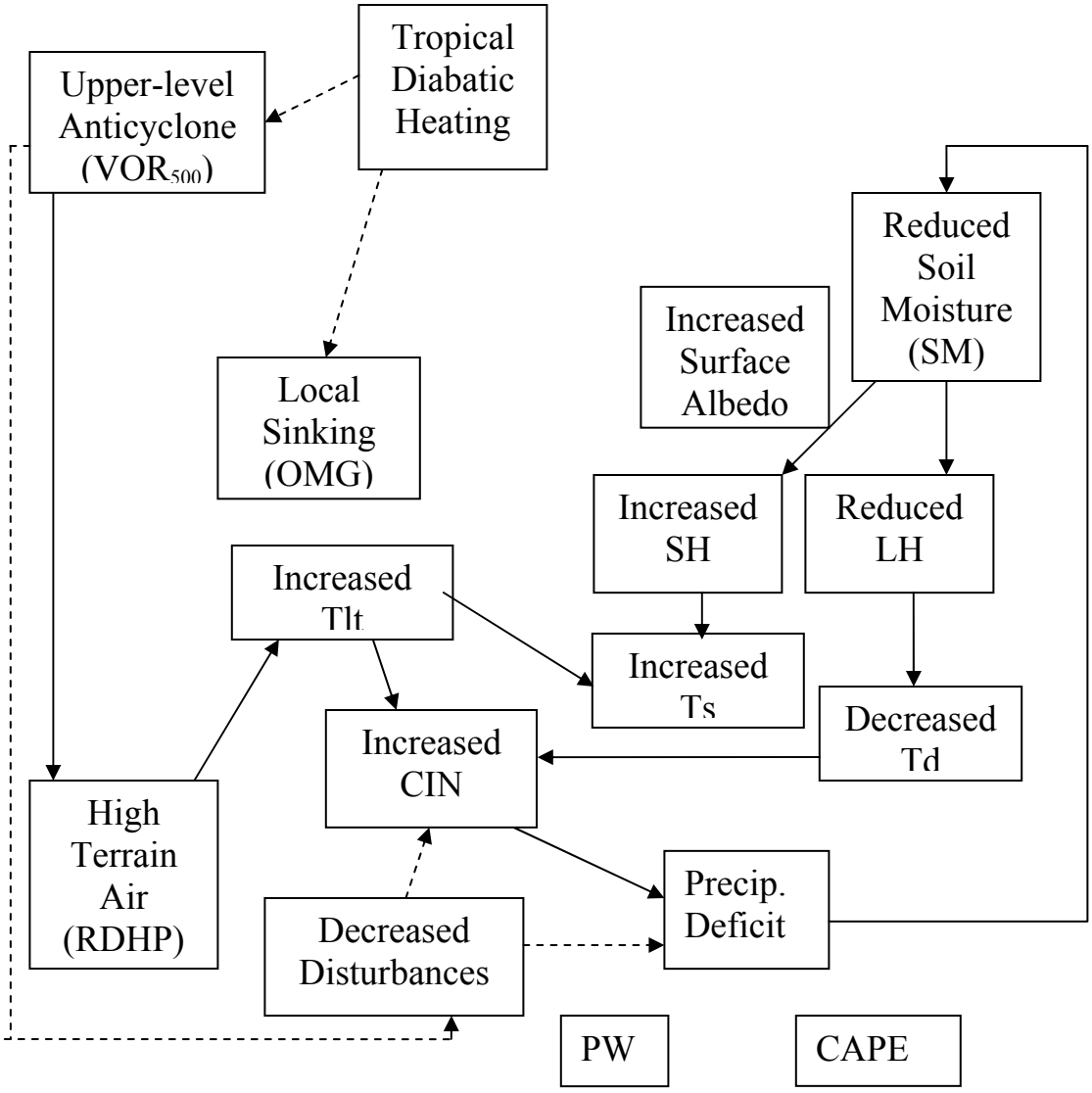

Fig. 6.12. Schematic showing verified processes by this study (solid) and unverified but possibly significant processes (dashed).

by increasing CIN, in turn, which demonstrates the soil moisture feedback on precipitation.

As seen in chapter IV, thermodynamic characteristics and changes in convective instability are significant to the interannual variability of summer precipitation in Texas. This study reveals that the amount of precipitation in summer in Texas is greatly modulated by upper-level circulations. Their influence is through changing thermodynamic structure and convective instability, especially CIN. Significant and tight linkages among OMG, VOR_{500}, SM, and PRCP project the key characteristics of the 1980, 1988, and 1998 droughts in the Great Plains and the south-central US: strong upper-tropospheric anticyclone, enhanced subsidence, and dry soil. This study succeeded in verifying the detailed processes resulting in precipitation deficit and drought quantitatively in the context of convective instability while the influences of VOR_{500} and SM are consistent with the mechanisms triggering and maintaining those droughts.

However, the origin of upper-level anticyclone, vertical motion, and their coupling does not seem to be typical of those droughts associated with quasi-stationary Rossby wave development. Dynamical mechanisms enhancing anticyclonic circulations over the south-western and south-central US demand more investigation.

We could not find critical impacts of subsidence on precipitation deficit despite the tight couplings of OMG with CIN and PRCP. In dry months, increments in Tlt and Ts are dominated by increases in RDHP and SH rather than by OMG. The existence of an anticyclone in the mid- and upper-troposphere would play the primary role of blocking disturbances rather than inducing subsidence. These results suggest that vertical

motion does not efficiently modify thermodynamic structure and convective instability, especially CIN, in summer in Texas. As mentioned in chapter II and chapter V, vertical motion rarely changes thermodynamics not only in the boundary layer but also in the free-troposphere because of the canceling effects of adiabatic cooling and subsidence warming (Ye et al. 1998; Gray 1973; Gray and Jacobson 1977). Rather than that, surface flux and convection are likely to modulate thermodynamic conditions in the tropics.

Our study is unique in finding a significant influence of warm air transport on precipitation deficit. In a NOAA news release in 2001 (NOAA 2001), it was reported that Texas and adjacent areas have had a higher frequency of droughts than other states in the western US, northern Plains and southeastern US during the 15-year period from 1985 to 2000. More frequent occurrence of drought in Texas may be attributed to the influence of the warm air over the high terrain. Therefore, we argue that studies and models of summer precipitation and drought in Texas have to take into careful account transport of diabatically heated air from the high terrain.

CHAPTER VII

SUMMARY AND CONCLUSIONS

We have examined the modulation of convective instability on summertime precipitation in Texas and the significant processes controlling convective instability. In doing so, the principal dynamical and physical processes modulating precipitation in summertime in Texas were revealed including the influences of upper-level circulation patterns and the feedback of soil moisture on precipitation. These processes are expected to play important roles on initiating and maintaining Texas summer droughts.

The principal motivation for this study is to bridge the gap between precipitation processes and remote/local forcings of the US summer droughts such as were identified in 1980 and 1988. A monthly time-scale was found to be useful for representing important processes such as the influence of precipitation on soil moisture, the feedback of soil moisture on precipitation, upper-tropospheric large-scale influences, and land-atmosphere interactions that cannot be characterized on either seasonal time-scales or weekly time-scales. The statistical relationships obtained from NCEP/NCAR reanalysis data and the physical background add to the understanding of the upper- and low-level and surface dynamics that accompanies precipitation deficit and droughts.

It was found that monthly mean precipitation is modified mainly by CIN rather than by CAPE or by precipitable water. This is supported by the fact that, despite the large CAPE and moisture availability, convection is inhibited when CIN is large since CIN is a measure of the amount of energy needed to initiate convection.

Linear regression analysis revealed that warming at 700 mb (high Tlt) and surface dryness (low Td) result in excessive CIN, leading to precipitation deficit on monthly time-scales. This is surprising, because previous drought studies have emphasized low relative humidity (large dewpoint depression) on surface as causing a reduction in rainfall. Surface temperature, Ts, is tightly coupled with CIN and precipitation and is affected by both the free-atmospheric temperature at 700 mb (Tlt) through entrainment and surface sensible heat flux. Therefore, the variability of CIN is explained mostly by Td and the rest is explained by Tlt rather than by Ts. The statistical independence of Tlt to Td suggests that different processes contribute to warming at 700 mb and surface dryness, resulting in excessive CIN in dry months.

Back trajectory analysis indicates that a significant contributor to warming at 700 mb is the inversion caused by warm air transport from the Rocky Mountains and Mexican Plateau where the surface potential temperature is greater than 307.5K rather than by subsidence. As mentioned above, this also increases surface temperature by entrainment of warm air into PBL, which results in elevated CIN. This effect reduces precipitation despite substantial low-level moisture.

While transport of diabatically heated warm air from the high terrain is associated with enhanced descent, the upper-level anticyclonic circulation in the south-central and south-west US seems to be responsible for their linkage. At 700 mb, an anticyclonic flow impedes climatological south-easterly flow, and then air transport from the west is enhanced, which results in the negative relationship between VOR_{500} and RDHP. But the physical reasons why downward motion is enhanced in Texas when

anticyclonic circulation prevails in the south-central US are not known. It is not due dynamically to the quasi-stationary Rossby wave propagation since the subtropical region lacks baroclinicity in summer. Downward motion associated with anticyclonic flow may be driven by convective heating adjacent to Texas.

Upper-level anticyclonic circulations in the southern US strongly affect Texas summertime precipitation by modulating the principal processes. Enhanced warm air transport from the high terrain reduces rainfall by increasing CIN. The existence of an upper-level anticyclone tends to inhibit convection by suppressing the occurrence of disturbances, allowing for CIN to accumulate. The resulting reduced precipitation decreases soil moisture. Reduced soil moisture significantly modulates surface temperature and dewpoint and then elevates CIN. The aforementioned chain-reaction of upper-level anticyclone influences can be understood in the context of CIN.

We could not find critical impacts of subsidence on precipitation deficit through modifying convective instability despite tight couplings of OMG with CIN and precipitation. In dry months, elevations of Tlt and Ts is dominated by increases in RDHP and SH rather than in OMG. Existence of an anticyclone in the mid- and upper-troposphere plays a primary role for blocking disturbances rather than subsidence does. Vertical motion is not likely to modify thermodynamic structure and convective instability in summer in Texas.

One limitation of this study is the lack of samples. We utilize 56 July months. Nevertheless, the use of the NCEP/ NCAR reanalysis data is found to provide a reasonable representation of several important processes affecting monthly precipitation:

1) the strong coupling between land surface and atmosphere by soil moisture (Koster et al. 2004) including feedbacks of soil moisture on precipitation, 2) the influence of large-scale circulations, and 3) suppression of convection by diabatically heated air from the west.

This study emphasizes the significant role of warm air transport from the Mexican Plateau and the Rocky Mountains associated with an upper-level anticyclone modulating convective instability and convective precipitation in Texas. Although this study focused on the convective precipitation processes in Texas, the impact of EMLs on convection emphasized in this study are not limited to Texas and can be applied to the south-central US and the southern Great Plains. It remains to be further investigated whether the mechanism is also causing warm season droughts over those regions.

REFERENCES

Atlas, R., N. Wolfson, and J. Terry, 1993: The effect of SST and soil moisture anomalies on GLA model simulations of the 1988 U.S. summer drought. *J. Climate*, **6**, 2034-2048.

Augustine, J. A., and F. Caracena, 1994: Lower-tropospheric precursors to nocturnal MCS development over the central United States. *Wea. Forecasting,* **9,** 116–135.

Betts A. K., J. H. Ball, A. C. M. Beljaars, M. J. Miller, and P. Viterbo, 1996: The land surface–atmosphere interaction: A review based on observational and global modeling perspectives. *J. Geophys. Res.*, **101**, 7209–7225.

Bony, S., and coauthors, 2006: How well do we understand and evaluate climate change feedback processes? *J. Climate*, **19**, 3445-3482.

Bowman, K. P., and G. D. Carrie, 2002: The mean-meridional transport circulation of the troposphere in an idealized GCM. *J. Atmos. Sci*., **59**, 1502–1514.

——, and T. Erukhimova, 2004: Comparison of global-scale Lagrangian transport properties of the NCEP Reanalysis and CCM3. *J. Clmate*, **17**, 1135– 1146.

Brenner, I. S., 2004: The relationship between meteorological parameters and daily summer rainfall amount and coverage in West-Central Florida. *Wea. Forecasting*, **19**, 286-300.

Brown, R. G., and C. S. Bretherton 1997, A test of the strict quasi-equilibrium theory on long time and space scales, *J. Atmos. Sci*., **54**, 624–638.

Brubaker K. L., D. Entekhabi, and P. S. Eagleson, 1993: Estimation of continental precipitation recycling. *J. Climate*, **6**, 1077–1089.

Brunetti, M., Maugeri, M., and T. Nanni, 2001: Changes in total precipitation, rainy days and extreme events in Northeastern Italy, Intern. *J. Climate*., **21**, 861-871.

Carlson, T. N., S. G. Benjamin, G. S. Forbes, and Y. –F. Li, 1983: Elevated mixed layers in the severe-storm environment-conceptual model case studies. *Mon. Wea. Rev*., **111**, 1453-1473.

Chang, F. C., and J. M. Wallace, 1987: Meteorological conditions during heat waves and droughts in the United States Great Plains. *Mon. Wea. Rev.,* **115,** 1253–1269.

——, and E. A. Smith, 2001: Hydrological and dynamical characteristics of summertime droughts over U.S. Great Plains. *J. Climate*, **14**, 2296-2316.

Charney, J. G., 1947: The dynamics of long waves in a baroclinic westerly current. *J. Meteor.,* **4,** 135–162.

——, 1975: Dynamics of deserts and drought in the Sahel.. *Quart.J. Roy. Meteor. Soc.,* **101**, 193-202.

——, W. J. Quirk, S. H. Chow, and J. Kornfield, 1977: A comparative study of the effects of albedo change on drought in semi-arid regions. *J. Atmos. Sci.,* **34,** 1366–1385.

Chen, P., and M. Newman, 1998: Rossby wave propagation and the rapid development of upper-level anomalous anticyclones during the 1988 U.S. drought. *J. Climate*, **11**, 2491-2504.

Clark, R. A., 1960: A study of convective precipitation as revealed by radar observation, Texas 1958-1959**.** *J. Atmos. Sci.,* **4,** 415-425.

Colby, F. P., Jr., 1980: The role of convective instability in an Oklahoma squall line. *J. Atmos. Sci*., **37**, 2113-2119.

——, 1984: Convective inhibition as a predictor of convection during AVE-SESAME II. *Mon. Wea. Rev.,* **112,** 2239–2252.

Cunnington, W. M., and P. R. Rowntree, 1986: Simulations of the Saharan atmosphere-dependence on moisture and albedo. *Quart, J. Roy. Meteor, Soc*., **112**, 971-999.

DeMott, C. A., and D. A. Randall, 2004: Observed variations of tropical convective available potential energy. *J. Geophys. Res.,* **109** (D02102): doi:10.1029/2003JD003784.

Doswell, C. A., III, 1987: The distinction between large-scale and mesoscale contribution to severe convection: A case study example. *Wea. Forecasting,* **2,** 3–16.

Eady, E. T., 1949: Long waves and cyclone waves. ***Tellus,* 1, 33–52.**

Eltahir, E. A. B., 1998: A soil moisture-rainfall feedback mechanism. 1. Theory and observations. *Water Resour. Res.,* **34,** 765–776.

Emanuel, K. A., 1994: *Atmospheric Convection.* Oxford University Press, 580 pp.

Fennessy, M. J., and J. Shukla, 1999: Impact of initial soil wetness on seasonal atmospheric prediction. *J. Climate*, **12**, 3167-3180.

Findell, K., and E. A. B. Eltahir, 1997: An analysis of the relationship between spring soil moisture and summer rainfall, based on direct observations from Illinois. *Water Resour. Res.,* **33,** 725–735.

——, and ——, 1999: Analysis of the pathways relating soil moisture and subsequent rainfall in Illinois. *J. Geophys. Res.* **104**, 31 565–31 574.

Firestone, J. K., and B. A. Albrecht, 1986: The structure of the atmospheric boundary layer in the cenral equatorial Pacific during January and February of FGGE. *Mon. Wea. Rev*., **114**, 2219-2231.

Foote and C. G. Wade, 1982: Case study of a hailstorm in Colorado. Part I: Radar echo structure and evolution. *J. Atmos. Sci*., **39**, 2828-2846.

Forman S.L., R. Olgesby, V. Markgraf, and T. Stafford, 1995: Paleoclimatic significance of late Quaternary eolian deposition on the piedmont and high plains, central United States. *Global Planet. Change,* **11,** 35–55.

Fu, R., B. Zhu, and R. Dickinson, 1999: How do the atmosphere and land surface influence the seasonal changes of convection in tropical Amazon? *J. Climate,* **12,** 1306–1321.

Gaffen, D. J., T. P. Barnett, and W. P. Elliott, 1991: Space and time scales of global tropospheric moisture, *J. Climate*., **4**, 989–1008.

Garratt, J. R., 1993: Sensitivity of climate simulations to land-atmospheric boundary layer treatments-A review, *J. Climate*., **6**, 419-449.

Gettelman, A., D. J. Seidel, M. C. Wheeler, and R. J. Ross (2002), Multidecadal trends in tropical convective available potential energy, *J. Geophys. Res*., **107**, 4606, doi:10.1029/2001JD001082.

Gray, W. M., 1973: Cumulus convection and larger scale circulations:I. Broadscale and mesoscale considerations. *Mon. Wea. Rev.,* **101,** 839–855.

——, and R. W. Jacobson, 1977: Diurnal variation of deep cumulus convection. *Mon. Wea. Rev.,* **105,** 1171–1188.

Groisman PY, Karl TR, Easterling DR, Knight RW, Jamason PF, Hennessy KJ, Suppiah R, Page CM, Wibig J, Fortuniak K, Razuvaev VN, Douglas A, Førland EJ, Zhai P., 1999: Changes in the probability of heavy precipitation: Important indicators of climatic change. *Climate Chang.,* **42**, 243–283.

Hao, W., and L. F. Bosart, 1987: A moisture budget analysis of the protracted heatwave in the southern Plains during summer of 1980. *Wea. Forecasting*, **2**, 269-288.

Hartmann D. L., H. H. Hendon, and R. A. Houze Jr., 1984: Some implications of the mesoscale circulations in tropical cloud clusters for large-scale dynamics and climate. *J. Atmos. Sci.*, **41**, 113–121.

Helfand, H. M., and S. D. Schubert, 1995: Climatology of the Great Plains low-level jet and its contribution to the continental moisture budget of the United States. *J. Climate,* **8,** 784–806.

Hering, W. S., and T. R. Borden, 1962: Diurnal variations in the summer wind field over the central United States. *J. Atmos. Sci.,* **19,** 81–86.

Higgins R. W., Y. Yao, E. S. Yarosh, J. E. Janowiak, and K. C. Mo, 1997a: Influence of the Great Plains low-level jet on summertime precipitation and moisture transport over the central United States. *J. Climate*, **10**, 481–507.

——, Y. Yao, and X. Wang, 1997b: Influence of the North American monsoon system on the United States summer precipitation regime. *J. Climate*, **10**, 2600–2622.

Holton, J. R., 1992: *Introduction to Dynamic Meteorology.* Academic Press, 511 pp.

Hong, S. Y., and E. Kalnay, 2002: The 1998 Oklahoma-Texas drought: Mechanistic experiments with NCEP global and regional Models. *J. Climate*, 1**5**, 945-963.

Horel, J. D., and J. M. Wallace, 1981: Planetary-scale atmospheric phenomena associated with the Southern Oscillation. *Mon. Wea. Rev.,* **109,** 813–829.

Hoskins, B. J., and D. J. Karoly, 1981: The steady linear response of a spherical atmosphere to thermal and orographic forcing. *J. Atmos. Sci.,* **38,** 1179–1196.

——, M. E. McIntyre, and A. W. Robertson, 1985: On the use and significance of isentropic potential-vorticity maps. *Quart. J. Roy. Meteor. Soc.,* **111,** 877–946.

Jin F. F., and B. J. Hoskins, 1995: The direct response to tropical heating in a baroclinic atmosphere. *J. Atmos. Sci.*, **52**, 307–319.

Johns, R. H., and C. A. Doswell III, 1992: Severe local storms forecasting. *Wea. Forecasting,* **7,** 588–612.

Johnson, D. R., M. Yanai, and T. K. Schaack, 1987: Global and regional distributions of atmospheric heat sources and sinks during the GWE. *Monsoon Meteorology,* C. P. Chang and T. N. Krishnamurti, Eds., Oxford University Press, 271–297.

Kalnay, E., and Coauthors, 1996: The NCEP/NCAR 40-year Reanalysis Project. *Bull. Amer. Meteor. Sco.*, **77**, 437-471.

Kingsmill, D. E., and R. M. Wakimoto, 1991: Kinematic, dynamic, and thermodynamic analyses of a weakly sheared severe thunderstorm over northern Alabama. *Mon. Wea. Rev.,* **119,** 262–297.

Kloesel, K. A., and B. A. Albrecht, 1989: Low-level inversions over the tropical Pacific—Thermodynamic structure of the boundary layer and above-inversion moisture structure. *Mon. Wea. Rev.,* **117,** 87–101.

Koster, R. D. and Coauthors, 2004: Regions of strong coupling between soil moisture and precipitation. *Science,* **305,** 1138–1140.

Lanicci J. M., and T. T. Warner, 1991: A synoptic climatology of the elevated mixed-layer inversion over the southern Great Plains in spring. Part I: Structure, dynamics, and seasonal evolution. *Wea. Forecasting*, **6**, 198–213.

——, and ——, 1997: A case study of lid evolution using analyses of observational data and a numerical model simulation. *Wea. Forecasting,* **12,** 228–252.

Lau K.-M., and L. Peng, 1987: Origin of low-frequency (intraseasonal) oscillations in the tropical atmosphere. Part I: Basic theory. *J. Atmos. Sci.*, **44**, 950–972.

Liu, J., R. E. Stewart, and K. K. Szeto, 2004: Moisture transport and other hydrometeorological features associated with the severe 2000/01 drought over the western and central Canadian Prairies. *J. Climate*, **17**, 305-319.

Livezey, R. E., and K. C. Mo, 1987: Tropical–extratropical teleconnections during the Northern Hemisphere winter. Part II: Relationships between monthly mean Northern Hemisphere circulation patterns and proxies for tropical convection. *Mon. Wea. Rev.,* **115,** 3115–3132.

Lyon, B., and R. M. Dole, 1995: A diagnostic comparison of the 1980 and 1988 U.S. Summer heat wave-drought. *J. Climate*, **8**, 1658-1675.

Maloney, E. D., and D. L. Hartmann, 1998: Frictional moisture convergence in a composite life cycle of the Madden–Julian oscillation. *J. Climate,* **11,** 2387–2403.

Manabe, S., J. Smagorinsky, and R. F. Strickler, 1965: Simulated climatology of a general circulation model with a hydrological cycle. *Mon. Wea. Rev.,* **93,** 769–798.

Mapes, B. E., 2000: Convective inhibition, subgrid-scale triggering energy, and stratiform instability in a toy tropical wave model**.** *J. Atmos. Sci.,* **57**, 1515-1535.

Matthews A. J., and G. N. Kiladis, 2000: A model of Rossby waves linked to submonthly convection over the eastern tropical Pacific. *J. Atmos. Sci.*, **57**, 3785–3798.

McNulty, R. P., 1995: Severe and convective weather: A central region forecasting challenge. *Wea. Forecasting,* **10,** 187–202.

Mintz, Y., 1984: The sensitivity of numerically simulated climates to land-surface boundary conditions. *The Global Climate,* J. T. Houghton, Ed., Cambridge University Press, 79–106.

Mo, K. C., J. R. Zimmerman, E. Kalnay, and M. Kanamitsu, 1991: A GCM study of the 1988 United States drought. *Mon. Wea. Rev.,* **119,** 1512–1532.

Namias, J., 1982: Anatomy of Great Plains protracted heat waves (especially the 1980 U.S. summer drought). *Mon. Wea. Rev.*, **110**, 824-838.

NCDC, cited 2006: Billion dollar US weather disasters 1980-2006. [Available online at http://www.ncdc.noaa.gov/oa/reports/billionz.html.]

NOAA, cited 2001: Texas droughts extreme for past 15 years, NOAA reports. [Available online at http://www.publicaffairs.noaa.gov/releases2001/mar01/noaa01r303.html.]

Oglesby, R. J., 1991: Springtime soil moisture, natural climatic variability, and North American drought as simulated by the NCAR Community Climate Model 1. *J. Climate,* **4,** 890–897.

——, and D. J. Erickson, 1989: Soil moisture and the persistence of North American drought. *J. Climate*, **2**, 1362-1380.

Plumb, R. A., 1985: On the three-dimensional propagation of stationary waves. *J. Atmos. Sci*., **42**, 217-229.

Rasmussen, E. N., and D. O. Blanchard, 1998: A baseline climatology of sounding-derived supercell and tornado forecast parameters. *Wea. Forecasting,* **13,** 1148–1164.

Ripley, E. A., 1976: Drought in the Sahara: Insufficient biogeophysical feedback? *Science*, **191**, 100.

Rowntree, P. R., and J. A. Bolton, 1983: Simulation of the atmospheric response to soil moisture anomalies over Europe, *Q, J. R. Meteorol. Soc*., **109**, 501-526.

Salby, M. L, 1996: *Atmospheric Physics*. Academic press, 627pp.

Sato, T., and F. Kimura, 2003: A two-dimensional numerical study on diurnal cycle of mountain lee precipitation, *J. Atmos. Sci*., 60, 1992-2003.

Schaack, T. K., and D. R. Johnson, 1994: January and July global distributions of atmospheric heating for 1986, 1987, and 1988. *J. Climate,* **7,** 1270–1285.

Schär C., D. Lüthi, U. Beyerle, and E. Heise, 1999: The soil–precipitation feedback: A process study with a regional climate model. *J. Climate*, **12**, 722–736.

Schumacher C., and R. A. Houze Jr., 2003: Stratiform rain in the Tropics as seen by the TRMM precipitation radar. *J. Climate*, **16**, 1739–1756.

Stensrud D. J., 1993: Elevated residual layers and their influence on surface boundary-layer evolution. *J. Atmos. Sci*, **50**, 2284–2293.

Stephens, G. L., and P. J. Webster, 1981: Clouds and climate: Sensitivity of simple systems. *J. Atmos. Sci.,* **38,** 235–247.

Sud, Y. C., and M. J. Fennessy, 1982: A study of the influence of surface albedo on July circulation in semi-arid regions using the GLAS GCM. *J. Climatol*., **2**, 105-125.

——, and ——, 1984: Influence of evaporation in semi-arid regions on the July circulation: A numerical study. *J. Climatol.*, **4**, 383-398.

——, and W. E. Smith, 1985: Influence of local land-surface processes on the Indian Monsoon: A numerical study. *J. Climate Appl. Meteor.*, **24**, 1015-1036.

——, D. M. Mocko, K. M. Lau, and R. Atlas, 2003: Simulating the Midwestern U.S. drought of 1988 with a GCM. *J. Climate*, **16**, 3946-3965.

Sun, W.-Y., and Y. Ogura, 1979: Boundary layer forcing as a possible trigger to a squall line formation. *J. Atmos. Sci.,* **36,** 235–254.

Ting, M., and H. Wang, 1997: Summertime U.S. precipitation variability and its relation to Pacific sea surface temperature. *J. Climate,* **10,** 1853–1873.

Trenberth, K. E., 1999: Atmospheric moisture recycling: Role of advection and local evaporation. *J. Climate,* **12,** 1368–1381.

——, and G. W. Branstator, 1992: Issues in establishing causes of the 1988 drought over North America. *J. Climate*, **5**, 159-172.

——, and C. J. Cuillemot, 1996: Physical process involved in the 1988 drought and 1993 floods in North America. *J. Climate*, **9**, 1288-1298.

——, G. W. Branstator, and P. A. Arkin, 1988: Origins of the 1988 North American drought. *Science*, **242**, 1640-1645.

——, G. W Branstator, D Karoly, A Kumar, N.-C Lau, and C Ropelewski, 1998: Progress during TOGA in understanding and modeling global teleconnections associated with tropical sea surface temperatures. *J. Geophys. Res.*, **103**, 14291–14324.

Tsonis, A. A., 1996: Widespread increases in low-frequency variability of precipitation over the past century, *Nature*, **382**, 700– 702.

van den Dool H. M., Coauthors,, 1998: 3rd annual review of skill of CPC real time long lead predictions: How well did we do during the great ENSO event of 1997–1998?, *Proc. 23d Climate Diagnostics and Prediction Workshop,* Miami, FL, NOAA/CPC, 9–12.

Weckwerth, T. M., 2000: The effect of small-scale moisture variability on thunderstorm initiation. *Mon. Wea. Rev*., **128**, 4017-4030.

Williams, E., and N. Renno, 1993: An analysis of the conditional instability of the tropical atmosphere, *Mon. Wea. Rev*., **121**, 21–36.

——, S. A. Rutledge, S. G. Geotis, N. Renno, E. Rasmussen, and T. Rickenbach, 1992: A radar and electrical study of tropical "hot towers." *J. Atmos. Sci.,* **49,** 1386–1395.

Woodhouse C. A., and J. T. Overpeck, 1998: 2000 years of drought variability in the central United States. *Bull. Amer. Meteor. Soc.*, **79**, 2693–2714.

Xie X., and B. Wang, 1996: Low-frequency equatorial waves in vertically sheared zonal flow. Part II: Unstable waves. *J. Atmos. Sci*, **53**, 3589–3605.

Ye, B., A. D. Del Genio, and K. K.-W. Lo, 1998: CAPE variation in the current climate and in a climate change, *J. Climate*., **11**, 1997–2015.

Ziegler, C. L., T. J. Lee, and R. A. Pielke Sr., 1997: Convective initiation at the dryline: A modeling study, *Mon. Wea. Rev*., **125**, 1001–1026.

Zipser, E. J., 1977: Mesoscale and convective-scale downdrafts as distinct components of squall-line circulation. *Mon. Wea. Rev.,* **105,** 1568–1589.

VITA

Boksoon Myoung was born in Korea on September 7, 1975 to Mr. Kwang-Young Myoung and Ms. Byoung-Yeol Ahn. She graduated from Ahn-Yang High School, Korea in 1994. She received a B.S. in astronomy and atmospheric Sciences from Yonsei University in Korea in 1998 and a M.S. in 2002 and a Ph.D. in 2007 in Atmospheric Sciences at Texas A&M University. At Texas A&M University she participated in the Texas Air Quality Study (TEXAQS 2000) in 2000. She can be reached through the Department of Atmospheric Sciences, Texas A&M University, College Station, TX 77843-3150. Her e-mail address is: springnite@gmail.com.